Anatomy of the Heart by Multislice Computed Tomography

Francesco Faletra • Natesa Pandian • Siew Yen Ho

WILEY-BLACKWELL

Anatomy of the Heart by Multislice Computed Tomography

Anatomy of the Heart by Multislice Computed Tomography
F. F. Faletra, N. G. Pandian and Siew Yen Ho. © 2008
Francesco Fulvio Faletra, Natesa G. Pandian and Siew Yen Ho.
ISBN: 978-1-4051-8055-9.

Anatomy of the Heart by Multislice Computed Tomography

Francesco Fulvio Faletra, MD

Head of Cardiac Imaging Laboratory
Fondazione Cardiocentro Ticino
Lugano, Switzerland

Natesa G. Pandian, MD

Professor of Medicine
Co-Director, Center for Cardiovascular Imaging
Tufts University Medical Center
Boston, MA, USA

Siew Yen Ho, PhD

Head of Cardiac Morphology
National Heart and Lung Institute
Imperial College London
London, UK

WILEY-BLACKWELL
A John Wiley & Sons, Ltd., Publication

This edition first published 2008, © 2008 by Francesco Fulvio Faletra, Natesa G. Pandian and Siew Yen Ho

Blackwell Publishing was acquired by John Wiley & Sons in February 2007. Blackwell's publishing program has been merged with Wiley's global Scientific, Technical and Medical business to form Wiley-Blackwell.

Registered office:
John Wiley & Sons Ltd, The Atrium, Southern Gate, Chichester, West Sussex, PO19 8SQ, UK

Editorial offices:
9600 Garsington Road, Oxford, OX4 2DQ, UK
The Atrium, Southern Gate, Chichester, West Sussex, PO19 8SQ, UK
111 River Street, Hoboken, NJ 07030–5774, USA

For details of our global editorial offices, for customer services and for information about how to apply for permission to reuse the copyright material in this book please see our website at www.wiley.com/wiley-blackwell

The right of the author to be identified as the author of this work has been asserted in accordance with the Copyright, Designs and Patents Act 1988.

All rights reserved. No part of this publication may be reproduced, stored in a retrieval system, or transmitted, in any form or by any means, electronic, mechanical, photocopying, recording or otherwise, except as permitted by the UK Copyright, Designs and Patents Act 1988, without the prior permission of the publisher.

Wiley also publishes its books in a variety of electronic formats. Some content that appears in print may not be available in electronic books.

Designations used by companies to distinguish their products are often claimed as trademarks. All brand names and product names used in this book are trade names, service marks, trademarks or registered trademarks of their respective owners. The publisher is not associated with any product or vendor mentioned in this book. This publication is designed to provide accurate and authoritative information in regard to the subject matter covered. It is sold on the understanding that the publisher is not engaged in rendering professional services. If professional advice or other expert assistance is required, the services of a competent professional should be sought.

The contents of this work are intended to further general scientific research, understanding, and discussion only and are not intended and should not be relied upon as recommending or promoting a specific method, diagnosis, or treatment by physicians for any particular patient. The publisher and the author make no representations or warranties with respect to the accuracy or completeness of the contents of this work and specifically disclaim all warranties, including without limitation any implied warranties of fitness for a particular purpose. In view of ongoing research, equipment modifications, changes in governmental regulations, and the constant flow of information relating to the use of medicines, equipment, and devices, the reader is urged to review and evaluate the information provided in the package insert or instructions for each medicine, equipment, or device for, among other things, any changes in the instructions or indication of usage and for added warnings and precautions. Readers should consult with a specialist where appropriate. The fact that an organization or Website is referred to in this work as a citation and/or a potential source of further information does not mean that the author or the publisher endorses the information the organization or Website may provide or recommendations it may make. Further, readers should be aware that Internet Websites listed in this work may have changed or disappeared between when this work was written and when it is read. No warranty may be created or extended by any promotional statements for this work. Neither the publisher nor the author shall be liable for any damages arising herefrom.

Library of Congress Cataloging-in-Publication Data
Data available

ISBN:978-1-4051-8055-9

A catalogue record for this book is available from the British Library.

CD produced by: Meg Barton and iBooks Book Production Services
Set in 9.5/12 pt Minion by Newgen Imaging Systems Pvt. Ltd, Chennai, India
Printed and bound in Singapore by Fabulous Printers Pte Ltd

1 2008

Contents

Preface, vi
Acknowledgments, vii

1 Basic Principles, 1
Additional contributor: A. Mayer, MD

2 Location of the Heart: Body Planes and Axis, 7

3 Cardiac Planes, 19

4 The Right Heart, 27

5 The Left Heart, 39

6 The Cardiac Valves, 55

7 The Cardiac Septum, 81

8 Coronary Artery Anatomy, 88
Additional contributor: Giovanni Pedrazzini, MD

9 Coronary Vein Anatomy, 108

10 Coronary Artery Bypass Grafts, 116
Additional contributor: Stefanos Demertzis

Index, 123

A CD-Rom with video clips is included at the back of the book.

Preface

Anatomy is perhaps the simplest of medical sciences, requiring little more than some curiosity plus careful observation of things as they are.

The new multislice computed tomography (MSCT) machines produce a volume data set with the highest isotropic spatial resolution ever seen. The 0.6-mm "pixel" (picture element) that CT has traditionally delivered in axial planes (x and y dimensions) is also extended to the z dimension as well. The spatial resolution of these new machines is such that they can scan a 10-mm diameter piece of heart in 20 axial sections to produce nearly 4000 pixels for each slice. In other words, these scanners are capable of digitizing the anatomy of a 70-kg human body into over half a billion individual voxels (volume elements).

Given this high spatial resolution, MSCT offers superb 3D images of the entire heart and great vessels. Relationships between cardiac structures can be shown as never before. Electronic casts and electronic dissections of the heart in any plane can show the internal and external cardiac structures. As a result, the anatomy of the heart and great vessels can be understood easily by young doctors, medical students and nurses. This atlas has been made for them.

MSCT is unique in its ability to image coronary arteries and it is likely to become one of the most used cardiac imaging techniques. Images of coronary vessels provided by MSCT can be interpreted both from radiological and cardiological standpoints. Indeed, radiologists are often not sufficiently familiar with cardiac anatomy, whereas cardiologists often lack adequate familiarity with the axial, coronal or sagittal planes used for visualization of cardiac MSCT images. This atlas has also been made to clarify the anatomy for both specialties.

The atlas is divided into 10 chapters. In each chapter, the body planes, cardiac planes and cardiac structures, such as cardiac chambers, cardiac valves, septa, coronary arteries and coronary veins, are displayed from many perspectives to give the reader a wider vision of living cardiac anatomy.

Acknowledgments

We wish to express our gratitude to Tiziano Mocetti, Elena Pasotti and Angelo Auricchio. This book would not have been possible without their support. We also appreciate and thank Chiara Carraro and Ermidio Rezzonico, technicians at the Radiology Department of Ospedale Civico in Lugano, for their skilful work.

Natesa wishes to thank his students and colleagues from whom he has learnt a great deal.

Ho wishes to thank the Cardiac Morphology team at the Royal Brompton Hospital for their continuing support.

Francesco Fulvio Faletra
Natesa G. Pandian
Siew Yen Ho

Video clips on CD-ROM

A companion CD-ROM with video clips is included at the back of the book

All video clips are referenced in the text where you see this symbol.

CHAPTER 1
Basic Principles

The images of this atlas are derived by a multislice computed tomography (MSCT) machine using the post-processing algorithms available. A brief, basic description of how the machine works and how the algorithms produce different image modalities is given in this introductory section. For more comprehensive descriptions of the post-processing algorithms see "Suggested reading".

The machine

The CT scanner has a ring with an x-ray tube on one side and detectors on the opposite side. This tube-detector unit rotates around the patient during data acquisition. The information (x-ray attenuation) obtained from the detectors during this rotation is processed through a computer, which can calculate the exact attenuation of a given point (pixel) in the examined volume. The width and length of a pixel depend on the size of the detector. With modern spiral CT (Fig. 1.1), the table moves through the ring so that the machine acquires data in a spiral trajectory during tube-detector unit rotation. This makes it possible to acquire attenuation information for a given point in a volume (three-dimensional, 3D) instead of a slice (two-dimensional, 2D). The volume element (voxel) has equal length in all three axes (x, y and z: isotropic voxel); this is important for reconstruction of images in different planes. To speed up data acquisition (and table movement) it is possible to calculate the attenuation information of one voxel from the detector data of less than one complete rotation (a 180° rotation is enough for a good image).

Anatomy of the Heart by Multislice Computed Tomography
F. F. Faletra, N. G. Pandian and Siew Yen Ho. © 2008
Francesco Fulvio Faletra, Natesa G. Pandian and Siew Yen Ho.
ISBN: 978-1-4051-8055-9.

The acquisition time depends on the number of detectors, rotation speed of the tube-detector unit, length of volume examined and speed of table movement.

Post-processing imaging modalities

Axial images

Axial images are the basic generated images used in MSCT. Axial images can be viewed directly for interpretation or used to create multiplanar or 3D images.

Multiplanar reconstruction (MPR)

Multiplanar reconstruction is the process of using data from axial MSCT images to create "non-axial" two-dimensional images. MPR images are generated from a plane of only one voxel in thickness transecting a set of axial images. In principle any plane can be generated from the volume data set but, by convention, the most used planes are the body planes (axial, sagittal and coronal) (see Chapter 2). Cardiac planes (parallel to the long axis of the left ventricle) are useful to evaluate the heart anatomy, and oblique planes (at any angulation) to display individual structures such as mitral leaflets or the aortic root (Fig. 1.2; see also Chapters 2 and 3).

Curved multiplanar reconstruction (cMPR)

This display modality produces a flattened representation of a curved plane. This modality is useful for the visualization of coronary arteries: a cMPR is reconstructed along the curved course of the vessel. All curved structures are represented on a flat plane. Because the plane is defined by the course of the coronary vessel of interest, the anatomical relationships of all other structures around the vessel are distorted (Fig. 1.3).

Figure 1.1 A modern multislice computed tomography machine (see text).

Figure 1.2 Multiplanar reconstruction. An oblique view aims to visualize the membranous septum (arrow). RA = right atrium; RV = right ventricle; Ao = aorta; LV = left ventricle.

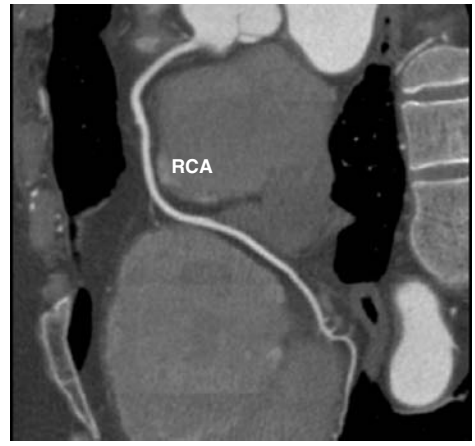

Figure 1.3 Curved multiplanar reconstruction of the right coronary artery (RCA). Although the artery has a tortuous course passing through many planes the algorithm projects the entire course of the vessel in a single plane. Note that the anatomic relationships between chambers are distorted.

Maximum intensity projection (MIP)

With this modality several voxels are stacked one on top of the other, so that slices thicker than one voxel are reconstructed. With MIP, only the voxels with the highest density are visualized. MIP is useful to evaluate small tortuous structures that are hyperdense (i.e., of higher density) compared with their surrounding structures (i.e., contrast-enhanced coronary vessels surrounded by fat). This display modality resembles the images of

Figure 1.4 The MIP image of the right coronary artery (RCA). This modality is similar to conventional coronary angiography.

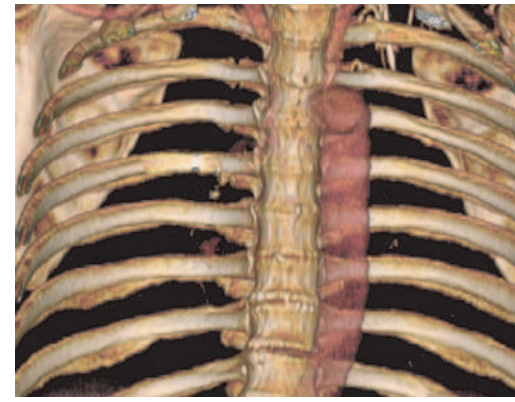

Figure 1.5 The white-yellow color assigned to the ribs makes the image of the chest cage similar to the actual anatomy.

conventional coronary angiography because the result is a projection of the highest attenuation values of the volume (Fig. 1.4).

Volume rendering technique

The 3D volume rendering technique is the computer algorithm used to transform serially acquired axial CT image data into 3D images. Each voxel is classified by calculating the probability that it contains a specific tissue type, with separate classifications for tissues such as bone soft tissue, contrast-enhanced vessels, air, and fat.

By applying color to the histogram tissue classification system, an intuitive perception of depth relationships can be achieved. The application of this "pseudo-color" to tissue classification can be used to enhance discrimination among structures. Although these color schemes (red for soft tissues such as heart and liver, yellow for vessels, white for bones, etc.) do not represent the true optical color of anatomical tissues (the color assignment is arbitrary and tailored for any individual applications), the volume-rendering computer algorithm of the heart displays the heart and great vessels as a nearly perfect copy of the anatomic specimen (Fig. 1.5). One of the strengths of 3D volume rendering is the ability to select a variety of viewing perspectives (Fig. 1.6).

Furthermore, an opacity value can be assigned to each voxel. By increasing or decreasing their opacity values the corresponding voxels become respectively more transparent or more opaque. The opacity setting can be arbitrarily selected according to the requirement of the observer. This display modality is useful for evaluating the coronary tree anatomy and its relationship with encased cavities (Fig. 1.7). Moreover, by making the coronary tree and the myocardium completely transparent and increasing the opacity of the intracavitary contrast, a high-resolution "electronic cast" of the cavities is produced (Fig. 1.8).

Virtual endoscopy

Another modality of imaging called "virtual endoscopy" can be obtained by making the contrast of the cavities transparent and the walls opaque. The viewpoint of the observer is within the cavity and can be moved in any direction. Although the clinical value of this modality in pathological states is not well defined, the comprehensive images are very useful for anatomical purposes (Fig. 1.9).

Endocardial surface modality

In this modality the contrast is made transparent and the endocardial surface of the wall is displayed. Cropping the entire volume data set in any desired planes makes visualization of the endocardial surfaces possible from any perspective (Fig. 1.10).

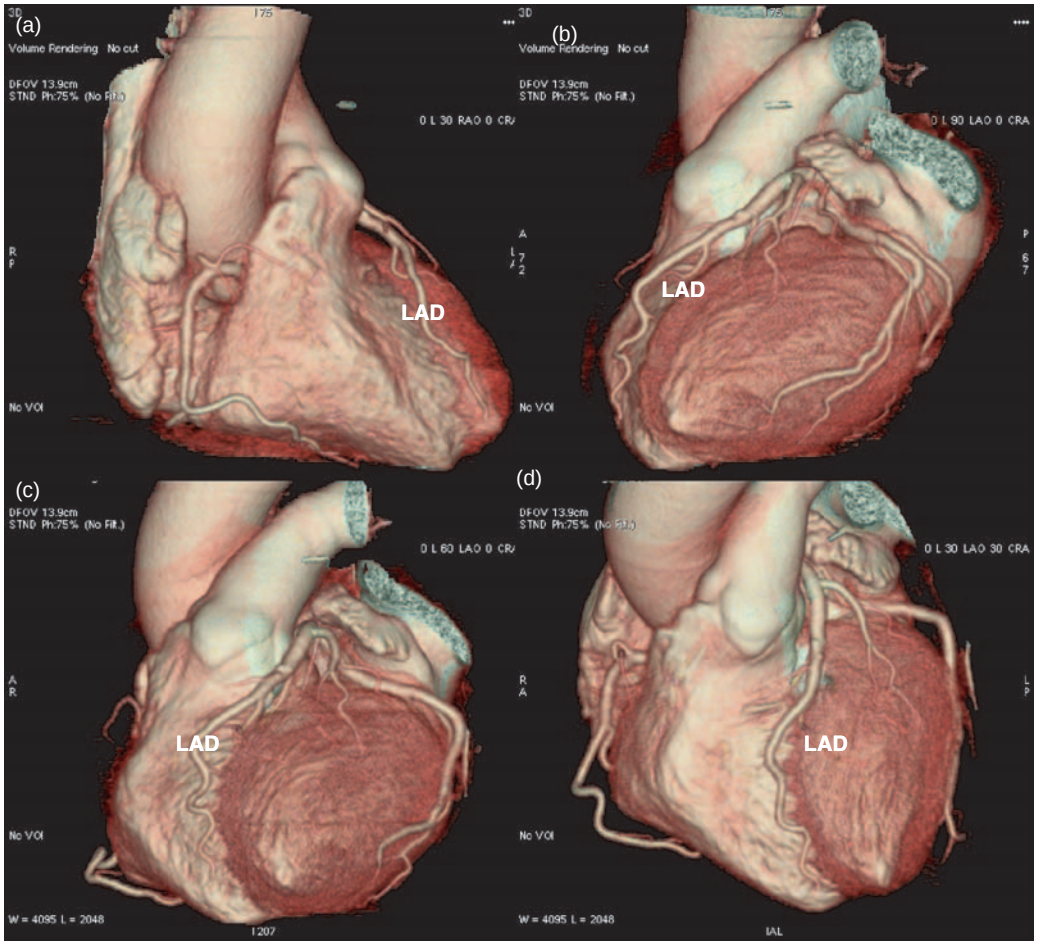

Figure 1.6 3D volume rendering is the most common method of display and assumes external visualization of an object, much like viewing a statue in a museum. 3D display is based on the assumption that light rays reaching our eyes are parallel, similar to seeing objects from a great distance. With this method a countless number of perspectives can be selected (a–d). LAD = left anterior descending coronary artery.

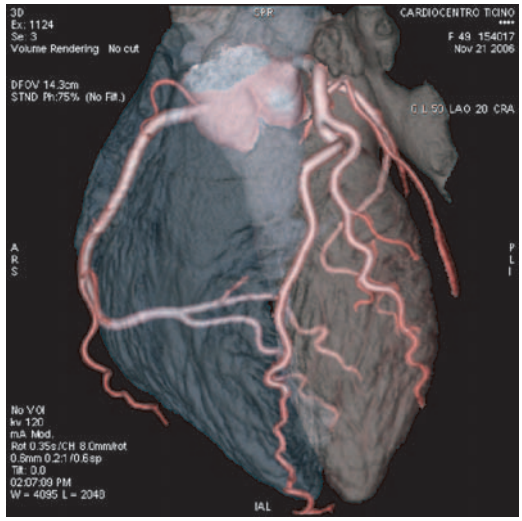

Figure 1.7 By increasing the opacity value of the coronary tree, decreasing the opacity of contrast inside the cavities and making the myocardium completely transparent, clear images of the coronary tree arborization and its relationship with encased cavities can be obtained.

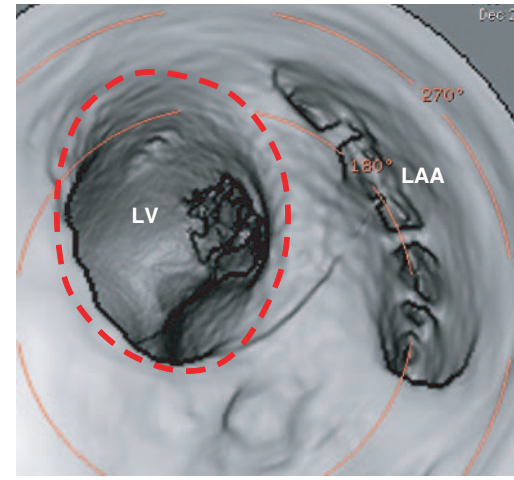

Figure 1.9 Virtual endoscopy. The perspective is inside the left atrium. The mitral valve annulus (red dotted circle), the left ventricle (LV) as well as the left atrial appendage (LAA) can be seen. Rather than light rays being parallel, projected light rays are focused to converge on the viewpoint, simulating natural light convergence on the human retina. The resulting distortion facilitates perception of distance on the basis of object size. Objects near the viewpoint appear large, whereas objects farther away appear small.

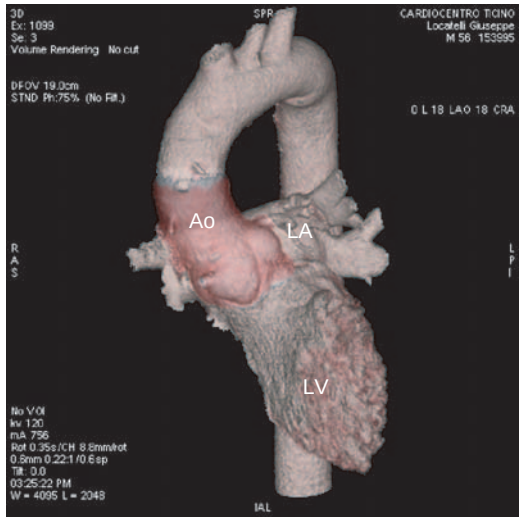

Figure 1.8 "Electronic casts" of the left heart cavities. The relationships between cavities are easily appreciated. LV = left ventricle; LA = left atrium; Ao = aorta.

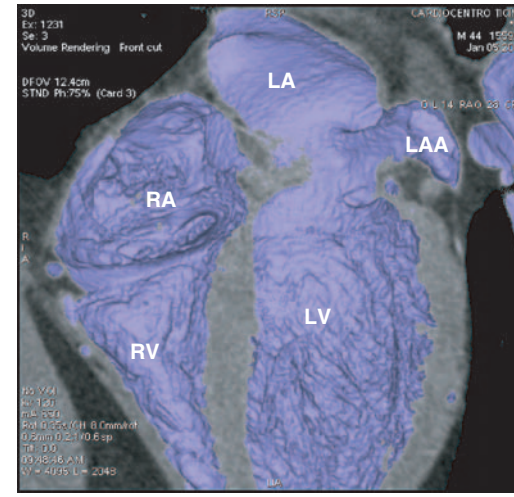

Figure 1.10 3D endocardial surface modality. The posterior endocardial surfaces of right atrium (RA), right ventricle (RV), left atrium (LA) and left ventricle (LV) are displayed viewed from an antero-superior perspective. LAA = left atrial appendage.

Suggested reading

Calhoun PS, Kuszyk BS, Heath DG, Carley JC, Fishman EK. Three-dimensional volume rendering of spiral CT data: theory and method. *RadioGraphics* 1999;19:745–776.

Cody DD. AAPM/RSNA physics tutorial for residents: topics in CT. *RadioGraphics* 2002;22:1255–1268.

Fishman EK, Drebin B, Magid D *et al.* Volumetric rendering techniques: applications for three dimensional imaging of the hip. *Radiology* 1987;163:737–738.

Van Ooijen PM, Ho KY, Dorgelo J, Oudkerk M. Coronary artery imaging with multidetector CT: visualization issues. *RadioGraphics* 2003;23:e16.

CHAPTER 2

Location of the Heart: Body Planes and Axis

Location of the heart

The heart is positioned within the mediastinum with one-third of its mass to the right of the midline, and with its own long axis directed from the right shoulder towards the left hip (Fig. 2.1a–d). It is bordered bilaterally by the lungs, anteriorly by the sternum and inferiorly by the diaphragm. The cardiac apex is located in the left hemithorax (Fig. 2.2a–d).

The right border of the silhouette, more or less vertical, is produced by the right atrium, with the caval veins entering at its top and bottom. The inferior border is made by the right ventricle, extending horizontally along the diaphragm to the cardiac apex, with the left border sloping upwards from the apex and formed by the wall of the left ventricle. At the top of the left border, the left atrial appendage contributes to the silhouette. The pulmonary trunk and aorta emerge from the superior border of the silhouette, with the aorta in a rightward position (Fig. 2.3).

The right heart is located anteriorly and the left heart posteriorly. The right heart structures (right ventricular infundibulum and pulmonary trunk) are therefore anterior relative to the left heart and not located directly to the right (Figs. 2.1a–d and 2.2a–d). The right ventricle is the most anteriorly situated cardiac chamber, lying behind the sternum (Figs. 2.1d and 2.2a). The atrial chambers are posterior and to the right of their respective ventricular chambers (Figs. 2.1d and 2.2d).

Furthermore, owing to the curvature of the ventricular septum, the outflow tract of the right ventricle sweeps antero-superiorly relative to that of the left ventricular outflow tract (Fig. 2.4a,b). The aortic root is thus centrally located in the heart. From its rightward position, the ascending aorta curves leftward to continue into the aortic arch, which passes to the left of the trachea and descends posteriorly as the thoracic aorta. The aortic arch is superior to the bifurcation of the pulmonary trunk (Fig. 2.5a,b).

The most anterior part of the left ventricle is the septum, which includes more than 40% of the cardiac mass. The anterior wall (A) of the left ventricle is actually superior, with the lateral wall lying superior and posterior (L), and the posterior wall inferior-posterior (P). Accordingly the "left anterior descending coronary artery" is superior and the "posterior" descending coronary artery is inferior (Fig. 2.6).

Body planes

Multislice computed tomography (MSCT) images are digital, and more than 1000 axis images are generated by the latest MSCT machines. Any slice has three dimensions: the width (x-axis), the height (y-axis) and the thickness (z-axis). Any slice is therefore divided into "voxels" (volume elements). In the modern MSCT the shape of voxels approximates closely to a small cube (isotropic, i.e., the x-, y-, and z-axes are almost equal). The volume data set of any MSCT examination consists of millions of voxels (Fig. 2.7).

Anatomy of the Heart by Multislice Computed Tomography
F. F. Faletra, N. G. Pandian and Siew Yen Ho. © 2008
Francesco Fulvio Faletra, Natesa G. Pandian and Siew Yen Ho.
ISBN: 978-1-4051-8055-9.

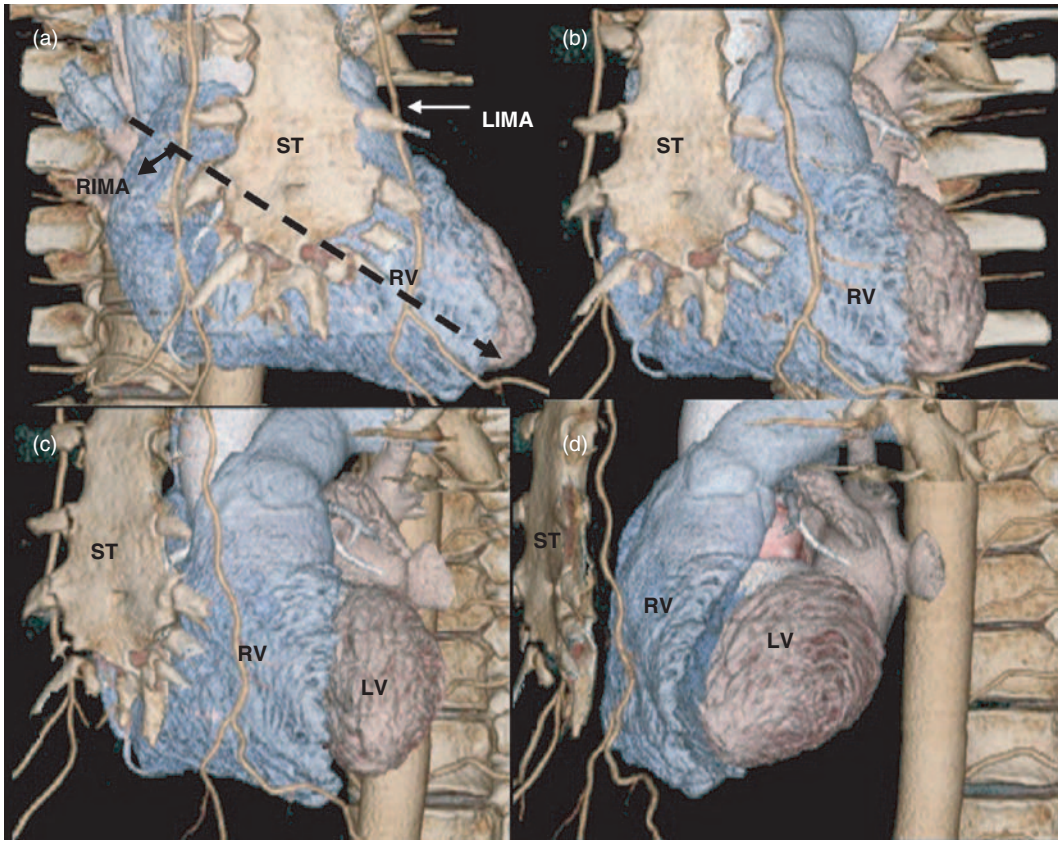

Figure 2.1 (a–d) Electronic cast showing the position of the heart in the thorax. Views from anterior (a) to left lateral (d) perspective. See text and Video clip 1, Position of the heart (Lateral rotation). RV = right ventricle; LV = left ventricle; ST = sternum; LIMA = left internal mammary artery; RIMA = right internal mammary artery.

In principle, any plane can be generated from this huge volume data set. However, by convention and with the subject standing in an upright position and facing the observer, three orthogonal planes are usually derived: sagittal, coronal and axial. For the body, two of these planes are in the long axis (sagittal and coronal), whereas the axial plane is transverse and in the short axis.

Axial planes

An axial plane divides the body into top and bottom portions (Figs. 2.8 and 2.9). These sections taken "from the head to the feet" usually produce a family of oblique cross-sections of the heart with truncated or expanded views of chambers and walls because of the oblique position of the heart within the thorax. Some of the transverse views appear similar to the echocardiographic short-axis views. Transverse sectioning at the level of the great arteries provides an anatomic display of the pulmonary trunk and its bifurcation into the right and left main pulmonary arteries and an adjacent cross-section of the ascending aorta. Moreover, from this plane the origins of the left and right coronary arteries can be appreciated (Fig. 2.10).

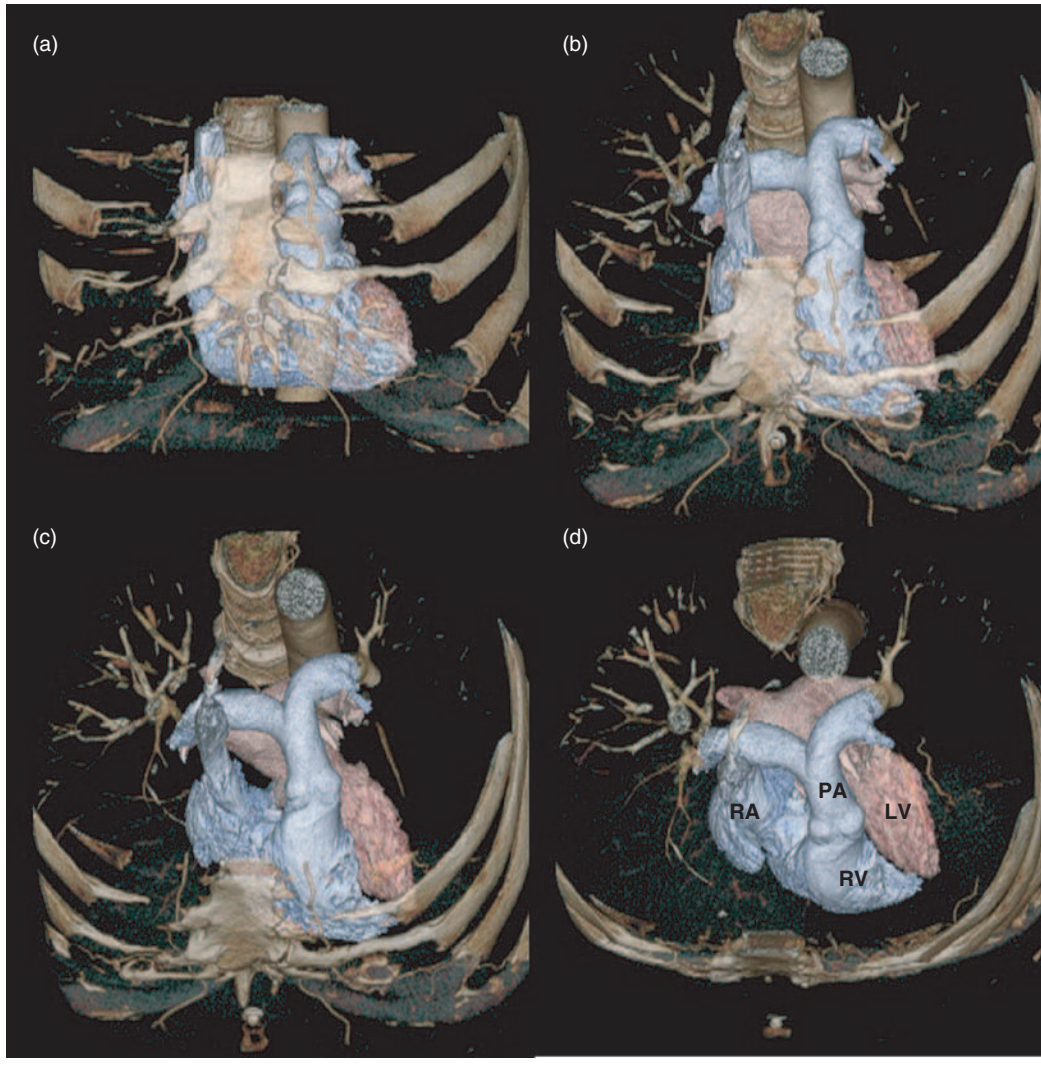

Figure 2.2 Electronic cast (see also Video clip 2, Position of the heart (supero-inferior rotation)). (a–d) Views from anterior (a) to above (d). RV = right ventricle; LV = left ventricle; RA = right atrium; PA = pulmonary artery.

Sagittal planes

The sagittal plane divides the body into right and left sides. Structures lying within different parts of the sagittal plane are then said to be anterior or posterior relative to each other (Figs. 2.11 and 2.12). The slices of the sagittal plane run from right to left or vice versa. This plane is useful for imaging the right ventricle outflow tract and the descending thoracic aorta (Fig. 2.13). Whenever the long axis of the left ventricle is horizontal, for example, in obese patients, the sagittal plane may be useful for imaging short axis views of the left ventricle.

Coronal planes

The coronal plane divides the body into front and back sections. Structures lying within different parts of the sagittal plane are then described as

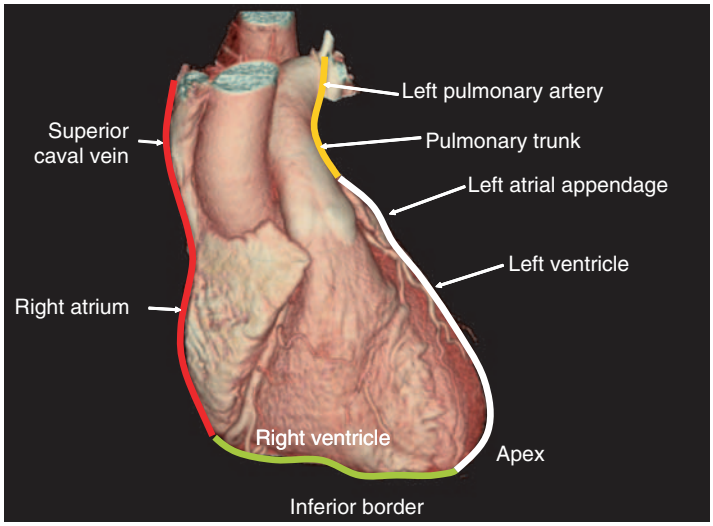

Figure 2.3 3D volume rendering. The cardiac silhouette (see text).

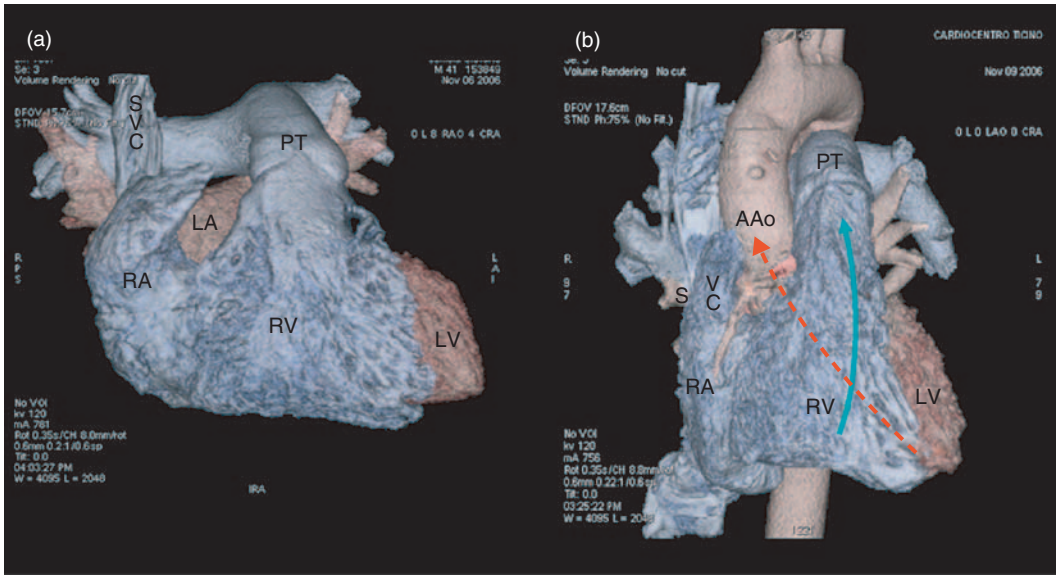

Figure 2.4 Electronic cast. (a) The right structures are anterior relative to the left structures. (b) The outflow tract of the right ventricle sweeps antero-superiorly relative to the left ventricular outflow tract (red and blue arrows). LA = left atrium; PT = pulmonary trunk; RV = right ventricle; LV = left ventricle; AAo = ascending aorta; RA = right atrium; SVC = superior vena cava.

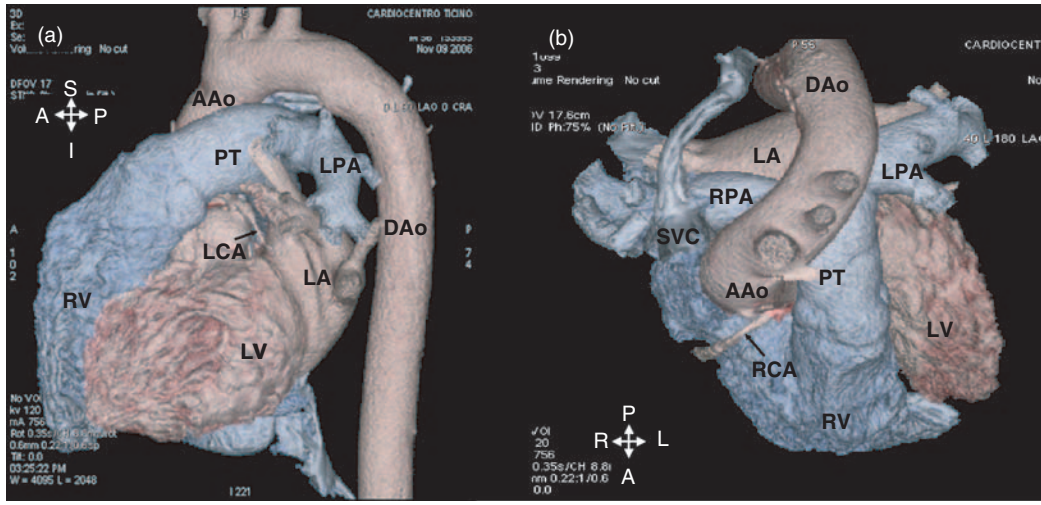

Figure 2.5 (a,b) Electronic cast showing the course of the aorta relative to the pulmonary trunk (see text). Note in this patient the right coronary artery (RCA) origins from the left Valsava sinus. PT = pulmonary trunk; RV = right ventricle; LV = left ventricle; LA = left atrium; AAo = ascending aorta; DAo = descending aorta; RPA = right pulmonary artery; LPA = left pulmonary artery; LCA = left circumflex artery.

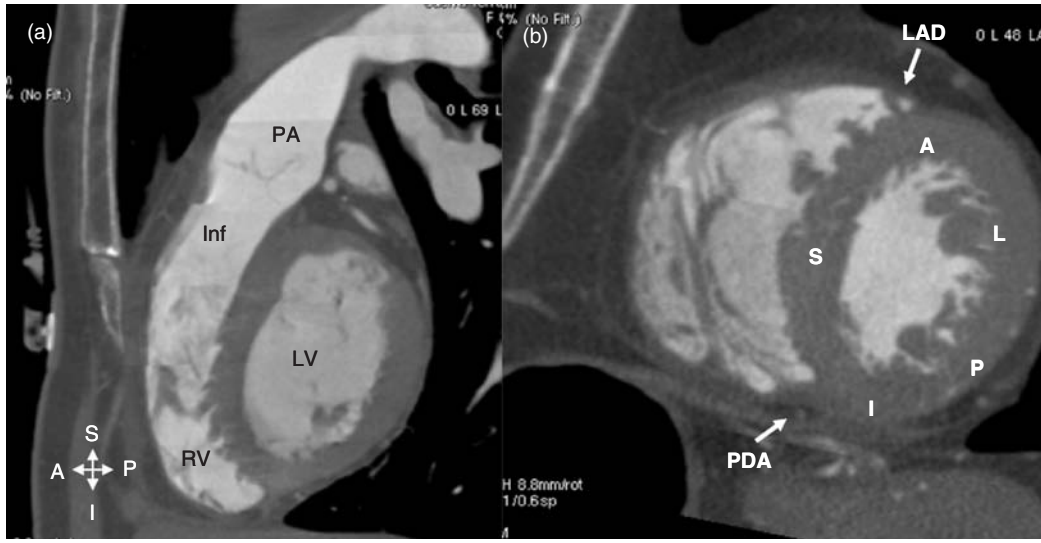

Figure 2.6 Axial (a) and short-axis (b) section showing the right ventricle as anterior and the left ventricle posterior, the anterior wall (A) superior, the lateral wall (L) superior-posterior and the posterior wall (P) inferior-posterior (I). The left anterior descending coronary artery (LAD) is actually superior and the posterior descending coronary artery (PDA) is inferior. RV = right ventricle; LV = left ventricle; PA = pulmonary artery; Inf = infundibulum.

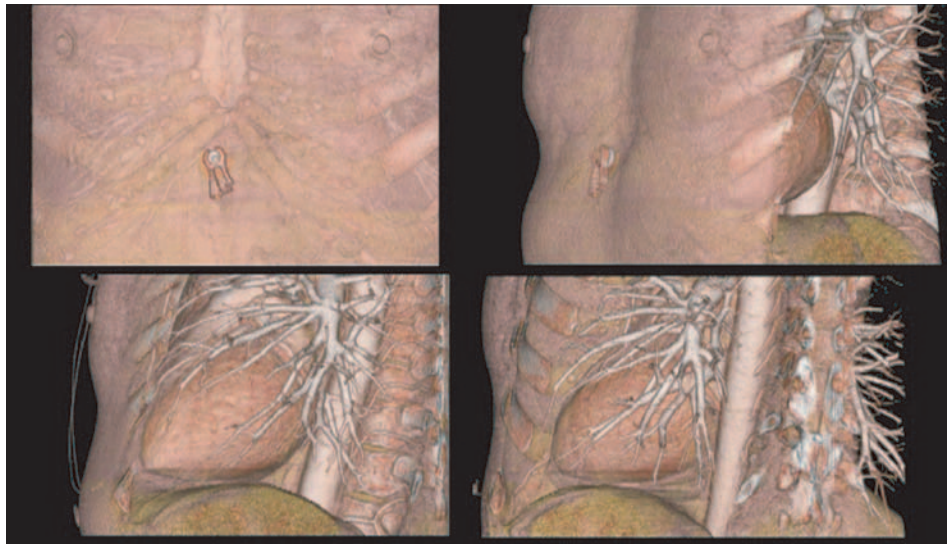

Figure 2.7 3D volume rendering. Volume data set of a patient who underwent CT coronary angiography. This data set comprises millions of voxels (see text and Video clip 3, Thorax).

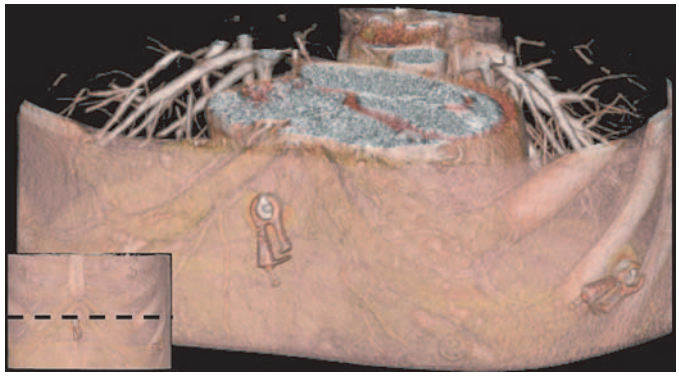

Figure 2.8 3D volume rendering. Axial view. The heart and thorax are cut along the axial plane. The inset shows the plane of the cut.

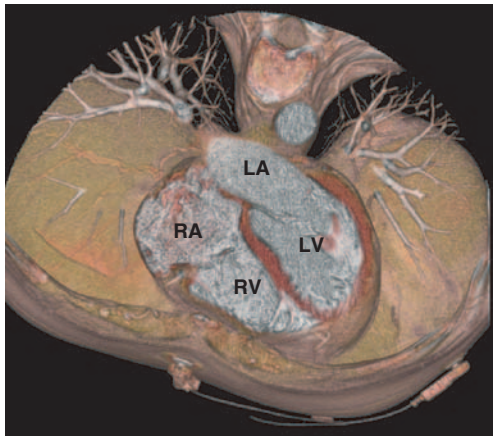

Figure 2.9 3D volume rendering. Axial view; perspective from above. LA = left atrium; LV = left ventricle; RA = right atrium; RV = right ventricle.

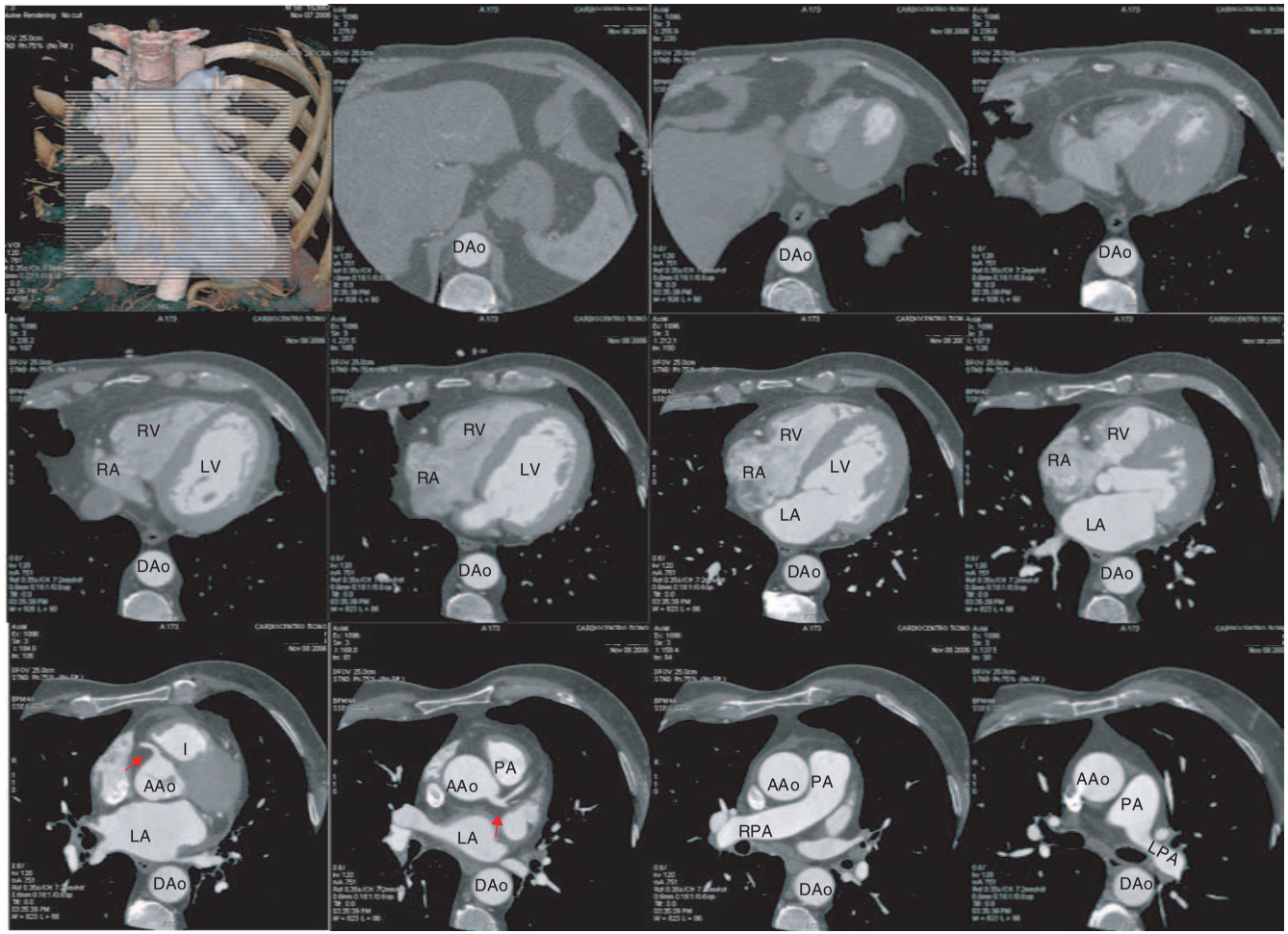

Figure 2.10 A collection of axial planes. These slices are as thin as 0.6 mm. PA = pulmonary artery; RA = right atrium; RV = right ventricle; LV = left ventricle; LA = left atrium; AAo = ascending aorta; DAo = descending aorta; RPA = right pulmonary artery; LPA = left pulmonary artery; red arrow = right and left coronary artery; I = infundibulum.

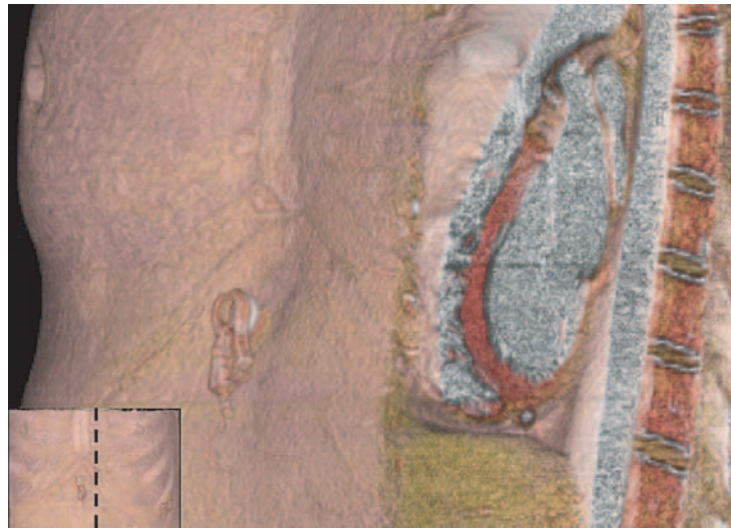

Figure 2.11 3D volume rendering. Axial view. The heart and thorax are cut along the sagittal plane. The inset shows the plane of the cut.

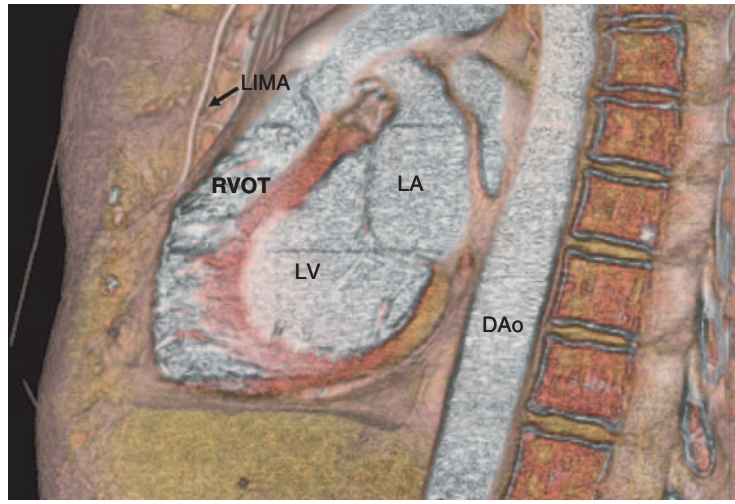

Figure 2.12 3D volume rendering. Sagittal view. Perspective from the left side (see text). LIMA = left internal mammary artery; RVOT = right ventricle outflow tract; LV = left ventricle; LA = left atrium; DAo = descending aorta.

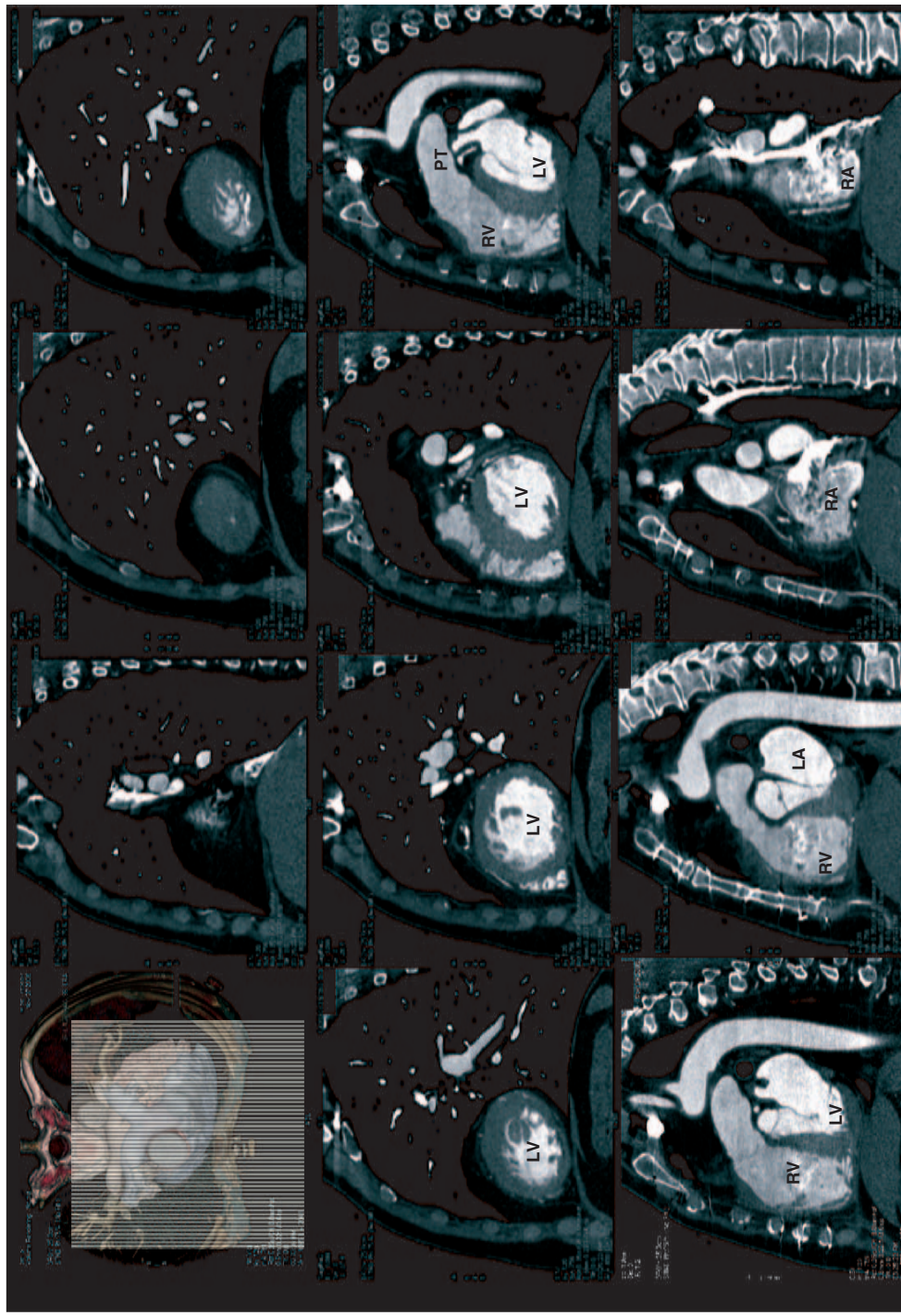

Figure 2.13 A collection of sagittal planes. Abbreviations as in previous figures.

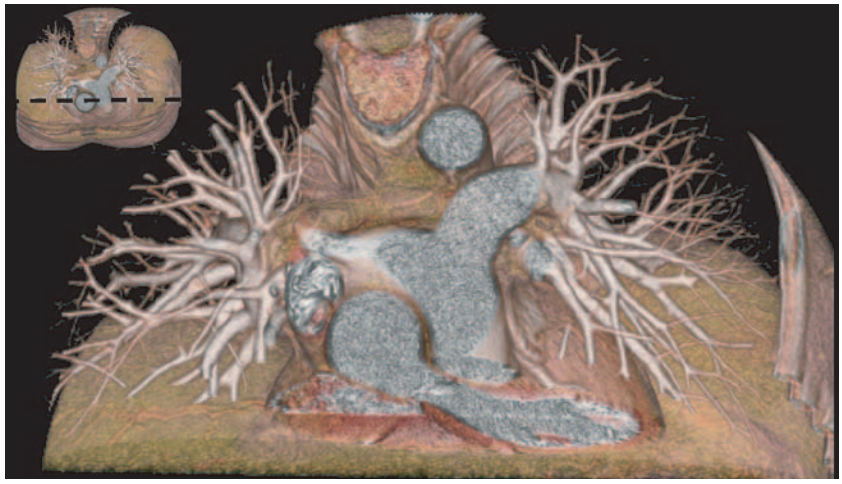

Figure 2.14 3D volume rendering. Axial view. The heart and thorax are cut along the coronal plane. The figure in the upper left corner shows the plane of the cut.

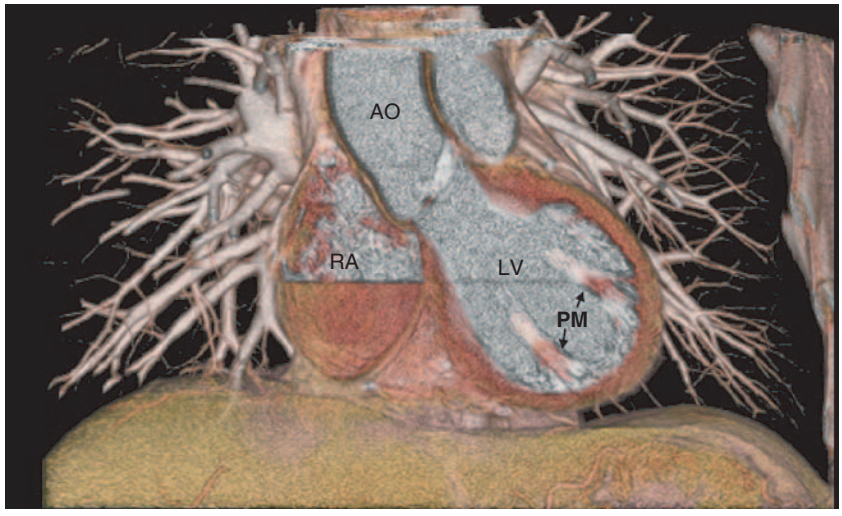

Figure 2.15 3D volume rendering. Coronal view. Perspective from anterior (see text). AO = aorta; LV = left ventricle; RA = right atrium; PM = papillary muscles.

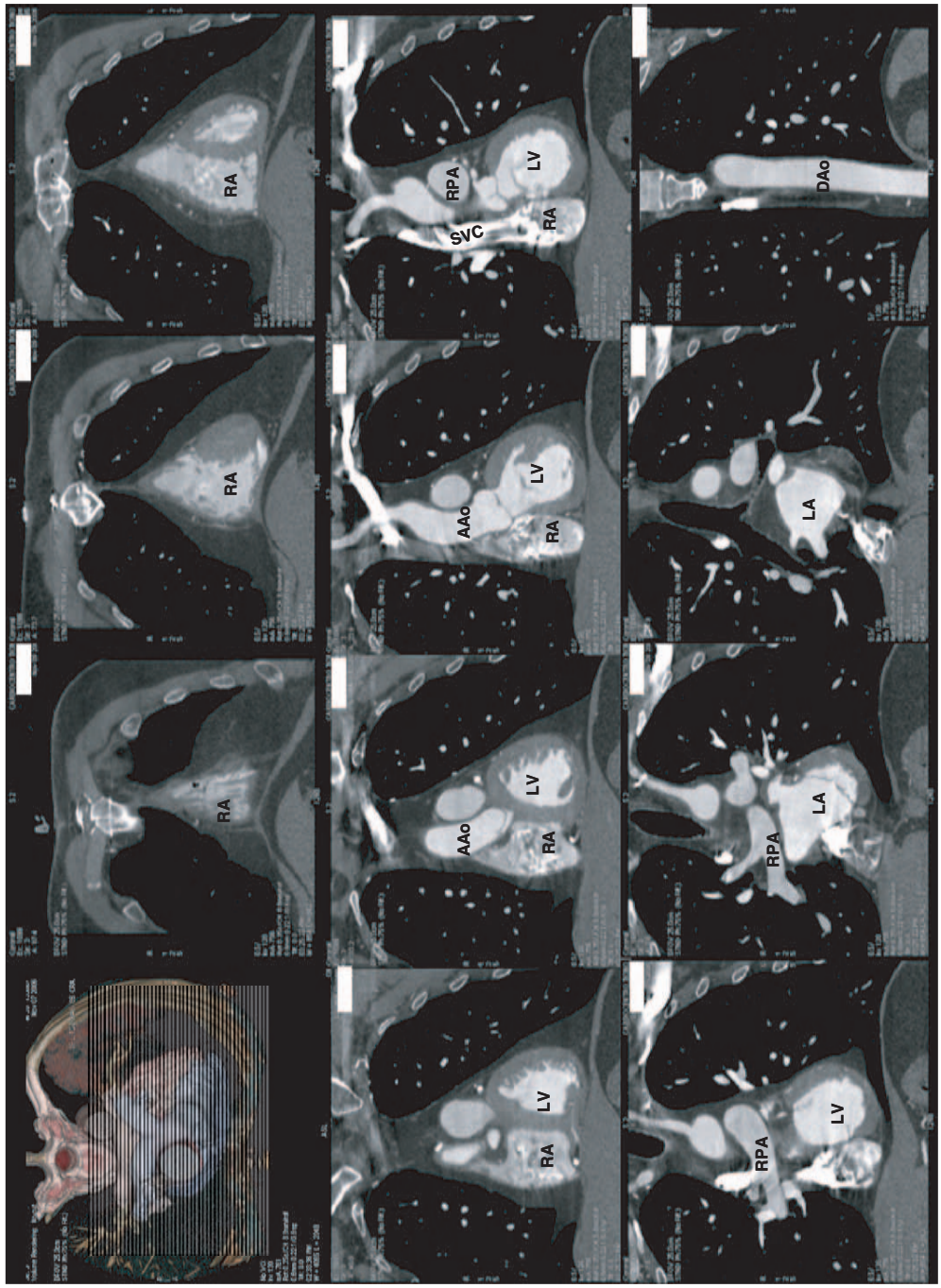

Figure 2.16 A collection of coronal planes. Abbreviations as in previous figures.

being right and left relative to each other (Figs. 2.14 and 2.15). Accordingly, the slices run from anterior to posterior and vice versa. Coronal planes are best for imaging the left ventricular outflow tract, aortic valve and descending thoracic aorta (Fig. 2.16).

Suggested reading

Anderson RH, Becker AE. *Cardiac Anatomy*. Edinburgh: Churchill Livingstone, 1980.

Anderson RH, Ho SY, Brecker SJ. Anatomic basis of cross-sectional echocardiography. *Heart* 2001;85:716–720.

Anderson RH, Razavi R, Taylor AM. Cardiac anatomy revisited. *J Anat* 2004;205:159–177.

Cosio FG, Anderson RH, Kuck KH *et al.* Living anatomy of the atrioventricular junctions. A guide to electrophysiologic mapping. A Consensus Statement from the Cardiac Nomenclature Study Group, Working Group of Arrhythmias, European Society of Cardiology, and the Task Force on Cardiac Nomenclature from NASPE. *Circulation* 1999;100:e31–e37.

McAlpine WA. Heart and Coronary Arteries. Berlin: Springer-Verlag, 1975.

CHAPTER 3
Cardiac Planes

Orthogonal views along the body planes are useful for evaluating the overall morphology of the heart. However, because these planes are not perpendicular to the wall or cavities, cardiac imaging planes are needed. These are the planes through the heart's long and short axes.

Three main long-axis views of the left ventricle oriented parallel to the long axis of the left ventricle are usually used (Figs. 3.1–3.4). These views are the long-axis view and the four- and two-chamber views. The long-axis view cuts through the anterior portion of the septum and the posterior left ventricular wall thus including both the inflow and outflow tracts of the left ventricle (Fig. 3.5a,b). This plane also cuts obliquely through the right ventricular outflow. As in an echocardiographic parasternal or apical long-axis view, the aortic valve with the right and non-coronary sinuses and the mid-portion of anterior (aortic) and posterior (mural) mitral leaflets are displayed. The posteriormedial papillary muscle can be well demonstrated. The upper and lower left pulmonary veins enter the roof of the left atrium (Fig. 3.5a, arrows). Finally, the proximal portion of the right coronary artery in cross-sectional view is also imaged.

The four-chamber plane cuts the heart along both lateral walls from the apex to base so that both ventricles and atria are included in the plane of section (Fig. 3.6a,b). As in echocardiography the four-chamber view displays the inflow chamber of the left and right ventricles, the mid-posterior septum and the left and right lateral walls. Usually this cut offsets papillary muscles, which are located in different planes. The so-called atrioventricular septum is easily imaged from this view (see Chapter 7 regarding septa). The left and right lower pulmonary veins can be seen (Fig. 3.6a, arrows). The mitral and tricuspid valves are also well demonstrated. The mid-portion of right coronary artery in cross axis view is imaged.

The two-chamber view mirrors the echocardiographic apical and transesophageal two-chamber view (Fig. 3.7a,b). The two-chamber view is obtained by cutting the heart immediately to the left of the ventricular septum from the left ventricular apex through the left mitral orifice and the left atrium (Fig. 3.3). The left anterior descending artery can be displayed in 3D volume rendering along its course in the interventricular sulcus (Fig. 3.7a). This section cuts the anterior and inferior walls. The posterior papillary muscle is usually depicted. The posterior course of the right coronary artery, in patients with right coronary dominance, and the coronary sinus (Fig. 3.7b) are visualized in cross-section. Finally, the section cuts the left atrial appendage.

Figure 3.8 shows the short-axis views of the heart. Short-axis cuts are oriented at 90° relative to the long axis of the left ventricle through the middle of the ventricle. They show the crescentic right ventricle and the circular left ventricle. The aorta and pulmonary trunk as well as left and right atria can be imaged in more cranial cuts (Figs. 3.9 and 3.10).

Anatomy of the Heart by Multislice Computed Tomography
F. F. Faletra, N. G. Pandian and Siew Yen Ho. © 2008
Francesco Fulvio Faletra, Natesa G. Pandian and Siew Yen Ho.
ISBN: 978-1-4051-8055-9.

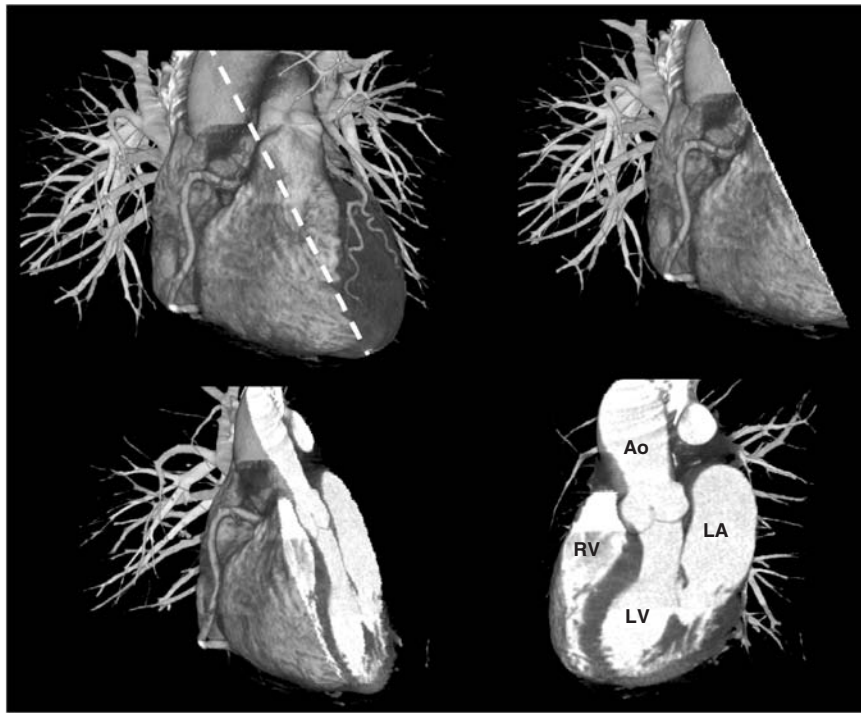

Figure 3.1 3D volume rendering. The heart is cut to show the long-axis view. RV = right ventricle; LA = left atrium; LV = left ventricle; Ao = aorta.

Figure 3.2 3D volume rendering. The heart is cut to show the four-chamber view. RA = right atrium; RV = right ventricle; LA = left atrium; LV = left ventricle.

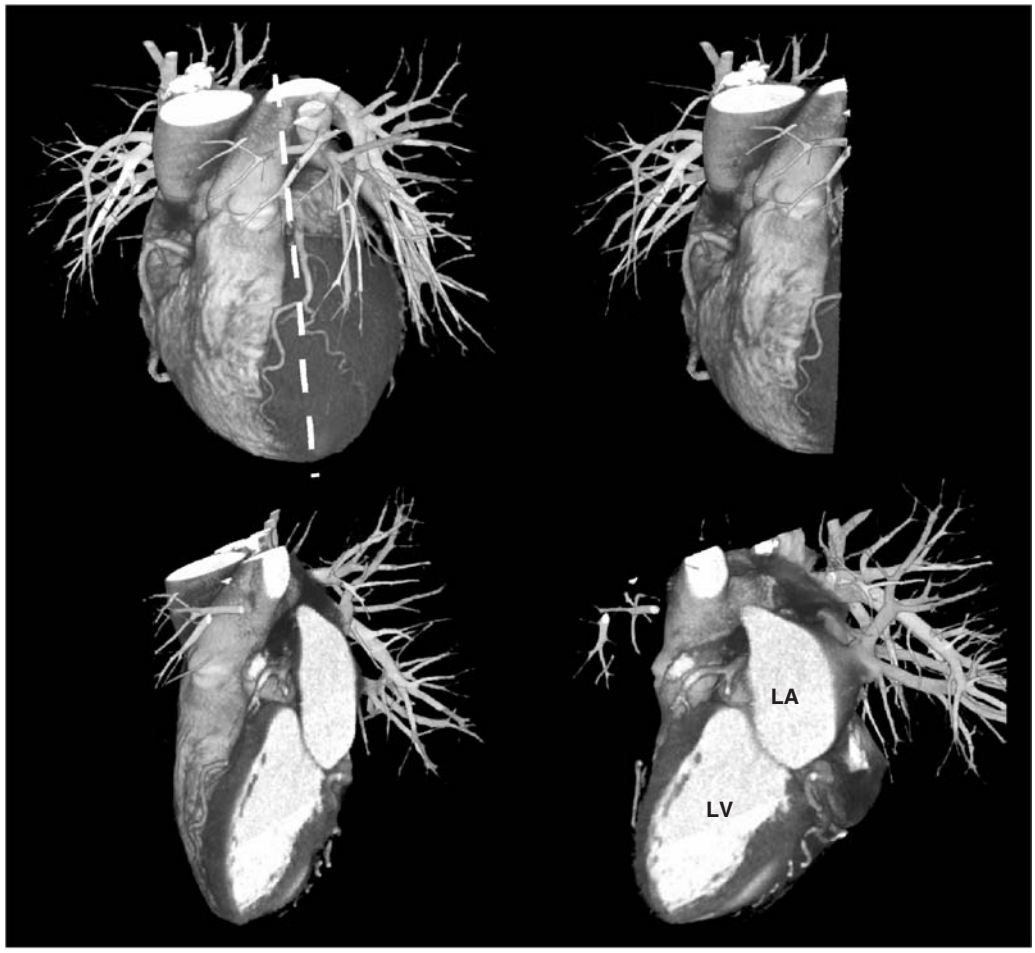

Figure 3.3 3D volume rendering. The heart is cut to show the two-chamber view. LA = left atrium; LV = left ventricle.

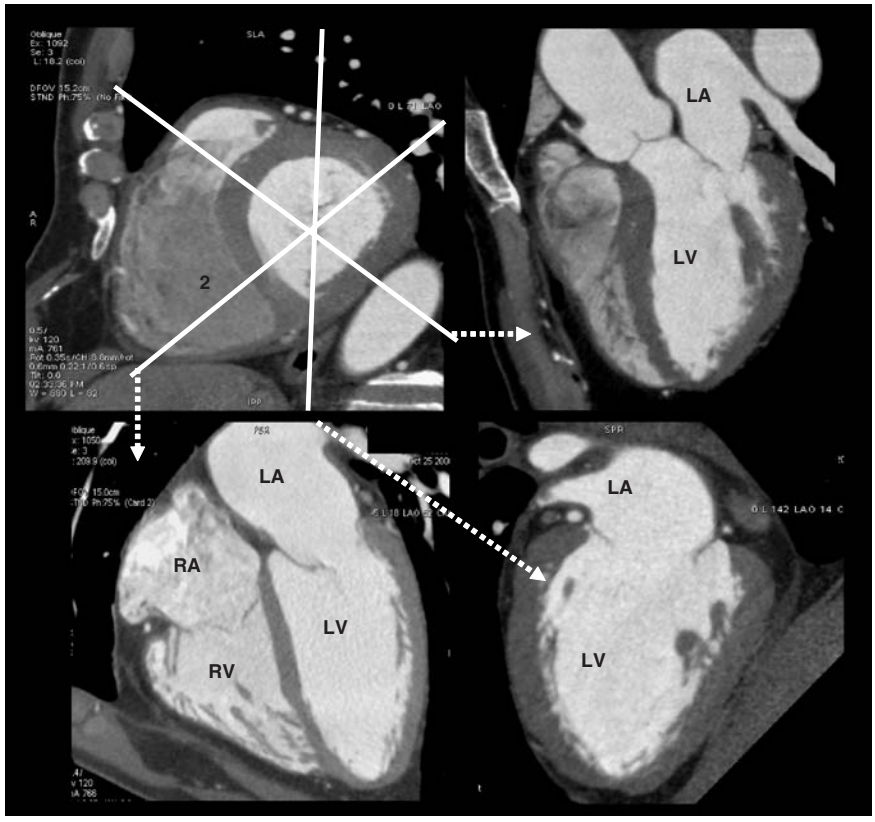

Figure 3.4 The three main long-axis planes. LA = left atrium; LV = left ventricle; RA = right atrium; RV = right ventricle.

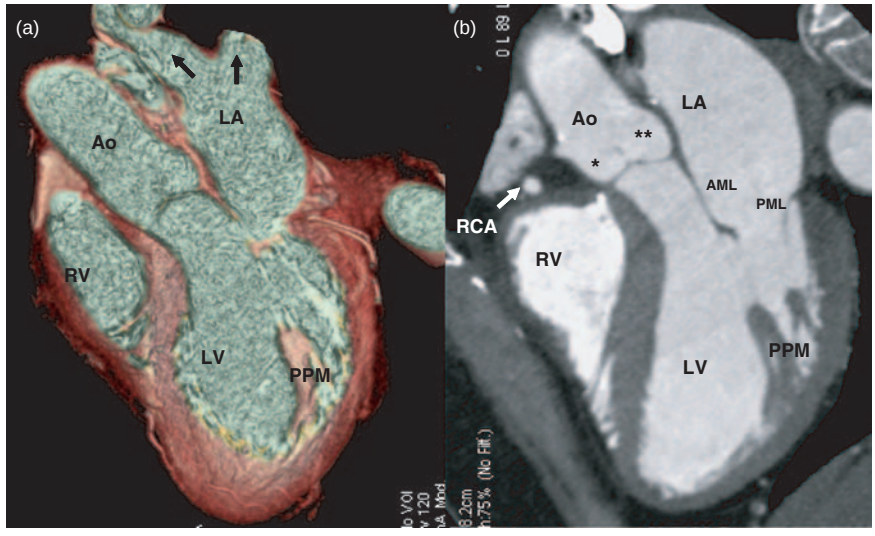

Figure 3.5 Long-axis view. (a) 3D volume rendering reconstruction and (b) the corresponding plane. The single and double asterisks in panel b mark the right and the non-coronary cusps. The arrows in panel a mark the upper and the lower left pulmonary veins (see text). RV = right ventricle; LV = left ventricle; LA = left atrium; Ao = aorta; PPM = posterior papillary muscle; RCA = right coronary artery; AML = anterior mitral leaflet; PML = posterior mitral leaflet.

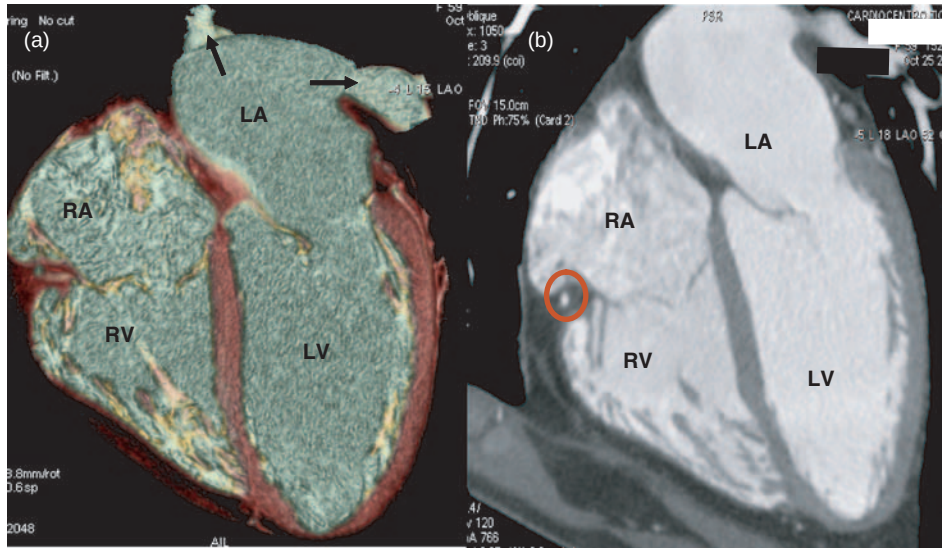

Figure 3.6 Four-chamber view. (a) 3D volume rendering reconstruction and (b) the corresponding plane. Arrows in panel a mark the left and right lower pulmonary veins. The right coronary artery is seen in cross section (red circle in panel b) (see text). RA = right atrium; RV = right ventricle; LA = left atrium; LV = left ventricle.

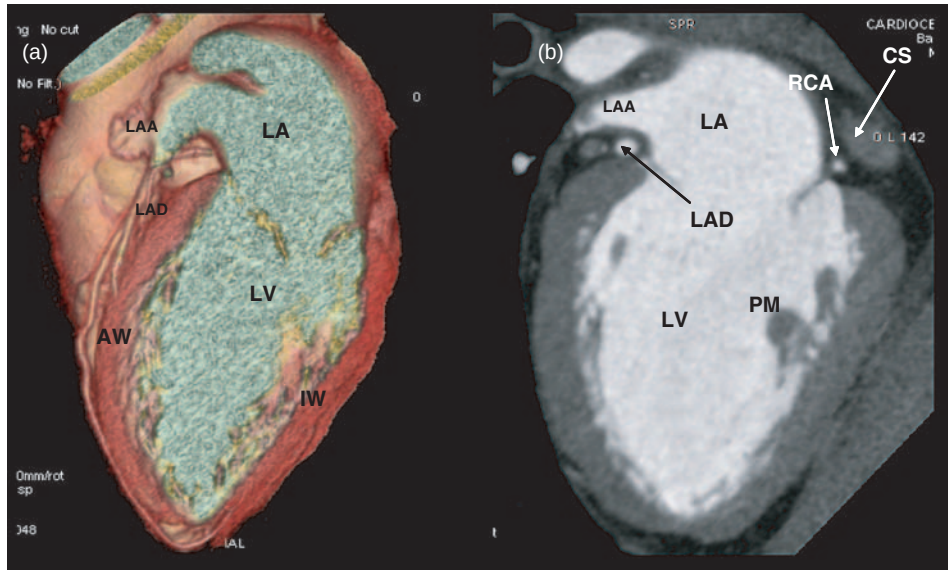

Figure 3.7 Two-chamber view. (a) 3D volume rendering reconstruction and (b) the corresponding plane (see text). LAA = left atrial appendage; LV = left ventricle; AW = anterior wall; IW = inferior wall; LAD = left anterior descending artery; RCA = right coronary artery; CS = coronary sinus; PM = papillary muscle.

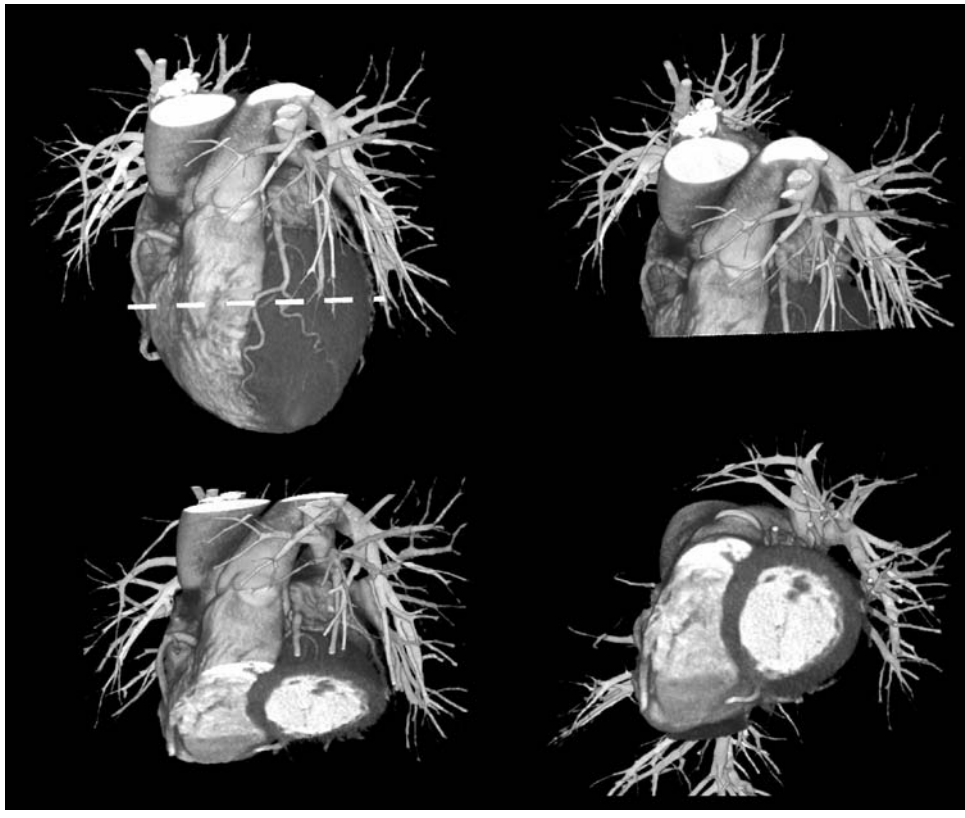

Figure 3.8 3D volume rendering. The heart is cut to show the short-axis view through the mid-ventricle. RV = right ventricle; LV = left ventricle.

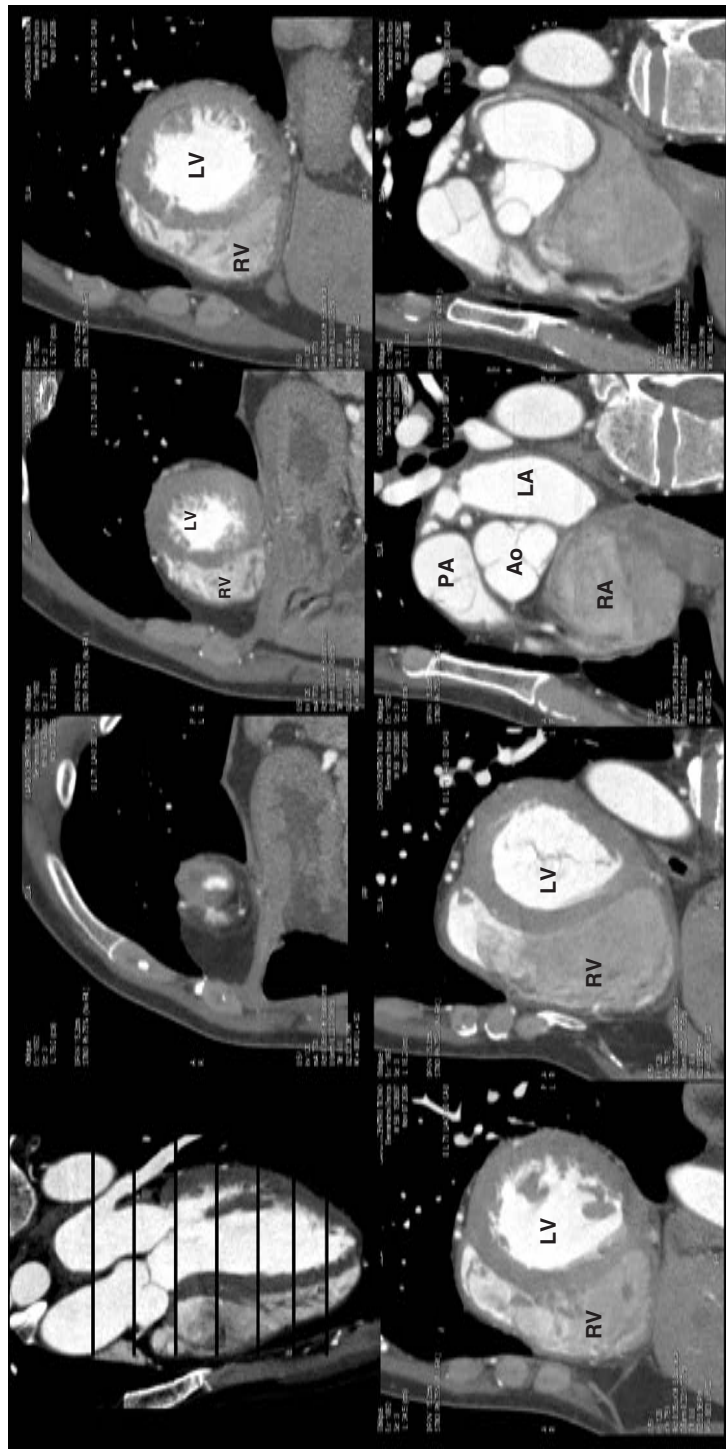

Figure 3.9 A collection of short-axis views from the apex to the base. RV = right ventricle; LV = left ventricle; RA = right atrium; LA = left atrium; Ao = aorta; PA = pulmonary artery.

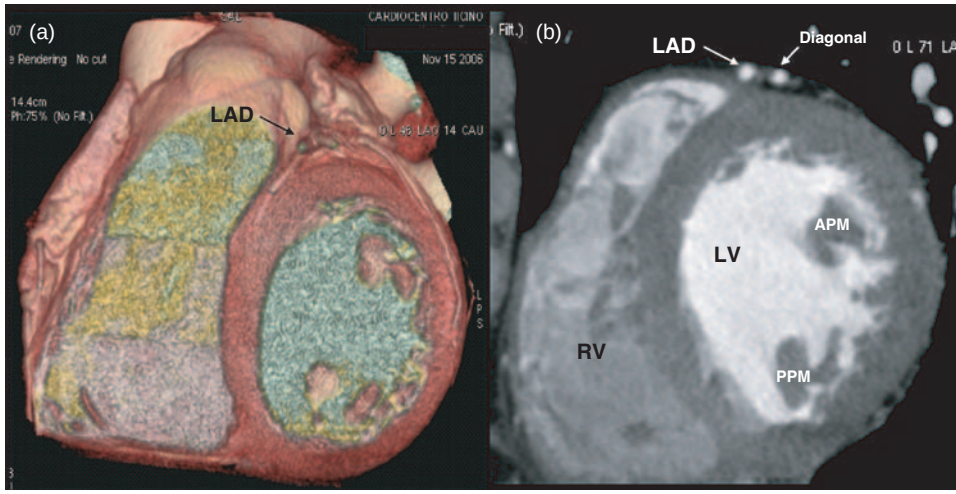

Figure 3.10 Short-axis view at the level of papillary muscles. 3D volume rendering reconstruction (a) and the corresponding oblique plane (b). Antero-lateral (APM) and postero-medial (PPM) papillary muscles can be imaged. Moreover, the left anterior descending coronary artery (LAD) and a diagonal branch are visualized in cross-section (arrows). RV = right ventricle; LV = left ventricle.

Suggested reading

American Heart Association, American College of Cardiology, and Society of Nuclear Medicine. Standardization of cardiac tomographic imaging. *Circulation* 1992;86:338–339.

Edwards WD, Tajik AJ, Seward JB. Standardized nomenclature and anatomic basis for regional tomographic analysis of the heart. *Mayo Clin Proc* 1981;56:479–497.

Waller BF, Taliercio CP, Slack JD *et al.* Tomographic views of normal and abnormal hearts: the anatomic basis for various cardiac imaging techniques, Part I. *Clin Cardiol* 1990;13:804–812.

Waller BF, Taliercio CP, Slack JD *et al.* Tomographic views of normal and abnormal hearts: the anatomic basis for various cardiac imaging techniques, Part II. *Clin Cardiol* 1990;13:877–884.

4 CHAPTER 4
The Right Heart

Although termed "right heart," this half of the heart is not located entirely in the right chest nor is it strictly to the right of the "left heart" (see Chapter 2). The "electronic" cast of the right heart,viewed from an anterior perspective, is displayed in Fig. 4.1. It shows the characteristic normal U-shape arrangement with the superior caval vein (superior vena cava) and right atrium forming one limb, the right ventricle forming the bend with its outflow tract (the infundibulum) and the pulmonary trunk forming the other limb. With this arrangement, the two valves in the right heart do not abut each other. Instead, a fold of muscle, the ventriculo-infundibular fold, interposes between the tricuspid and pulmonary valves (Figs. 4.1 and 4.2).

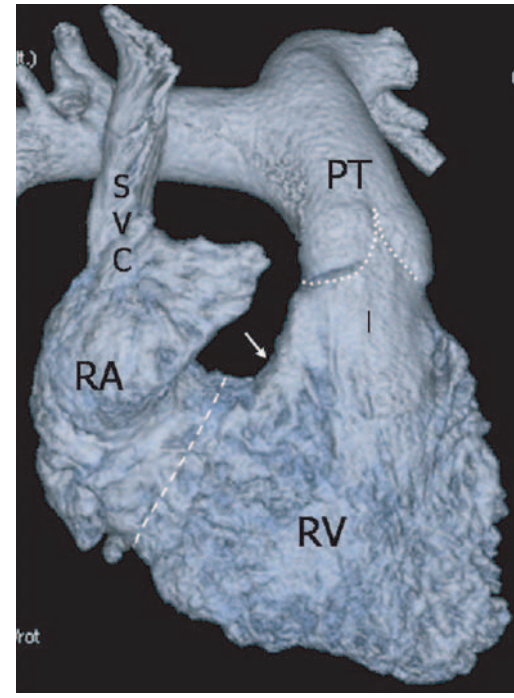

Figure 4.1 The "electronic" cast of the right heart. Anterior perspective. Superior vena cava (SVC), right atrium (RA), right ventricle (RV), infundibulum (I) and pulmonary trunk (PT) form a U-shaped structure. The ventriculo-infundibular fold (arrow) separates the right heart valves (broken lines).

Right atrium

The right atrium comprises a venous component, an appendage, and a vestibular portion that leads to the orifice of the tricuspid valve. The venous component receives the superior (SVC) and inferior caval veins. It forms the posterior wall of the right atrium (Fig. 4.3). The junction between the appendage and the venous component is marked on the epicardial aspect by the sulcus terminalis (terminal groove) (Fig. 4.4), which is usually filled with fatty tissue. The sulcus corresponds to a muscular crest named the crista terminalis (terminal crest) on the endocardial surface. This is a prominent muscular band that separates the smooth wall of the venous component from the rough wall of the atrial appendage (Fig. 4.5). The crista terminalis is a roughly C-shaped band that originates from the antero-medial wall of the right atrium, passes along the anterior border of the superior cavo-atrial junction, sweeps laterally and descends toward the entrance of the inferior caval vein

Anatomy of the Heart by Multislice Computed Tomography
F. F. Faletra, N. G. Pandian and Siew Yen Ho. © 2008
Francesco Fulvio Faletra, Natesa G. Pandian and Siew Yen Ho.
ISBN: 978-1-4051-8055-9.

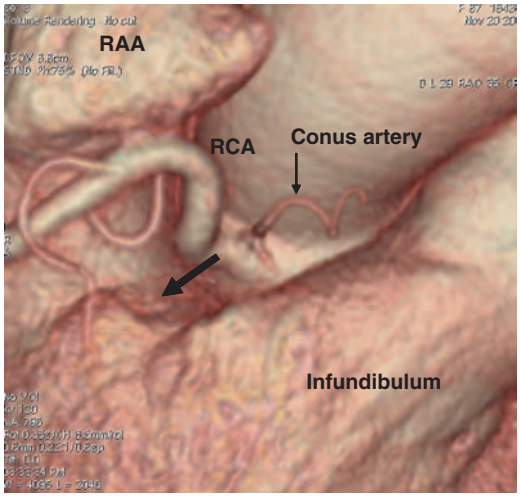

Figure 4.2 3D volume rendering showing the ventriculo-infundibular fold (arrow). View from above and right. Note the conus artery originating independently from the aorta. RAA = right atrial appendage; RCA = right coronary artery.

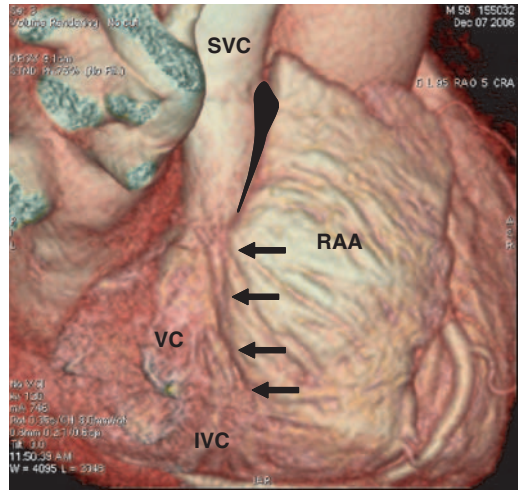

Figure 4.4 3D volume rendering. Postero-lateral view of the right atrium showing the superior (SVC) and inferior (IVC) venae cavae, the venous component (VC) and the right atrial appendage (RAA). Arrows point to the sulcus terminalis. The black-filled shape represents the location of the sinus node.

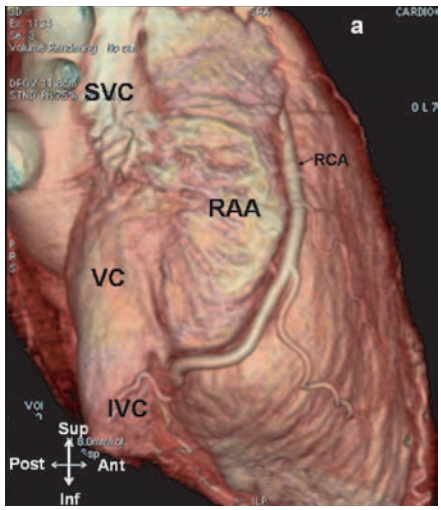

Figure 4.3 3D volume rendering. Postero-lateral view of the right atrium showing the superior (SVC) and inferior (IVC) venae cavae, the venous component (VC) and the right atrial appendage (RAA). RCA = right coronary artery.

(Fig. 4.6). It is of variable thickness and breadth. When cut in cross-section, the muscular band appears like a bump protruding into the atrial cavity (Fig. 4.5c,d). The cephalad portion of the sinus node, the cardiac pacemaker, is located in the antero-superior part of the crista terminalis whereas its tail portion descends within the musculature of the band (Fig. 4.4). In the right anterior oblique view (RAO), the crista terminalis marks the right atrial border (Fig. 4.7). The appendage of the right atrium is triangular and has a broad junction with the atrial chamber. Antero-medially, the appendage protrudes from the right atrium and overlaps the aortic root (Fig. 4.8). On the endocardial aspect, the wall of the appendage is lined with pectinate muscles. These bundles emerge in branching fashion from the crista terminalis, terminating at the vestibule. Because the right atrial appendage is a large part of the atrium, the pectinate muscles are distributed extensively (Figs. 4.9 and 4.10).

The vestibule is the portion of the atrium lying immediately proximal to the orifice of the tricuspid valve. Characteristically it is smooth walled. Its distal margin is marked circumferentially by the hingeline (annulus) of the valvar leaflets (Fig. 4.11).

The segment of the vestibule that is located inferiorly on RAO view (see Fig. 4.7) is part of the cavo-tricuspid isthmus (Fig. 4.12). The inferior isthmus is recognized by electrophysiologists as the region

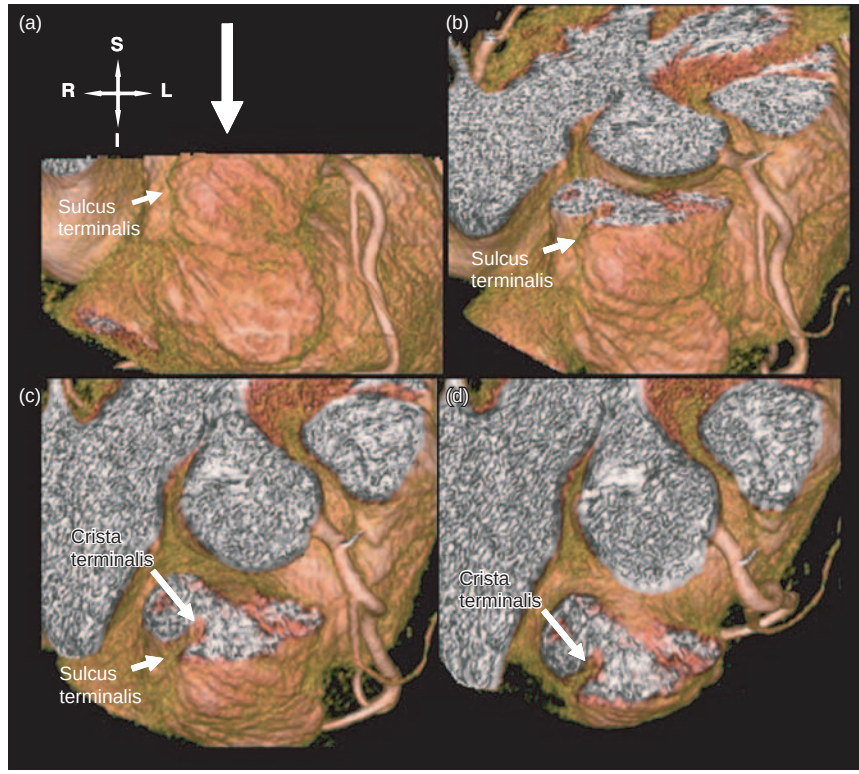

Figure 4.5 (a–d) 3D volume rendering. The data set has been properly cropped and rotated to show the sulcus and the crista terminalis (arrows; see Video clip 4, Right atrium).

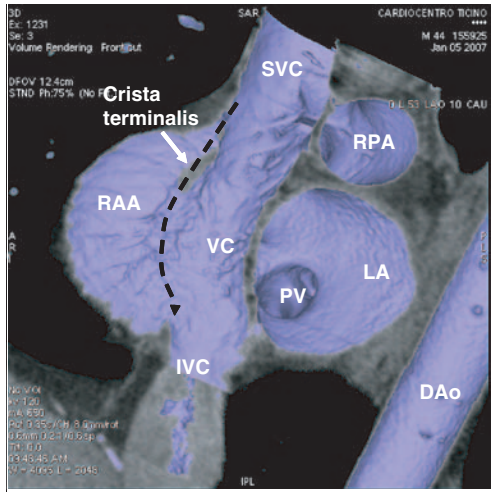

Figure 4.6 3D endocardial perspective showing the C-shaped crista terminalis (dotted line). SVC = superior vena cava; IVC = inferior vena cava; RAA = right atrial appendage; LA = left atrium; PV = pulmonary vein; RPA = right pulmonary artery; DAo = descending aorta; VC = venous component.

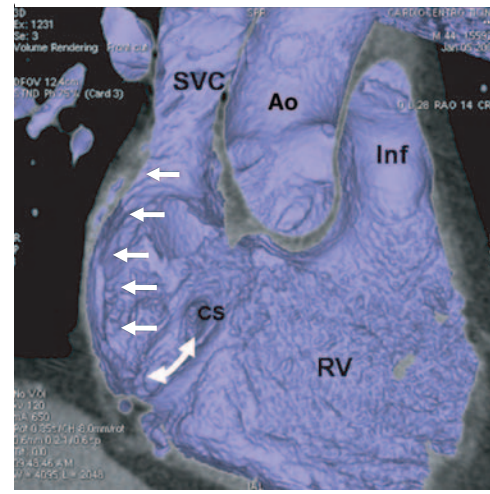

Figure 4.7 3D endocardial surface modality. Right anterior oblique view. The crista terminalis marks the right border of the atrium. The double white arrow marks the region of the inferior isthmus. SVC = superior vena cava; Ao = aorta; RV = right ventricle; Inf = infundibulum; CS = coronary sinus.

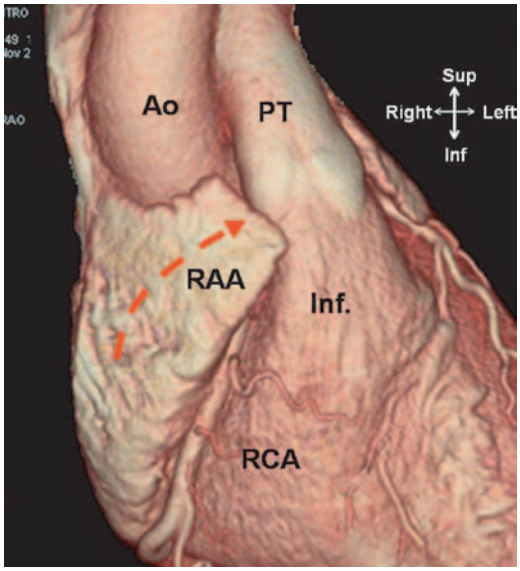

Figure 4.8 The right atrial appendage (RAA) overlaps (red dotted line) the aortic root (Ao) when the heart is viewed from the front. RCA = right coronary artery; Inf = infundibulum; PT = pulmonary trunk.

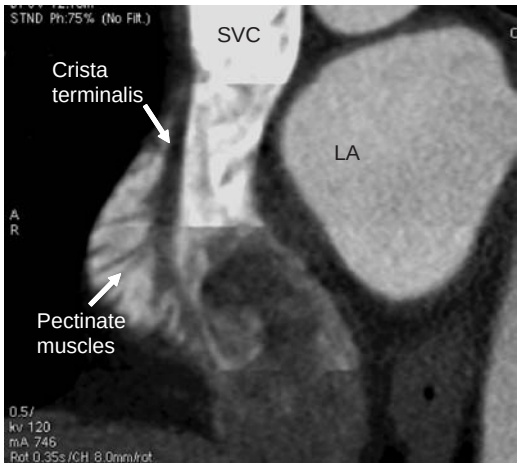

Figure 4.9 A slice image showing pectinate muscles. These muscles originate as branching fibers that emerge at right angles from the terminal crest. SVC = superior vena cava; LA = left atrium.

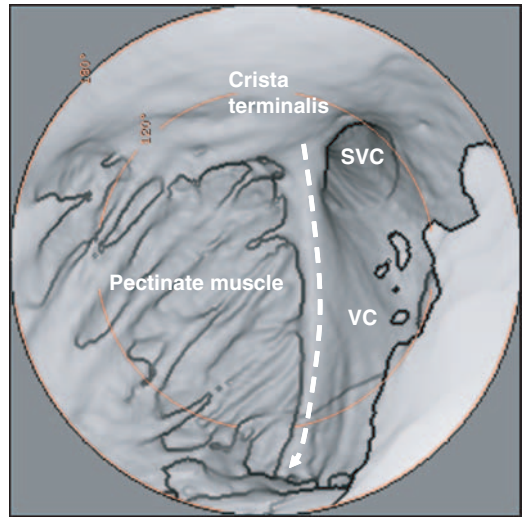

Figure 4.10 Virtual endoscopy. The crista terminalis (dotted line) and the pectinate muscles are clearly visible. SVC = superior vena cava; VC = venous component.

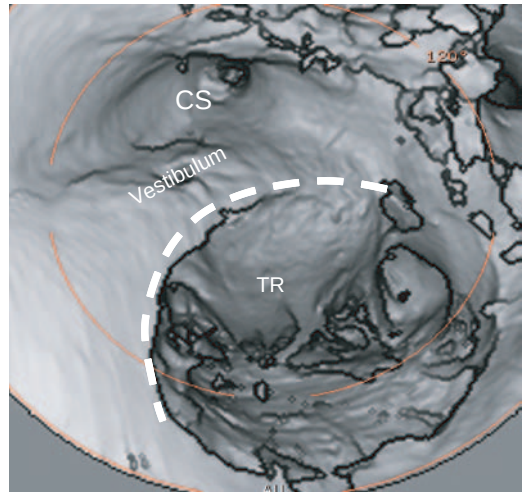

Figure 4.11 Virtual endoscopy showing the vestibule between the ostium of coronary sinus (CS) and the tricuspid annulus (dotted line).

that is ablated to interrupt the circuit of common atrial flutter.

Superiorly, on the septal aspect lies the triangle of Koch with the atrioventricular node toward its apex (Fig. 4.13a,b). A thin fibrous cord known as the tendon of Todaro runs within the musculature of the sinus septum, from the insertion of the eustachian valve, to reach the central fibrous body. The course of the tendon marks the posterior border of the nodal triangle, which is the anatomic landmark for the location of the atrioventricular node of the cardiac conduction system. The anterior border is marked by the hingeline of the septal

leaflet whereas the inferior border is the orifice of the coronary sinus together with the vestibule (Fig. 4.13b).

Right ventricle

The right ventricle is the most anteriorly situated cardiac chamber, lying directly behind the sternum.

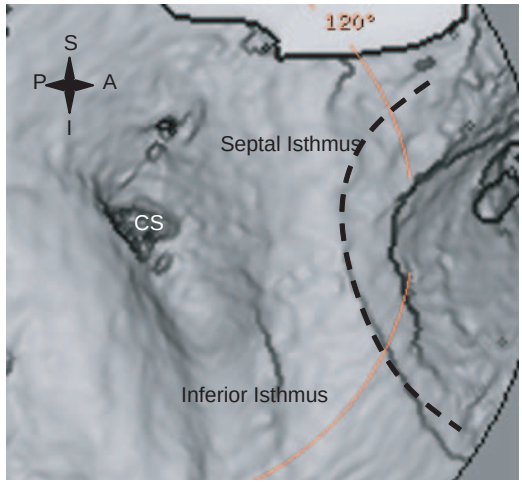

Figure 4.12 Virtual endoscopy showing the ostium of coronary sinus (CS), the annulus of the tricuspid valve (dotted line) and the septal isthmus and inferior isthmus.

The right ventricle's cavity is therefore anterior, overlapping much of the left ventricle (Fig. 4.14). Most of the inferior border of the frontal roentgenogram view of the heart consists of the right ventricle. The right ventricle can be identified externally by its pyramidal shape (Fig. 4.15). When seen from the cardiac apex, the right edge of the right ventricle is a sharp angle, forming the acute margin of the heart (Fig. 4.16). The right ventricle sweeps antero-cephalad to "wrap around" the left ventricle (Fig. 4.17). Viewed from the diaphragmatic aspect of the heart, the right and left ventricles can be seen to lie side by side. The term "crux" of the heart (crux cordis) refers to the intersection between the planes of the atrial and ventricular septa upon the inferior atrioventricular junction. Because the left atrioventricular junction is at not at the same level as the right atrioventricular junction, the crux is not a perfect cross (Fig. 4.18). In the normal heart the wall of the right ventricle is considerably thinner than that of the left ventricle. It ranges in thickness from 3 to 7 mm. At the tip of the apex, however, the wall is particularly thin (Fig. 4.19). The internal appearance of the right ventricle is typical. The shape of the cavity can be imaged as an open "V" with a wide muscular separation between tricuspid and pulmonary valves.

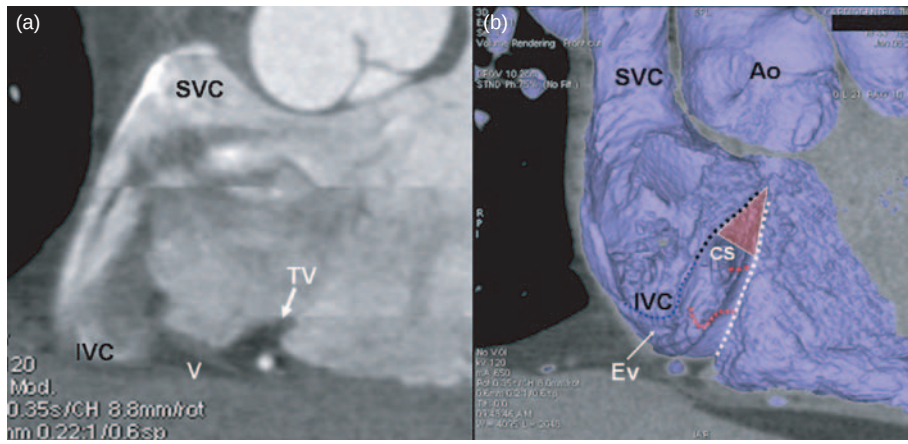

Figure 4.13 (a) Slice image in a simulated right anterior oblique view through the cavo-tricuspid isthmus. Its anterior portion is the smooth vestibular wall (v). (b) The 3D endocardial surface modality shows the eustachian valve (Ev) and coronary sinus (CS). The red triangle marks the location of Koch's triangle. The long red dotted line indicates the inferior isthmus whereas the short red line marks the "septal" isthmus. The white dotted line represents the hingeline of the septal leaflet of the tricuspid valve, and the black dotted line represents the tendon of Todaro, which adjoins the free margin of the eustachian valve (blue dotted line).

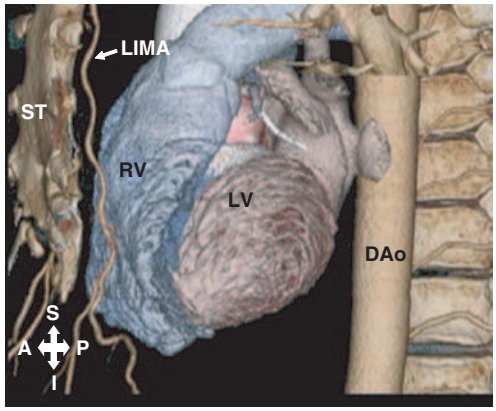

Figure 4.14 Electronic cast. The right ventricle overlaps most of the left ventricle. ST = sternum; RV = right ventricle; LV = left ventricle; LIMA = left internal mammary artery; DAo = descending aorta.

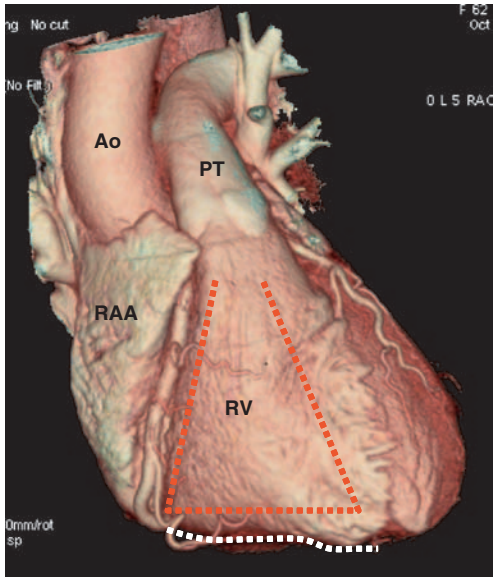

Figure 4.15 3D volume rendering showing the right ventricle. Almost all the inferior border of the frontal view of the heart consists of the right ventricle (dotted white line). The red triangle (dotted red line) illustrates the shape of the right ventricle when viewed from the front. Ao = aorta; PT = pulmonary trunk; RAA = right atrial appendage; RV = right ventricle.

The right ventricle can be divided into three components: the inlet, apical and outlet components (Fig. 4.20).

The most constant characteristic feature of the right ventricle is the presence of coarse apical

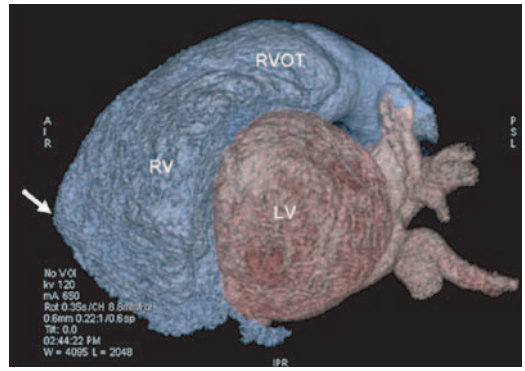

Figure 4.16 Electronic cast viewed from the apex. The arrow marks the acute margin. RV = right ventricle; LV = left ventricle; RVOT = right ventricle outflow tract.

trabeculations, in contrast to the fine trabeculations found in the left ventricle. In addition, the right ventricle is characterized by the presence of other structures such as (a) the crista supraventricularis (or supraventricular crest), (b) the moderator band and (c) the trabecula septomarginalis (or septomarginal trabeculation) (Fig. 4.21). The crista supraventricularis is the prominent muscular structure that separates tricuspid from pulmonary valves. It comprises the ventriculoinfundibular fold (Fig. 4.21) and its septal insertion into the trabecula septomarginalis. The trabecula septomarginalis is a Y-shaped muscle band that appears like a column supporting the ventriculoinfundibular fold in between its arms (Fig. 4.22). The posterior arm points toward the tricuspid valve and the membranous septum. Deeper cuts into the crista supraventricularis reveal the aortic root and a thin part of the ventricular septum, the membranous septum (Fig. 4.23a,b). Usually, but not always, the body of the Y is adherent to the septum, and in sectional imaging it can appear as a bump on the septum (Fig. 4.24). When abnormally formed or hypertrophied, it can divide the ventricular cavity into two chambers.

The body of the "septomarginal trabeculation" ends near the apex, splitting into several smaller muscle bundles. One of these usually takes a characteristic course crossing the right ventricular cavity. This branch has been named the moderator band because it was thought, wrongly, to limit the diastolic expansion of the chamber (Figs. 4.25 and

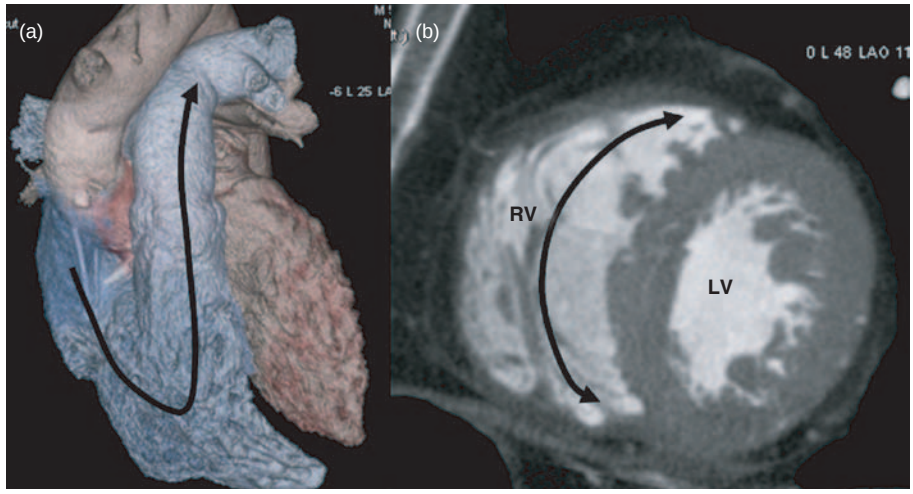

Figure 4.17 (a) The black line in the electronic cast traces the inflow and outflow tracts through the right ventricle. (b) In short-axis view the right ventricle is crescent shaped, curving around the left ventricle. RV = right ventricle; LV = left ventricle.

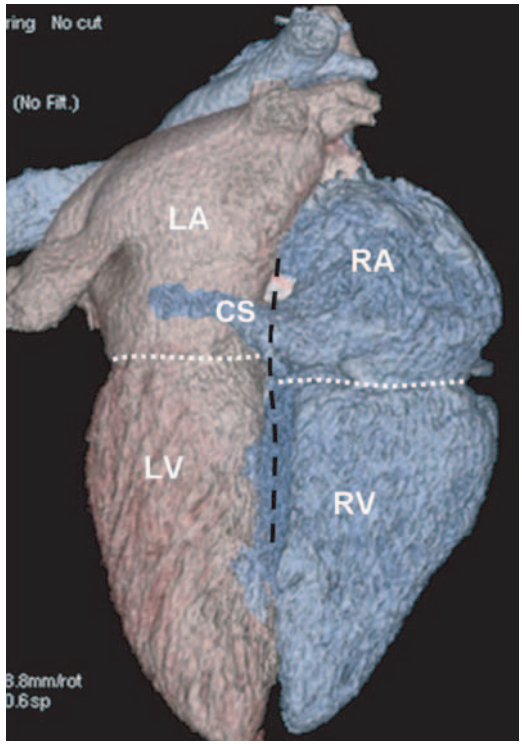

Figure 4.18 Electronic cast of both ventricles. This view from the diaphragmatic aspect shows the course of the coronary sinus (CS) and the cardiac crux, which is the intersection between the plane of the cardiac septa (black broken line) and the inferior atrioventricular junction (white broken lines). RV = right ventricle; LV = left ventricle; RA = right atrium; LA = left atrium.

4.26). The moderator band runs toward the anterior wall, and joins the base of anterior papillary muscle (Fig. 4.27a,b).

The outlet portion of the right ventricle consists of the infundibulum, a circumferential muscular structure that supports the leaflets of the pulmonary valve. Because of the semilunar shape of the pulmonary leaflets, this valve does not have an annulus in the traditional sense of a ring-like attachment. The leaflets have semilunar attachments that cross the musculoarterial junction in a corresponding semilunar fashion (Fig. 4.28a). The outlet component, or infundibulum, is a free-standing and completely muscular structure. The pulmonary valve leaflets are supported entirely by this free-standing musculature. There is an extensive external tissue plane between the walls of the aorta and the pulmonary infundibulum. The leaflets of the pulmonary and aortic valves have markedly different levels of attachments within their respective ventricles. These features allow the pulmonary valve, including its basal attachments within the infundibulum, to be harvested during the Ross procedure without creating a ventricular septal defect (Fig. 4.28b). Another important spatial relationship to note is that the posterior (paraseptal) wall of the infundibulum is in close proximity to the main branches of the coronary arteries (Fig. 4.28).

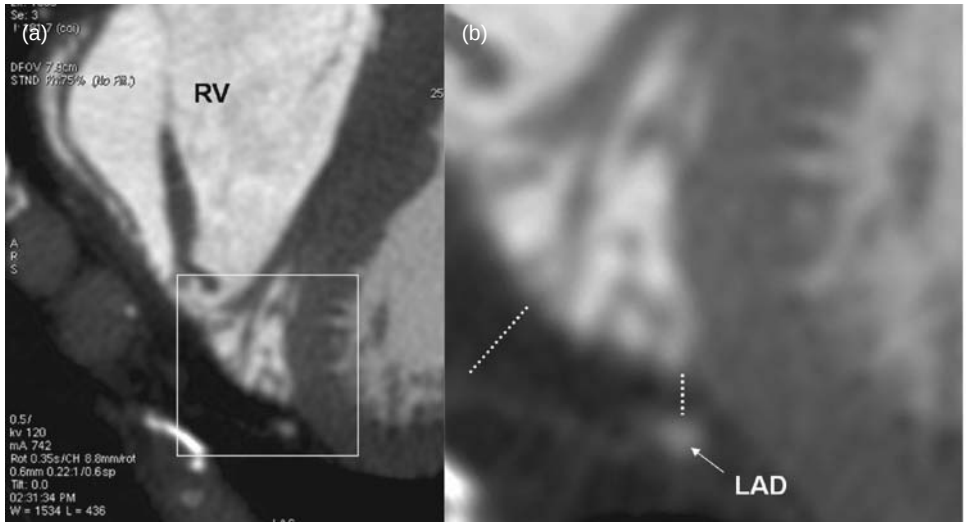

Figure 4.19 The remarkably thin wall of the right ventricle (RV) at its apex (dotted lines) in comparison with the wall nearby. Note the course of the left descending coronary artery (LAD) in cross-section. Figure (b) is the magnified image of figure (a) which is shown as an inset.

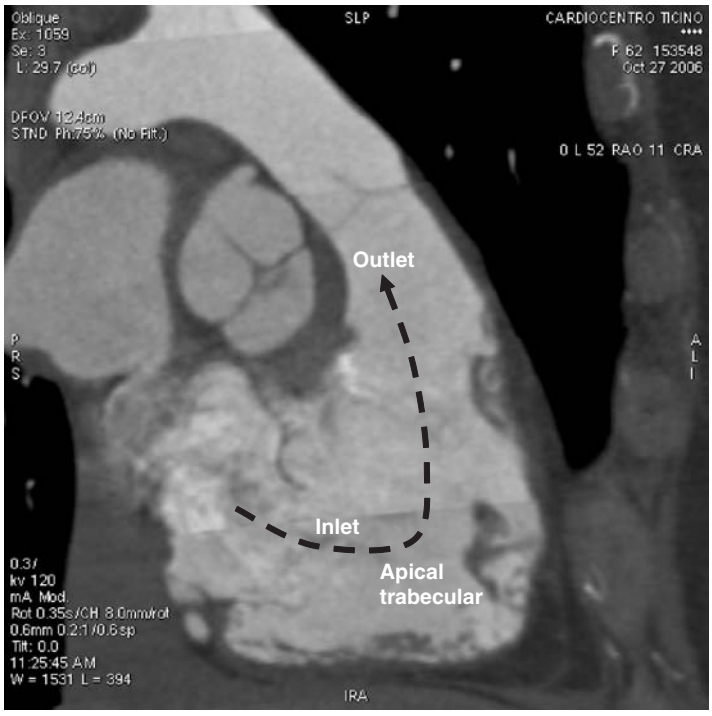

Figure 4.20 A slice image showing the three components of the right ventricle: the inlet, the apical trabecular and the outlet. The dotted line marks the V-shaped cavity. Note the aortic valve imaged in cross-section in the middle.

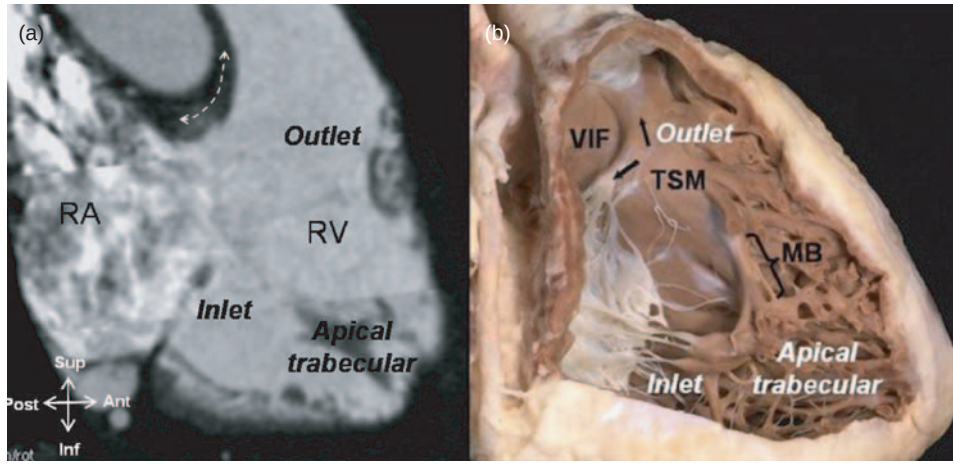

Figure 4.21 (a) A slice image and (b) a specimen showing the inlet, apical trabecular and outlet components of the right ventricle. The ventriculo-infundibular fold (white double-headed arrow; VIF) separates the tricuspid valve from the pulmonary valve. It inserts between the arms (black arrows) of the trabecula septomarginalis (TSM). The moderator band (MB) arises from the TSM and crosses the ventricular chamber as a well-defined muscular bundle to insert into the antero-lateral ventricular wall. The anterior papillary muscle of the tricuspid valve is usually attached to it.

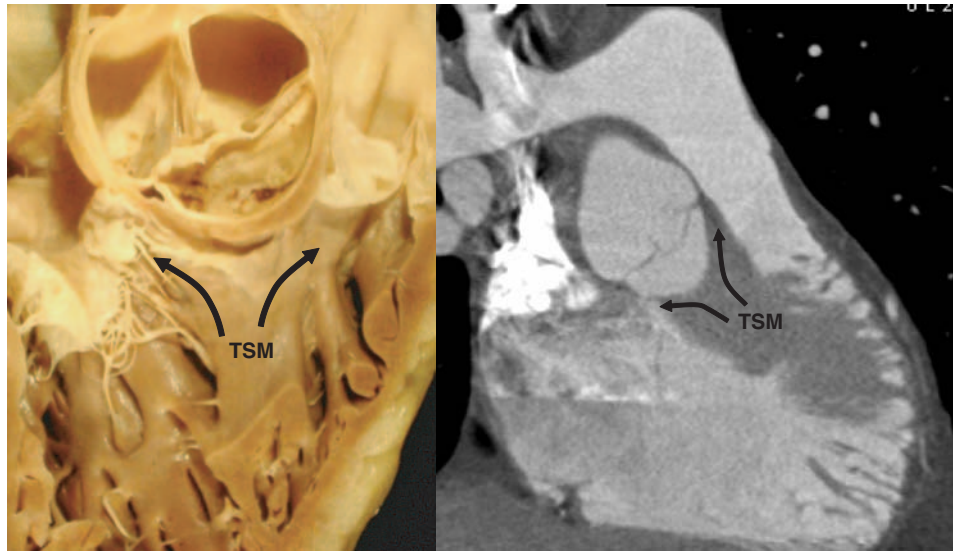

Figure 4.22 Anatomic specimen and a slice image showing the trabecula septomarginalis (TSM) and its arms (arrows).

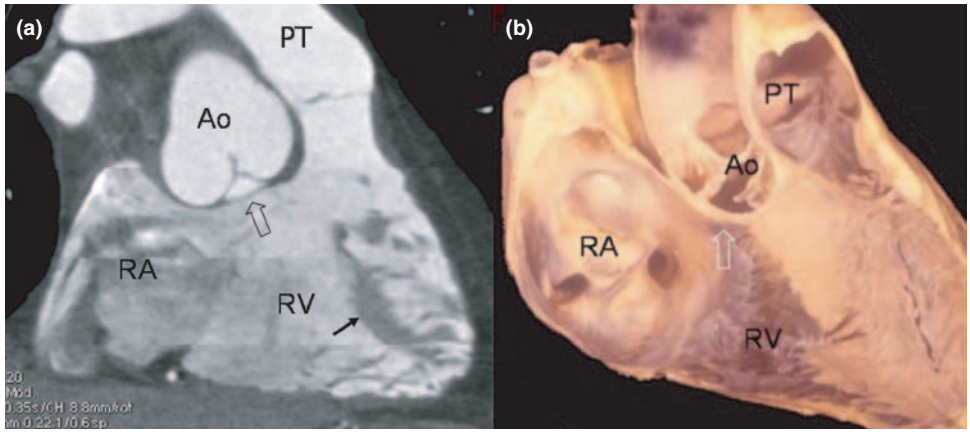

Figure 4.23 (a) This slice cuts into the body of the trabecula septomarginalis (black arrow), the aortic root and the region of thin ventricular septum (open arrow). (b) The heart specimen is displayed in similar orientation but the cut is deeper into the muscular septum and through the thin part of the septum adjacent to the membranous septum (open arrow). Ao = aorta; PT = pulmonary trunk; RA = right atrium; RV = right ventricle.

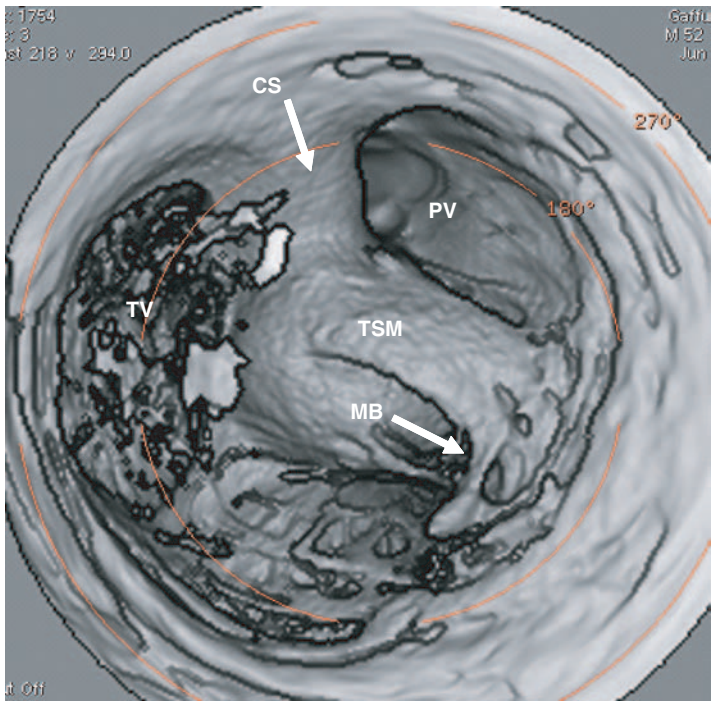

Figure 4.24 3D virtual endoscopy. View from the apex. The crista supraventricularis (CS), the trabecula septomarginalis (TSM) and the moderator band (MB) can be recognized. TV = tricuspid valve; PV = pulmonary valve.

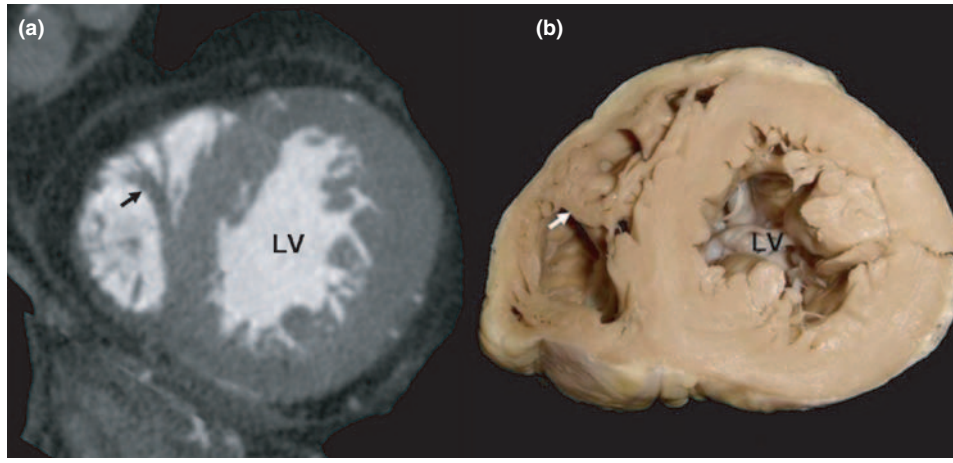

Figure 4.25 Short-axis view (a) and anatomic specimen (b) showing the moderator band (arrow) spanning the septum and the antero-lateral wall of the right ventricle. LV = left ventricle.

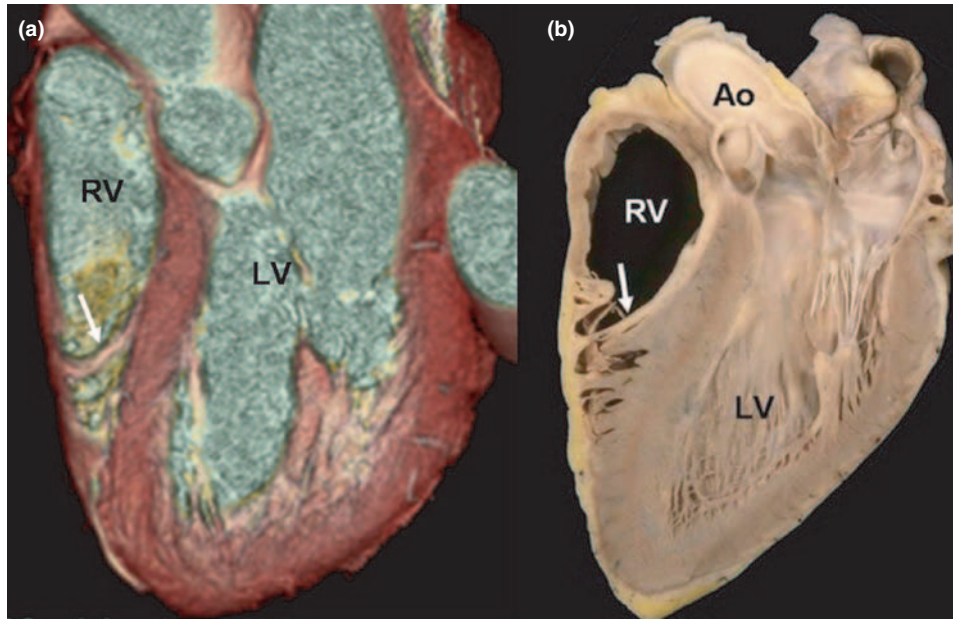

Figure 4.26 (a,b) 3D volume rendering long-axis view and comparable cut of specimen showing the moderator band (arrow). Ao = aorta; LV = left ventricle; RV = right ventricle.

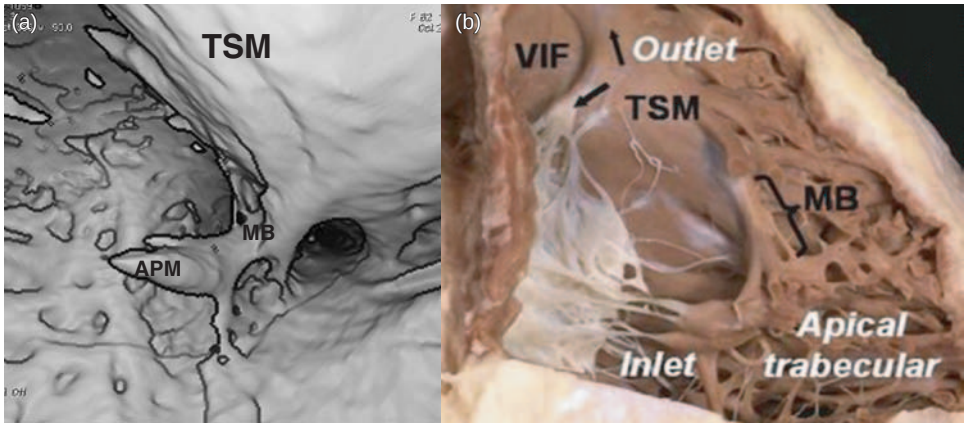

Figure 4.27 (a,b) 3D Virtual endoscopy and anatomic specimen showing the anatomic continuity between the trabecula septomarginalis (TSM), the moderator band (MB) and the anterior papillary muscle (APM). VIF = ventriculo-infundibular fold.

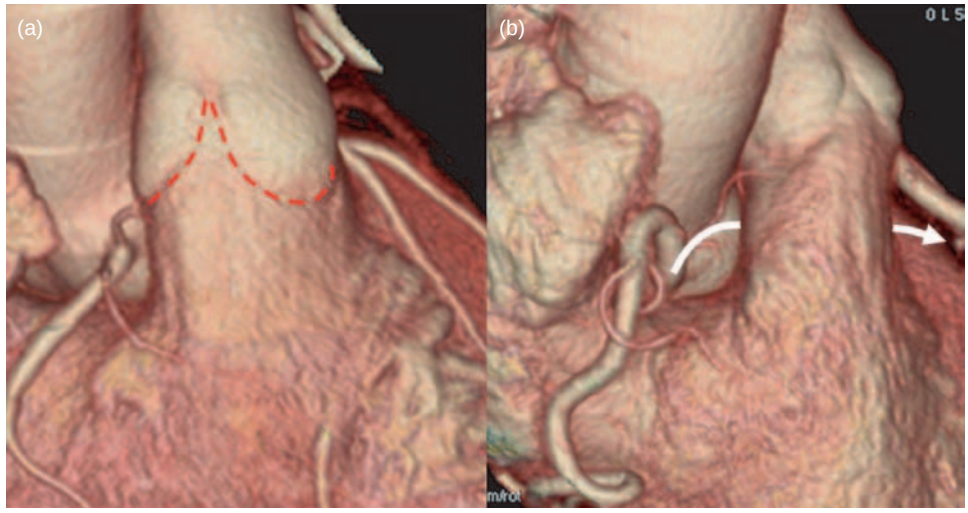

Figure 4.28 (a) 3D volume rendering of the subpulmonary infundibulum and the pulmonary root. The infundibulum elevates the pulmonary valve above the ventricular mass. The crown-shaped hingelines of pulmonary leaflets are indicated by the dotted red lines. (b) The curved white arrow passes through the extracardiac tissue plane between the infundibulum and the aorta. This feature makes it possible to detach the pulmonary valve for use in the surgical Ross procedure without creating a ventricular septal defect.

Suggested reading

Cabrera JA, Sanchez-Quintana D, Farre J, Rubio JA, Ho SY. The inferior right atrial isthmus: further architectural insights for current and coming ablation technologies. *J Cardiovasc Electrophysiol* 2005;16:402–408.

Foale R, Nihoyannopoulos P, McKenna W *et al.* Echocardiographic measurement of the normal adult right ventricle. *Br Heart J* 1986;56:33–44.

Ho SY, Anderson RH, Sanchez-Quintana D. Atrial structure and fibres: morphological basis of atrial conduction. *Cardiovasc Res* 2002;54:325–336.

Ho SY, Nihoyannopoulos P. Anatomy, echocardiography, and normal right ventricular dimensions. *Heart* 2006; 92:2–13.

5 CHAPTER 5
The Left Heart

Pulmonary veins

Anatomic details of the pulmonary veins, especially at the venous insertions into the left atrium, have become clinically important owing to the use of catheter ablation in treating patients with atrial fibrillation. The pulmonary veins are considered to have an important role in initiating and maintaining atrial fibrillation. Current commonly used ablation strategies aim to isolate the veins from the left atrium.

The pulmonary veins originate from a capillary network on the walls of the air sacs, where they are continuous with the capillary ramifications of the pulmonary artery. Joining together, they form one vessel for each lung lobule. These vessels merge together into a single vein for each lobe – three for the right lung and two for the left lung. The vein from the middle lobe of the right lung usually unites with that from the upper lobe. The most common pattern is to have two veins from the hilum of each lung. They open separately into the posterior part of the left atrium (Fig. 5.1).

The pulmonary vein ostia are the atriopulmonary venous junctions. However, it is often not possible to identify the precise location of the junctions especially when the veins are funnel-shaped and have a gradual "entrance" to the atrium. Multislice computed tomography can provide clearer anatomic delineation thereby reducing the risk of ablating within the vein and causing venous stenosis. Ablating within the right superior pulmonary vein also increases the risk of injuring the right phrenic nerve. There are many variants from the usual pattern of four pulmonary veins. For example, the right hilum may have three veins when the upper and middle lobes drain independently. Not infrequently, the veins on the left or the right, or both sides, join together into a common vein (or veins) before entering the left atrium. The common segment is often very short and described as the antrum. On gross examination, it is not clear where the atriopulmonary venous junction lies precisely in these hearts. The venous ostia are ellipsoidal rather than round, with greater superior–inferior dimensions than antero-posterior dimensions (Fig. 5.2).

The distal or central pulmonary veins are the portions of the pulmonary veins in proximity to the left atrium. Electrophysiologists name the pulmonary vein segments between branch

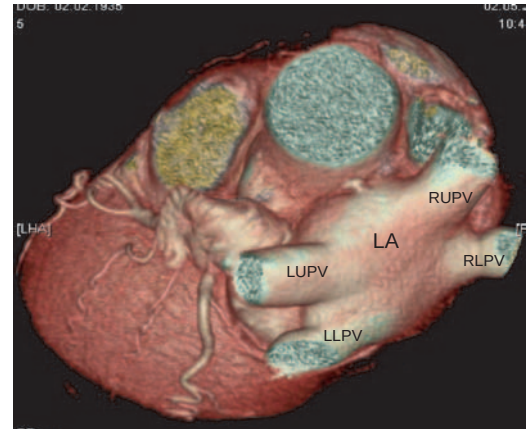

Figure 5.1 3D volume rendering. External view of the four pulmonary veins and their atriopulmonary junctions. LUPV = left upper pulmonary vein; LLPV = left lower pulmonary vein; RUPV = right upper pulmonary vein; RLPV = right lower pulmonary vein.

Anatomy of the Heart by Multislice Computed Tomography
F. F. Faletra, N. G. Pandian and Siew Yen Ho. © 2008
Francesco Fulvio Faletra, Natesa G. Pandian and Siew Yen Ho.
ISBN: 978-1-4051-8055-9.

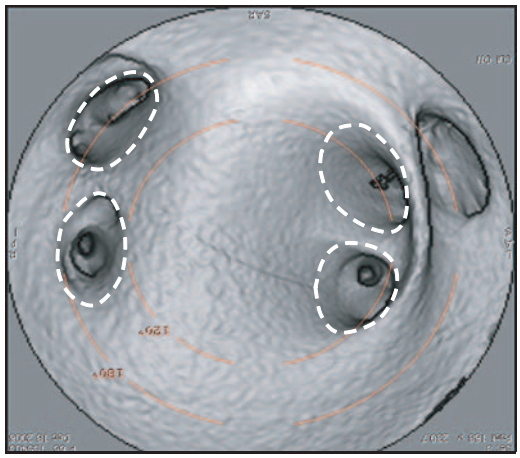

Figure 5.2 Virtual endoscopy. The ostia of pulmonary veins are ellipsoidal with longer superior–inferior dimensions than antero-posterior dimensions.

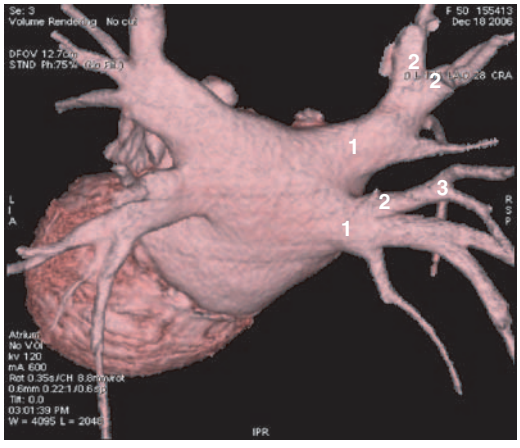

Figure 5.3 Electronic cast. Segments of the distal pulmonary veins from V1 through V3. The V1 segment is the most important segment to include on epicardial views.

points retrogradely from the atriopulmonary venous junctions. For example, the V1 segment extends retrograde from the ostium to the "first" branch point, which anatomically is the last junction or confluence of branches (Fig. 5.3).

The intervenous "saddle" is the region of atrial wall lying between separate ipsilateral pulmonary veins. The pulmonary vein inflow vestibule includes the ipsilateral pulmonary vein ostia and the intervenous saddle atrial wall. The posterior left

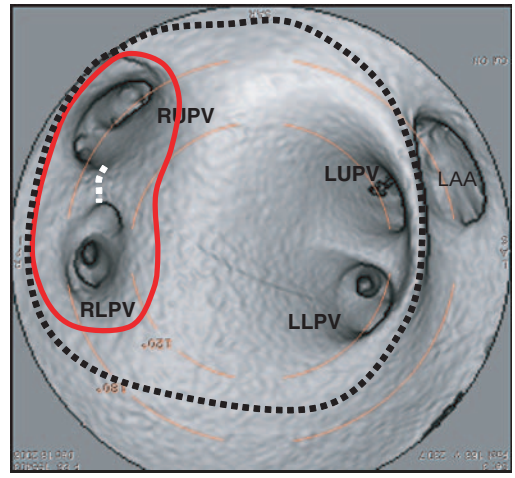

Figure 5.4 Virtual endoscopy. A view from inside looking at the roof of the left atrium. The right intervenous saddle is marked by a white dotted line. The right pulmonary vein inflow vestibule is circled by the solid red line. The black dotted line encircles the whole posterior left atrium. RUPV = right upper pulmonary vein; RLPV = right lower pulmonary vein; LUPV = left upper pulmonary vein; LLPV = left lower pulmonary vein; LAA = left atrial appendage.

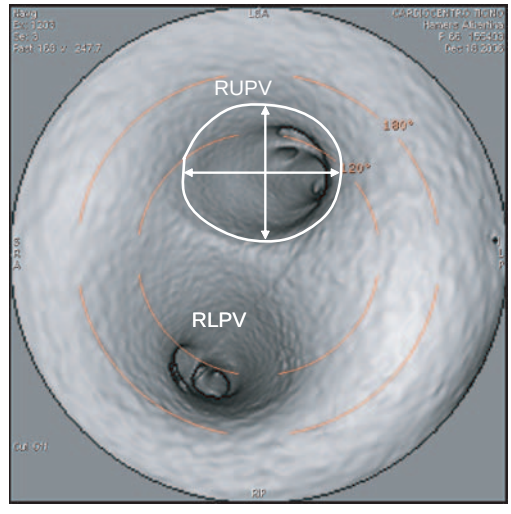

Figure 5.5 Navigator modality. Normal lower and upper veins with the ostial diameters and circumferences measured.

atrium includes the bilateral pulmonary vein inflow vestibules and the interposed posterior atrial wall (Figs. 5.4 and 5.5).

On the endocardial aspect, the left atrial wall has a smooth ridge between the entrance of the left

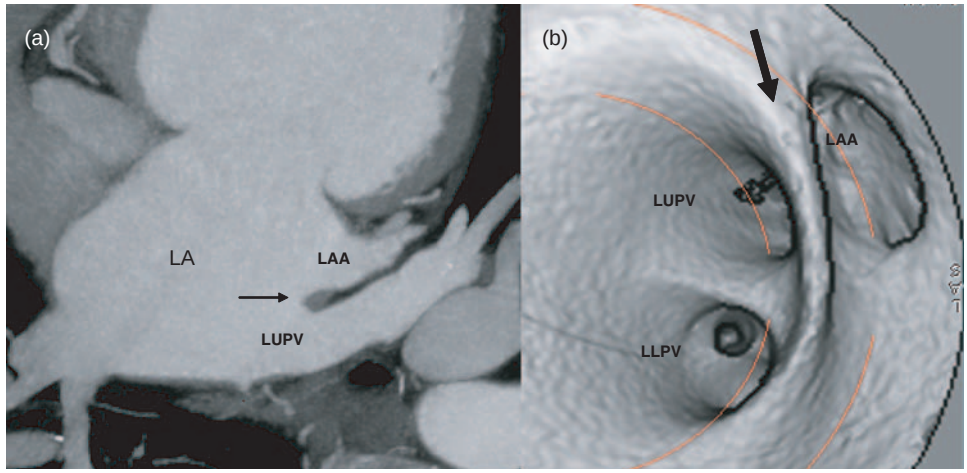

Figure 5.6 (a) Maximum intensity projection (MIP) oblique projection and navigator modality showing a ridge (arrow) projecting into the left atrium (LA). This ridge is caused by an infolding of the wall of the left atrium between the left atrial appendage (LAA) anteriorly and the left upper pulmonary vein (LUPV) posteriorly. (b) A bulbous tip (pointed by arrow) may be misdiagnosed as a mass. LLPV = left lower pulmonary vein.

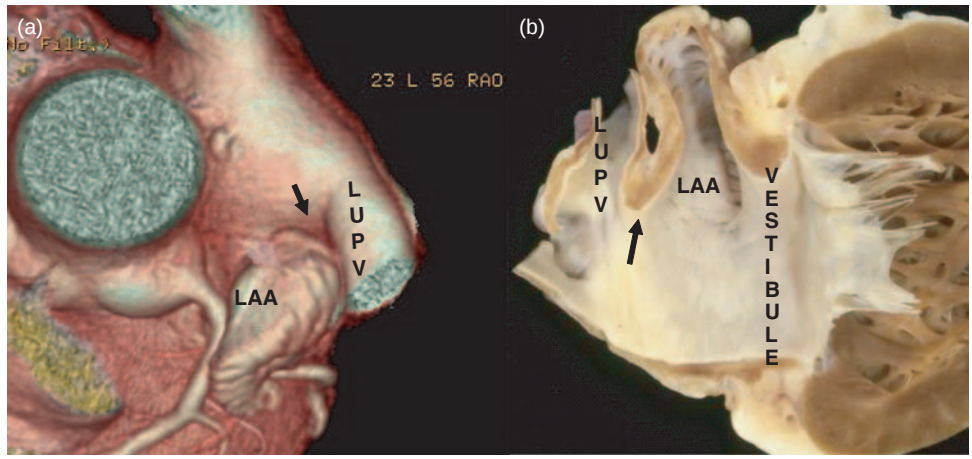

Figure 5.7 (a) 3D volume rendering showing the infolding of the wall of the left atrium (arrow) between the left atrial appendage (LAA) anteriorly and the left upper pulmonary vein (LUPV) posteriorly. (b) The left side of the heart cut longitudinally to show the infolding (arrow) that appears like a ridge on the endocardial surface. The LAA is trabeculated on the endocardial surface whereas the rest of the atrial wall is smooth.

atrial appendage and the ostium of the left superior pulmonary vein. This ridge may have a bulbous tip and can be mistaken for a pedunculated mass or thrombus arising from the lateral wall of the left atrium (Fig. 5.6).

Anatomically, this ridge is an infolding of the wall of the left atrium. Its prominence and width vary considerably (Fig. 5.7) with implications for isolating the atriopulmonary venous junction.

Left atrium

The left atrium is located superiorly and in the midline. It is the most posteriorly situated cardiac

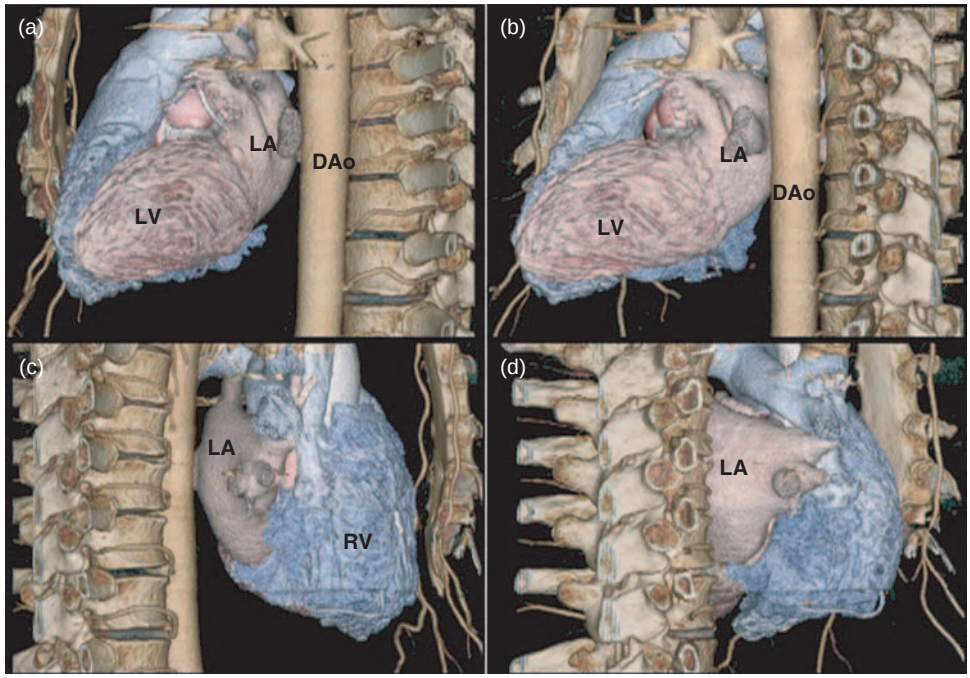

Figure 5.8 3D electronic cast showing the superior–posterior position of left atrium from the left (a,b) and the right and right-posterior (c,d) perspectives. LA = left atrium; LV = left ventricle; DAo = descending aorta; RV = right ventricle.

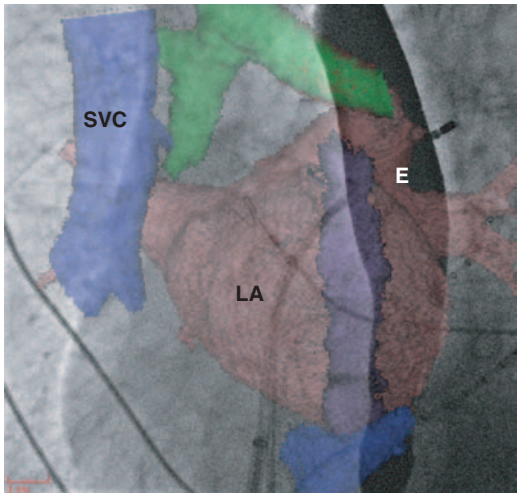

Figure 5.9 "Fusion imaging" between MSCT of the left atrium (LA) and barium swallow of the esophagus (E). SVC = superior vena cava.

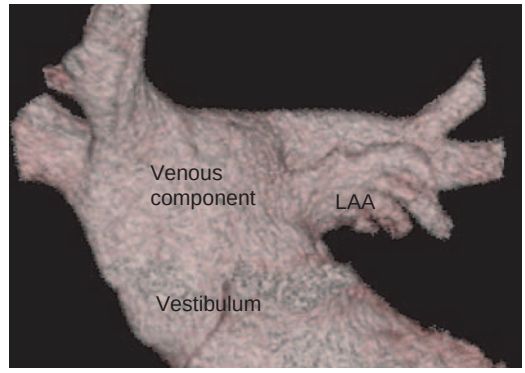

Figure 5.10 Electronic cast of the left atrium. The left atrium, similarly to the right atrium, consists of a smooth-walled venous component that receives the four pulmonary veins, the vestibule and the left atrial appendage (LAA).

chamber. Consequently, its posterior wall is adjacent to the course of the esophagus, separated only by the pericardium (Fig. 5.8).

The descent of the esophagus has a variable relationship with the atrial wall and with the atriopulmonary venous junctions, in the middle, or more to the right or the left. Delineation of the location of the esophagus can help reduce the risk of causing atrioesophageal fistulas when carrying out ablations for atrial fibrillation (Fig. 5.9).

Like the right atrium, the left atrium consists of three components: the appendage, vestibule,

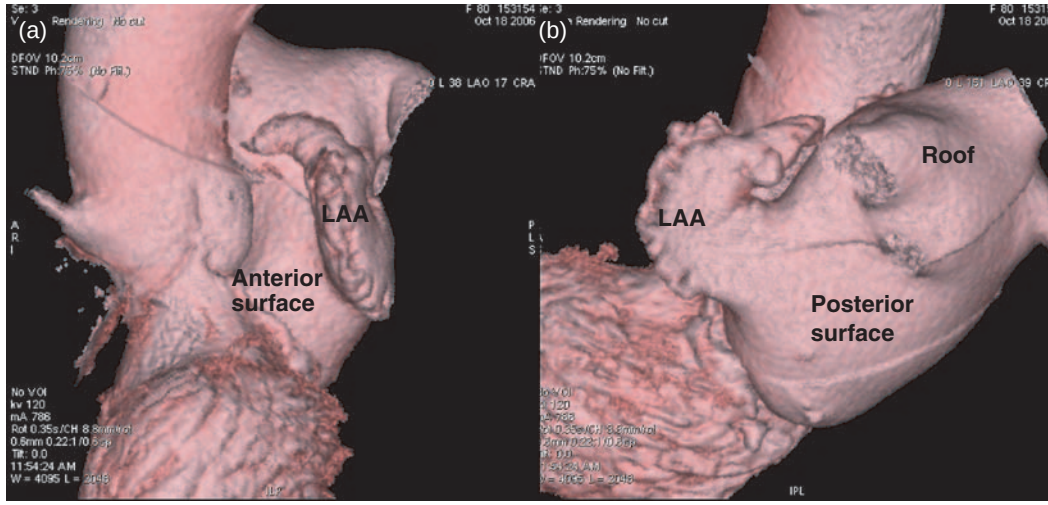

Figure 5.11 Electronic cast showing the anterior (a), the posterior surfaces and the roof (b) of the left atrium. LAA = left atrial appendage.

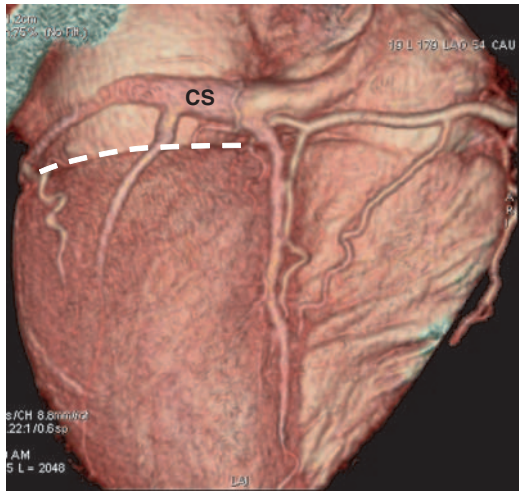

Figure 5.12 3D volume rendering of the posterior aspect of the heart. The coronary sinus (CS) runs superiorly from the level of the mitral valve hingeline.

and venous component. It is mainly smooth walled because its venous component is considerably larger than the appendage. The smooth wall continues into the vestibule that surrounds the atrial outlet, leading to the mitral valve (Figs. 5.10 and 5.11).

Related to the epicardial aspect of the inferior quadrant of the vestibule is the coronary sinus. It runs a centimeter or so distant from the level of the mitral valve hingeline (annulus) (Fig. 5.12) (see also Chapter 9). When the coronary sinus can be traced to the remnant of the oblique left atrial vein (ligament of Marshall), the remnant can be seen to run in the fold of atrial wall ("ridge," as described above) that lies between the left atrial appendage and the left superior pulmonary vein.

Left atrial appendage

Because the left atrium is situated posteriorly relative to the other cardiac chambers, only its appendage is visible when the heart is viewed from the front. The appendage forms the superior part of the left cardiac border (Fig. 5.13; see also Chapter 2).

Characteristically, the left appendage is a finger-like extension from the atrial chamber and it usually points anteriorly and superiorly, overlying the left ventricular wall. Its ostium (the orifice opening into the chamber) lies immediately above the level of the left atrioventricular groove. The circumflex branch of the left coronary artery runs close to the basal margin of the ostium (Fig. 5.14).

Usually the left phrenic nerve descends along the fibrous pericardium in close relation to the location of the appendage. As the appendage is within the confines of the pericardium, lying between the free wall of the left ventricle and the pericardial sac, its

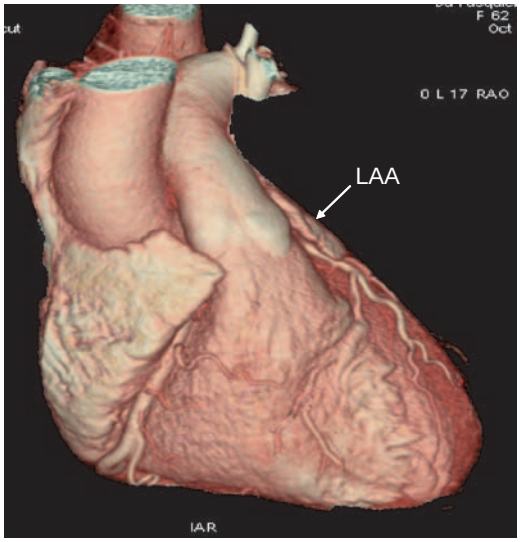

Figure 5.13 3D volume rendering of the entire heart from the anterior perspective. The left atrial appendage (LAA) forms the superior part of the left heart border.

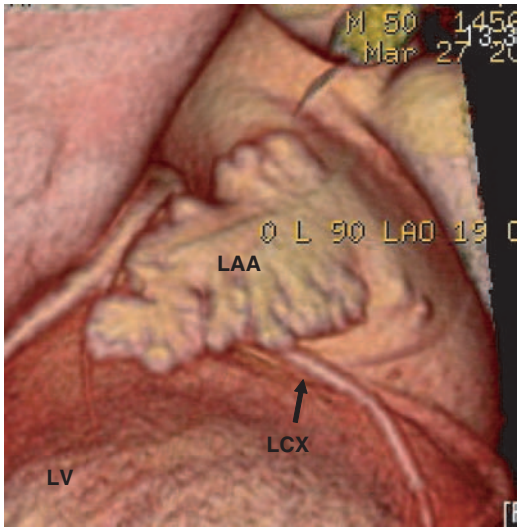

Figure 5.14 3D volume rendering of the left atrial appendage (LAA) and its relationships with surrounding structures. LV = left ventricle; LCX = left circumflex artery.

emptying and filling may be significantly affected by left ventricular function (Fig. 5.15).

Anatomically, the left appendage is likely the most variable structure of the entire heart. It may be a long, tubular, hooked structure with one, two, three or more lobes that spread in different directions (Fig. 5.16). It has a narrow junction with the

Figure 5.15 MIP projection coronal view. The arrows point to the course of the left phrenic nerve.

venous component of the atrium. Unlike the right side, the junction of the left appendage with its own atrium is not marked either externally or internally by a crest or groove (Fig. 5.17).

The pectinate muscles appear as interlacing fine ridges lining the lumen of the appendage. Without a terminal crest for anchorage, these ridges tend to be less regularly arranged than in the right appendage (Fig. 5.18).

Left ventricle

The morphological left ventricle forms the apex and the lower part of the left heart border. It is shaped like a cone (ellipsoid of revolution) with its long axis directed from the apex to the base (Figs. 5.19 and 5.20). Short-axis cross-sections, perpendicular to the long axis, reveal a roughly circular geometry (Fig. 5.21). The endocardial surface is irregular relative to the epicardial surface because of the two groups of papillary muscles and trabeculations (Fig. 5.22). Sections parallel to the ventricular long axis reveal an ellipsoid geometry. There are important variations in wall thickness, caused mainly by variation in the amount of circumferentially oriented mid-wall fibers (Fig. 5.23).

Stress develops when pressure is applied to a cross-sectional area. According to the Laplace law, wall stress in the left ventricle is determined by the intracavitary pressure × radius of curvature/twice the wall thickness (Fig. 5.24). Because of the conical shape of the left ventricle, the end-diastolic

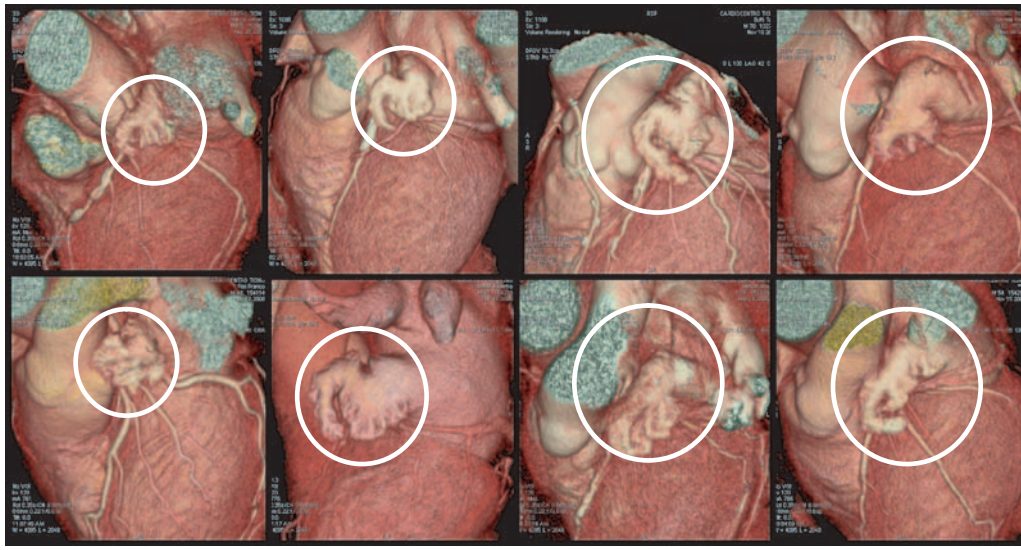

Figure 5.16 A composition of eight consecutive patients showing the extreme variability of the shape of the left atrial appendage (white circle). It may be long, tubular, or hooked with one, two, three or more lobes spreading in different directions.

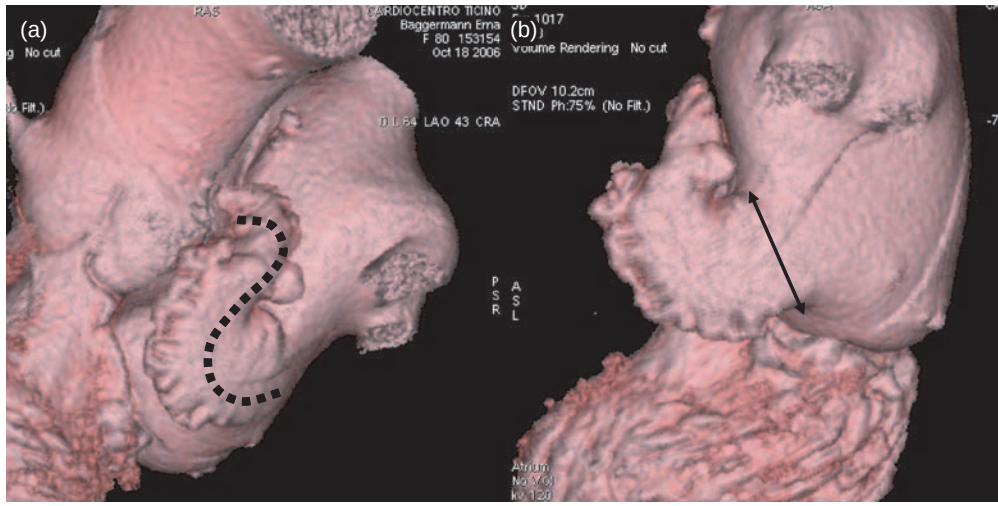

Figure 5.17 (a,b) The electronic cast shows the hooked structure of the left atrial appendage and its narrow junction with the venous component of the atrium (arrow). The junction between the left atrium and the left atrial appendage is not marked by any sulcus or crest.

circumferential radius of curvature gradually decreases from base to apex. Radius of curvature and wall thickness are related: wall thickness is smallest at the apex where the radius of curvature is also smallest. According to the Laplace law, the small radius of curvature compensates for the greater stress acting over the thinner apical wall (Fig. 5.25).

During systole the ventricle thickens radially (from the epicardium to the center of the cavity, in the direction of radii perpendicular to the long axis) (Fig. 5.26) and shortens from the base to apex

along meridians (curved lines parallel to the long axis) (Fig. 5.27). Moreover, shortening also occurs circumferentially along curved lines in short-axis planes and, finally, the apex twists relative to the base (see also 3D Video clip 8, Left ventricle rotation). These simultaneous movements in different directions can be explained by the complex architecture of muscle fiber orientation. In the mid-wall (halfway between the epicardium and the endocardium) the fibers lie in the circumferential plane, aligned with the short-axis section. In the subendocardium (approximately 10% of wall thickness from the endocardial surface), the fibers course upward and to the right averaging 60° oblique to the circumferential plane. Finally, in the subepicardium (10% of wall thickness closest to epicardial surface), the fibers course downward to the right averaging 60° oblique to the circumferential plane thus overlapping the subendocardial fibers at 120° (Fig. 5.28). The 3D electronic cast of left ventricle shows the helical disposition of the trabeculations. Whether this disposition is related to the subendocardial fibers is unknown (Fig. 5.29a,b).

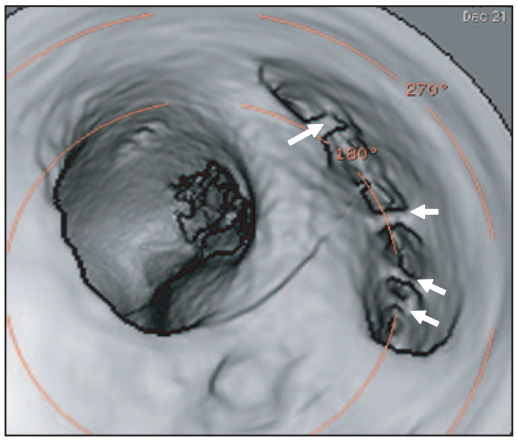

Figure 5.18 Virtual endoscopy of the left atrial appendage with its pectinate muscles (arrows).

Like the right ventricle, the left ventricle possesses an inlet, an apical trabecular component, and an outlet. The inlet component contains the mitral valve and extends from the atrioventricular junction to the attachment of the papillary muscles (Fig. 5.30a,b). The apical trabecular portion is the most characteristic feature of the morphological left ventricle and contains fine trabeculations (Fig. 5.31). This part helps identification because the left ventricle never possesses a septomarginal trabeculation or a moderator band.

In a sizable minority (in 40–50% of autopsy series) fibrous or fibromuscular bands (also known as false tendons) stretch across the left ventricle from the septum to the free wall. They can also tether to a papillary muscle, but unlike the chordae

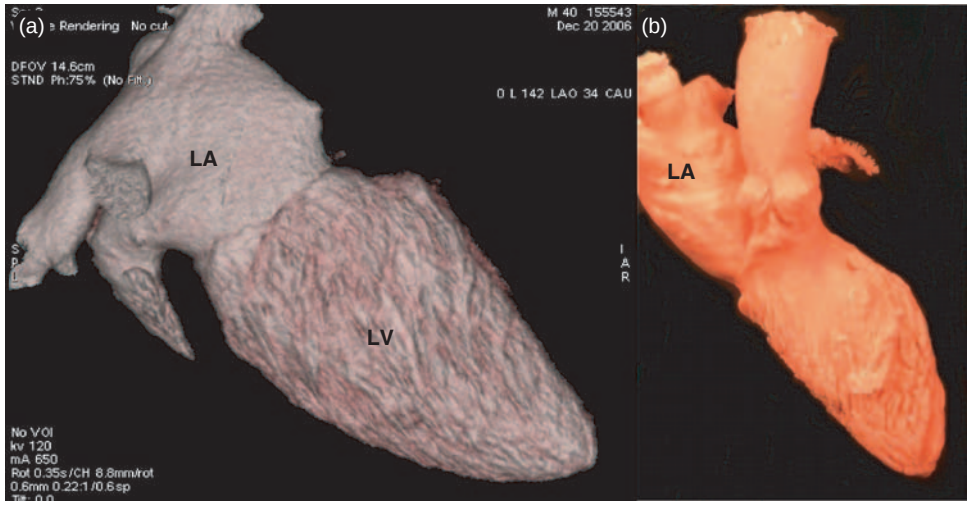

Figure 5.19 (a) "Electronic cast" showing the shape of the left ventricle. (b) Endocast preparation from a specimen in antero-posterior view. LA = left atrium; LV = left ventricle.

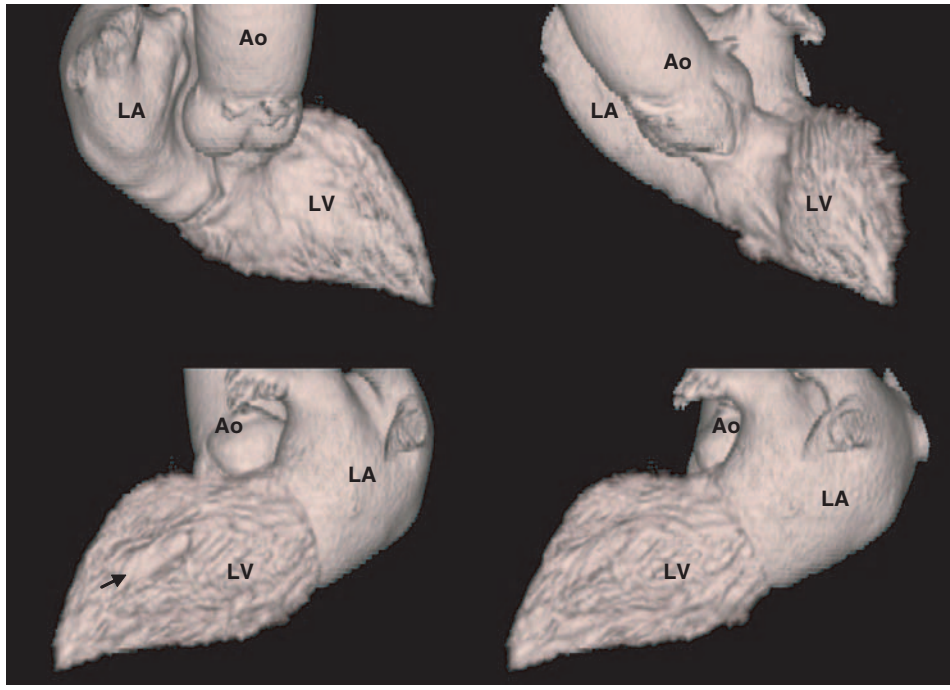

Figure 5.20 Electronic cast of the left ventricle (LV), left atrium (LA), and aorta (Ao) from different perspectives. The geometry of the left ventricle resembles an ellipsoid of revolution. The arrow marks the imprint of the anterior papillary muscle (see Video clip 5, Left ventricle).

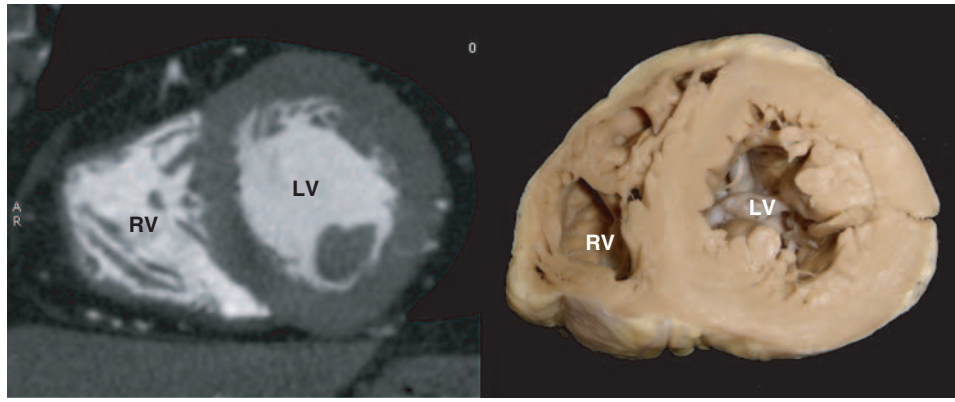

Figure 5.21 Short-axis cross-sectional slices and a specimen showing a roughly circular left ventricle with irregular endocardial surface. LV = left ventricle; RV = right ventricle.

tendineae, do not connect to the mitral leaflets. They are anatomic variants that should not be mistaken for abnormalities such as tumors, subaortic membranes, thrombus borders, and septal hypertrophy. Histological examination shows the false tendons to be composed of cardiac muscle, blood vessels, fibrous tissue, and Purkinje cells. False tendons might play a role in innocent murmurs or premature beats. Moreover, these fibromuscular bands may be involved as a part of the circuit in the genesis of ventricular tachycardia (Figs. 5.32a,b and 5.33).

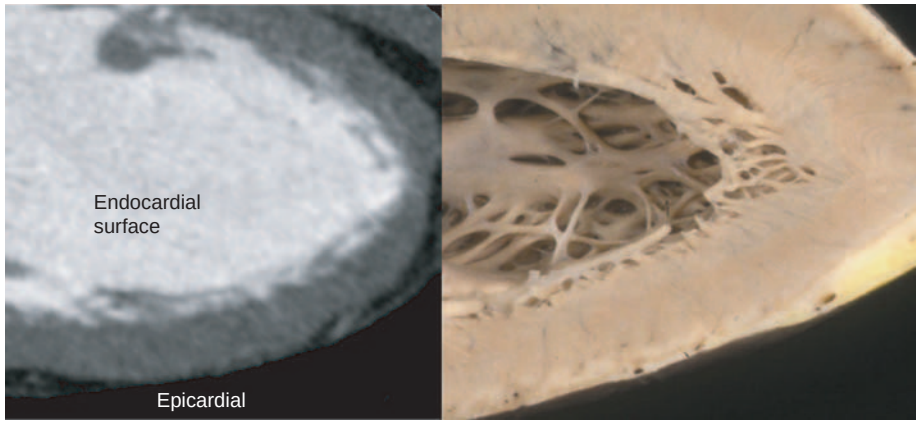

Figure 5.22 Magnified images of a portion of the left ventricular wall. The endocardial surface is more irregular than the epicardial surface because of the trabeculations.

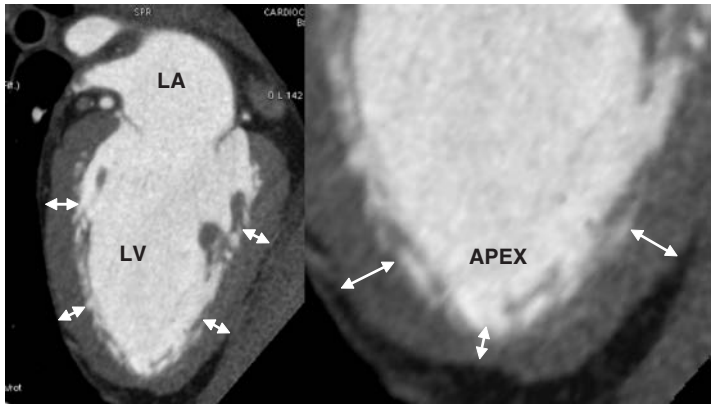

Figure 5.23 Long-axis slices showing the differences in wall thickness between anterior and inferior walls and the thin apex. LA = left atrium; LV = left ventricle.

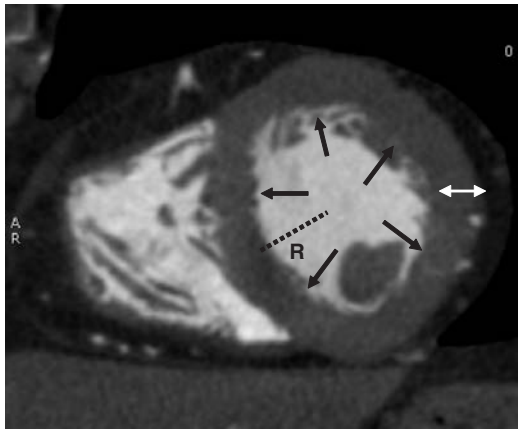

Figure 5.24 Short-axis view of the left ventricle showing the determinants of wall stress: the pressure inside the cavity (black arrows), the radius (dotted line), and the wall thickness (double white arrow). According to the Laplace law: stress = pressure × radius/twice the wall thickness.

The outlet component supports the aortic valve and consists of both muscular and fibrous portions. This is in contrast to the infundibulum of the right ventricle, which is comprised entirely of muscle. The septal portion of the left ventricular outflow tract, although primarily muscular, also includes the membranous portion of the ventricular septum (see Chapter 7). The posterior quadrant of the outflow tract consists of an extensive fibrous curtain that extends from the fibrous skeleton of the heart across the aortic leaflet of the mitral valve (Fig. 5.34), and supports the leaflets of the aortic valve in the area of aortic–mitral fibrous continuity (see Chapter 6). The lateral quadrant of the outflow tract is again muscular and consists of the lateral margin of the inner curvature of the heart.

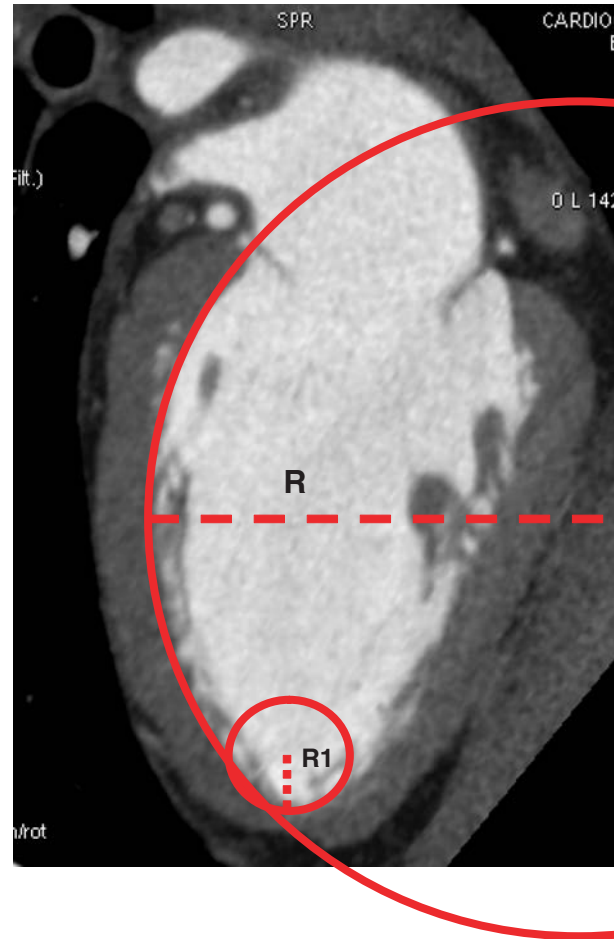

Figure 5.25 Long-axis slice of left ventricle. The radius of curvature of anterior wall (R) is greater than that of the apical wall (R1). According to the Laplace law, the small radius of curvature reduces the stress at the apex.

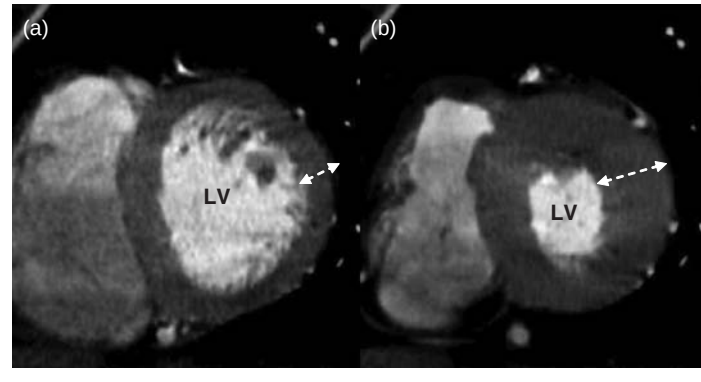

Figure 5.26 Short-axis view in diastole (a) and in systole (b) (see text and Video clip 6, Short axis function). LV = left ventricle.

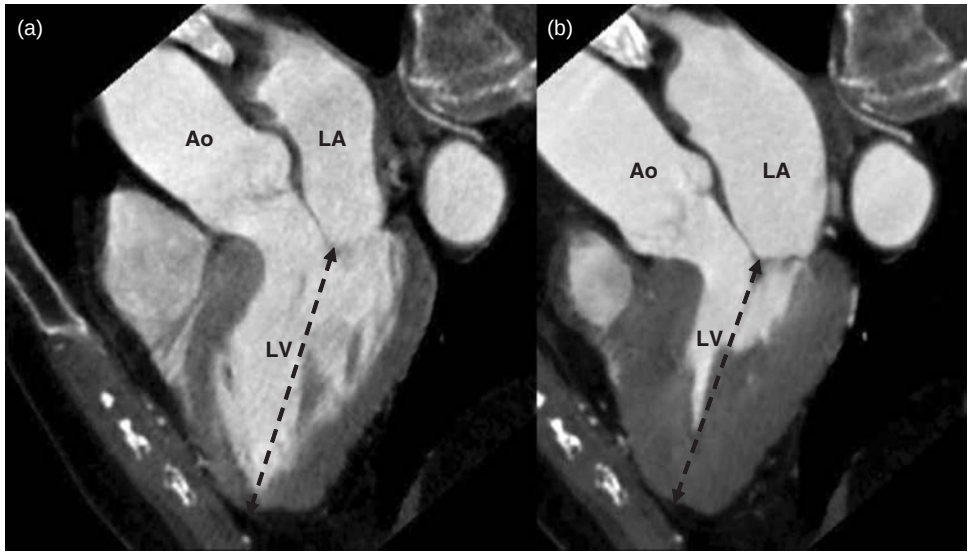

Figure 5.27 Long-axis view in diastole (a) and in systole (b) (see text and Video clip 7, Long axis function). Ao = aorta; LA = left atrium; LV = left ventricle.

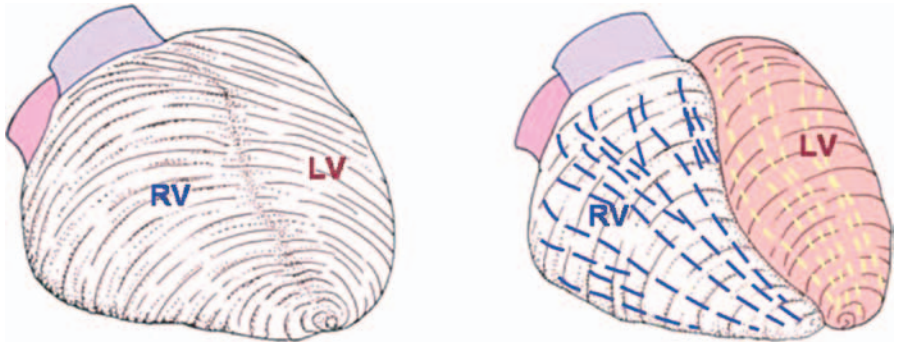

Figure 5.28 The left ventricular wall has three major orientations of myofibers. The left-hand panel shows the oblique orientation in the subepicardium for both right and left ventricles (RV and LV). The right-hand panel shows the thick "layer" of circumferentially oriented myofibers in the mesocardium and the thin "layer" of myofibers in the subendocardium (broken lines).

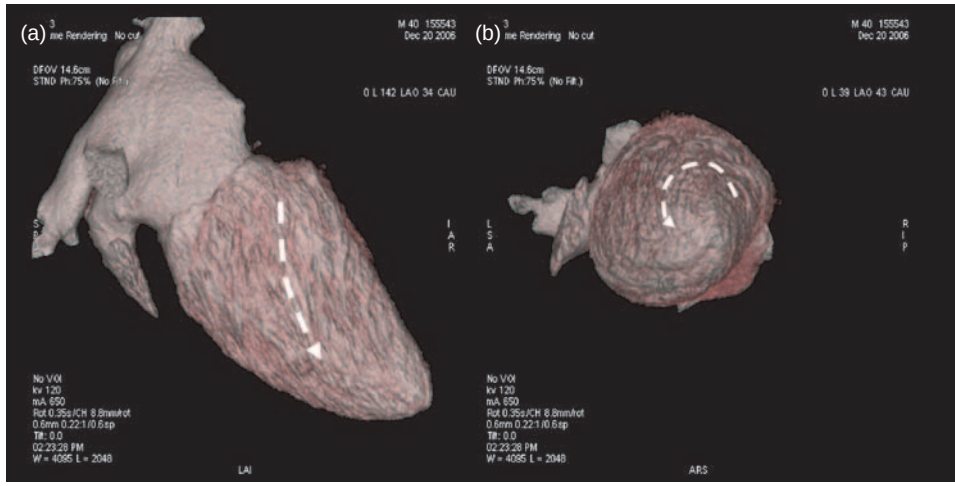

Figure 5.29 Electronic cast. (a) Anterior view showing the oblique course of trabeculations. (b) A view from the apex shows the helical disposition of the trabeculations.

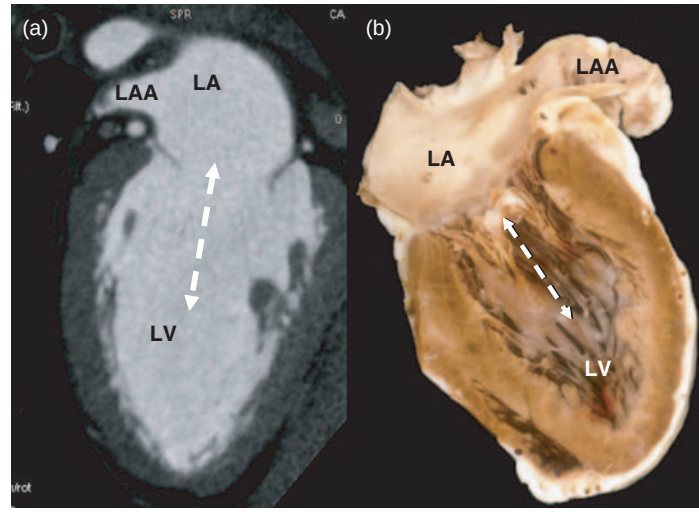

Figure 5.30 (a) Two-chamber-view slice, and (b) anatomic specimen showing the inlet part of the left ventricle extending from the atrioventricular junction to the attachment of papillary muscles (arrow). LV = left ventricle; LA = left atrium; LAA = left atrial appendage.

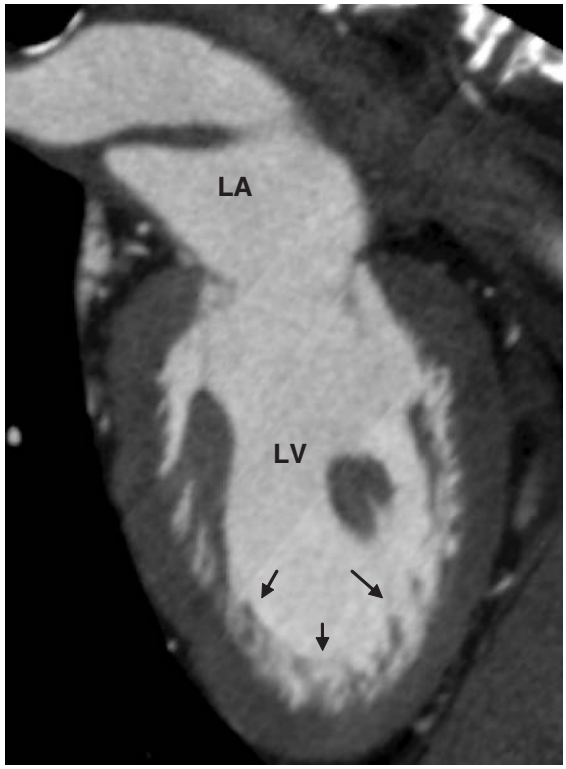

Figure 5.31 Two-chamber-view slice showing the fine trabeculations of the left ventricle. LA = left atrium; LV = left ventricle.

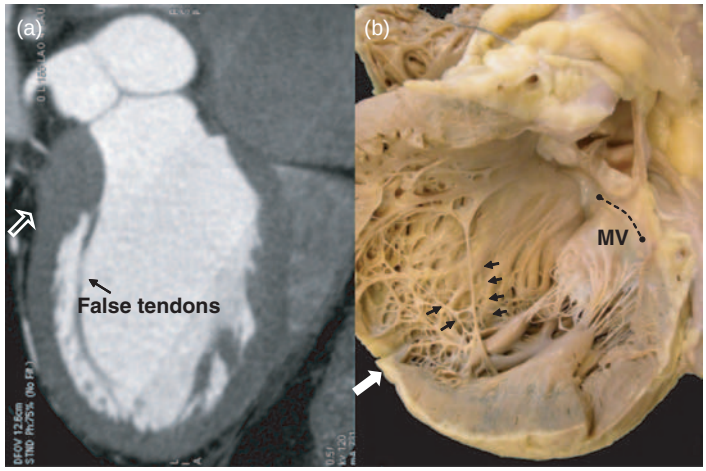

Figure 5.32 (a) Long-axis-view slice showing a false tendon running from the septum to the apex. (b) Anatomic specimen. The left ventricle is splayed open to show several false tendons (arrows) crossing the cavity of the left ventricle. Note the area of fibrous continuity between the aortic and the mitral valves (MV) (broken line) and the very thin muscular wall at the apex (white arrow).

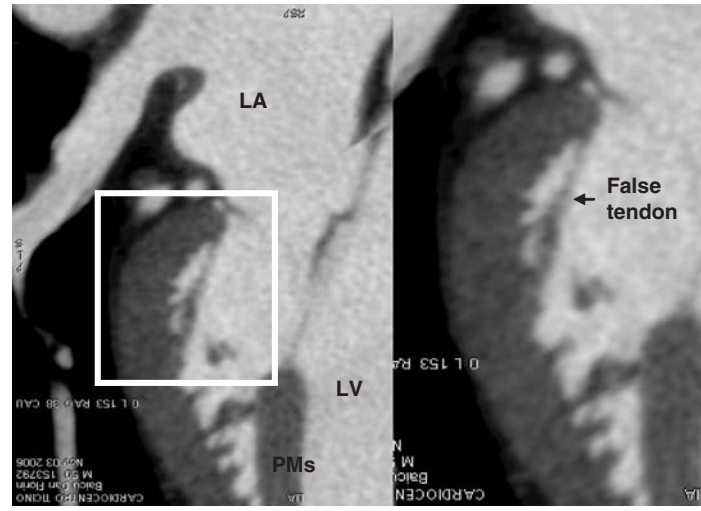

Figure 5.33 False tendon in the posterior wall. LA = left atrium; LV = left ventricle; PMs = papillary muscle.

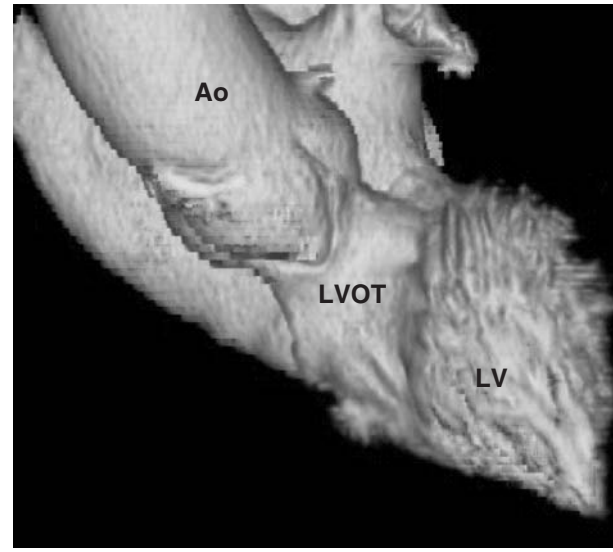

Figure 5.34 Electronic cast (left anterior oblique view) showing the left ventricular outflow tract cavity (LVOT). Ao = aorta; LV = left ventricle.

Suggested reading

Becker AE. Left atrial isthmus: anatomic aspects relevant for linear catheter ablation procedures in humans. *J Cardiovasc Electrophysiol* 2004;15:809–812.

Buckberg GD, Castella M, Gharib M, Saleh S. Structure/function interface with sequential shortening of basal and apical components of the myocardial band. *Eur J Cardiothorac Surg* 2006;29(Suppl 1):S75–S97.

Cirillo S, Bonamini R, Gaita F *et al.* Magnetic resonance angiography virtual endoscopy in the assessment of pulmonary veins before radiofrequency ablation procedures for atrial fibrillation. *Eur Radiol* 2004;14:2053–2060.

Ernst G, Stollberger C, Abzieher F *et al.* Morphology of the left atrial appendage. *Anat Rec* 1995;242:553–561.

Greenbaum RA, Ho SY, Gibson DG, Becker AE, Anderson RH. Left ventricular fibre architecture in man. *Br Heart J* 1981;45:248–263.

Ho SY, Sanchez-Quintana D, Cabrera JA, Anderson RH. Anatomy of the left atrium: implications for radiofrequency ablation of atrial fibrillation. *J Cardiovasc Electrophysiol* 1999;10:1525–1533.

Kato R, Lickfett L, Meininger G *et al.* Pulmonary vein anatomy in patients undergoing catheter ablation of atrial fibrillation: lessons learned by use of magnetic resonance imaging. *Circulation* 2003;107:2004–2010.

Le Grice IJ, Takayama Y, Covell JW. Transverse shear along myocardial cleavage planes provides a mechanism for normal systolic wall thickening. *Circ Res* 1995;77:182–193.

Lorenz CH, Pastorek JS, Bundy JM. Delineation of normal human left ventricular twist throughout systole by tagged cine magnetic resonance imaging. *J Cardiovasc Magn Reson* 2000;2:97–108.

McCulloch AD, Omens JH. Myocyte shearing, myocardial sheets, and microtubules. *Circ Res* 2006;98:1–3.

Rademakers FE, Rogers WJ, Guier WH *et al.* Relation of regional cross-fiber shortening to wall thickening in the intact heart. Three dimensional strain analysis by NMR tagging. *Circulation* 1994;89:1174–1182.

Sanchez-Quintana D, Cabrera JA, Climent V, Farre J, Weiglein A, Ho SY. How close are the phrenic nerves to cardiac structures? Implications for cardiac interventionalists. *J Cardiovasc Electrophysiol* 2005;16:309–313.

Sanchez-Quintana D, Garcia-Martinez V, Climent V, Hurle JM. Morphological changes in the normal pattern of ventricular myoarchitecture in the developing human heart. *Anat Rec* 1995;243:483–495.

Schwartzman D, Lacomis J, Wigginton WG. Characterization of left atrium and distal pulmonary vein morphology using multidimensional computed tomography. *J Am Coll Cardiol* 2003;41:1349–1357.

6 CHAPTER 6
The Cardiac Valves

Aortic valve

Aortic root

The aortic root may be defined as the portion of the left ventricular outflow tract that supports the leaflets of the aortic valve, delineated by the sinutubular ridge superiorly and the bases of the valve leaflets inferiorly. It comprises the aortic valve leaflets and their hingelines, the sinuses, the interleaflet triangles, the ventriculo-arterial junction, and the sinutubular junction. These components all work in concert to accomplish the role of the aortic root, which is to allow unimpeded forward flow when open and prevention of backflow when closed. Like the mitral valve apparatus, the complex interactions of all the components of the aortic root are both its strength and its potential weakness. Disruption of any component by disease processes such as aortic annuloectasia affects all the other components and can alter the biomechanics of the whole system. The aortic root is centrally located in the heart. Seen in profile, it lies behind the subpulmonary muscular infundibulum and anterior to the atria (Fig. 6.1). Because of its central location, the aortic valve is related to each of the cardiac chambers and cardiac valves (Fig. 6.2).

The annulus (ring hingeline)

Similar to the pulmonary valve, the semilunar hingelines of the aortic leaflets give a crown-shaped appearance to the fibrous thickening that forms the so-called annulus. It is a condensation of collagenous tissue that follows the semilunar contour of the valvar attachment. As with the pulmonary valve, the semilunar attachment extends across the ventriculo-arterial junction. Importantly, the "annulus" is not shaped like a conventional ring. The summits are at the commissures, which are the highest points of the valvar closure lines. They reach to the level of the sinutubular junction whereas the nadirs cross into ventricular tissues. This arrangement gives the valve the flexibility that would not be possible if the ring was a circular band (Figs. 6.3 and 6.4).

Aortic leaflets

The normal aortic valve has three semilunar leaflets. The leaflets seldom are perfectly equal in size. Each leaflet has a semicircular hingeline, a body, and a coapting surface (Fig. 6.5).

The three leaflets meet centrally along zones of apposition where adjacent leaflets coapt (Fig. 6.6). At the center of each zone is a thickened nodule, called the nodule of Arantius. Peripherally, adjacent to the commissures, the surfaces of coaptation are thinner and may contain small perforations in normal valves. These perforations have no hemodynamic impact because they occur on or above (distal to) the zones of apposition.

During systole, the leaflets are pushed aside, away from the center of the aortic lumen and into the sinuses, whereas during diastole they fall back passively to obliterate the lumen. The curvilinear attachment between the aortic valve leaflets and aortic root wall allows for stress sharing. This arrangement enables the high stresses carried by each leaflet during closure to be shared with the aortic root wall (Fig. 6.7).

The sinuses of Valsalva

Behind each leaflet, the aortic wall bulges outward to form the sinus of Valsalva. The sinuses of

Anatomy of the Heart by Multislice Computed Tomography
F. F. Faletra, N. G. Pandian and Siew Yen Ho. © 2008
Francesco Fulvio Faletra, Natesa G. Pandian and Siew Yen Ho.
ISBN: 978-1-4051-8055-9.

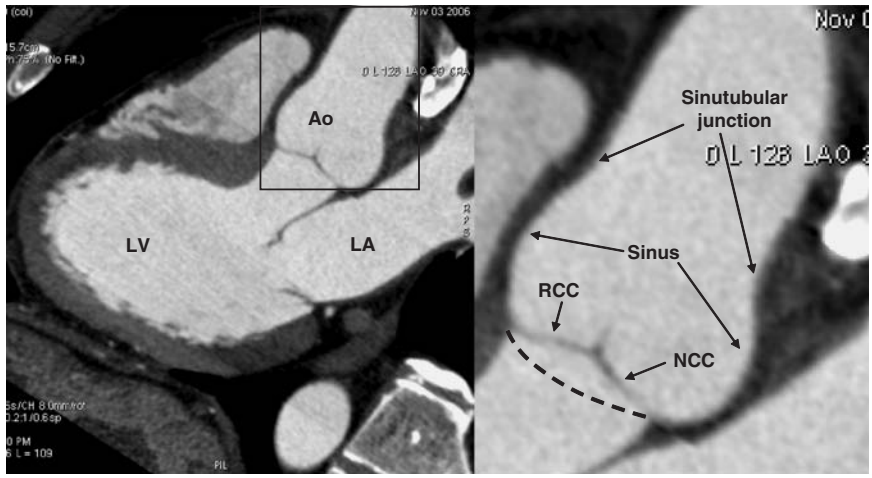

Figure 6.1 The aortic valve apparatus is composed of several components: the leaflets, the sinuses of Valsalva, the sinutubular junction, the ventriculo-arterial junction (black dotted line), and the interleaflet triangles (not seen in this figure). Note the location of the aortic valve behind the right ventricular outflow tract (RVOT) and in front of the transverse pericardial sinus (*). Ao = aorta; LV = left ventricle; LA = left atrium; RC = right coronary leaflet; NC = non-coronary leaflet.

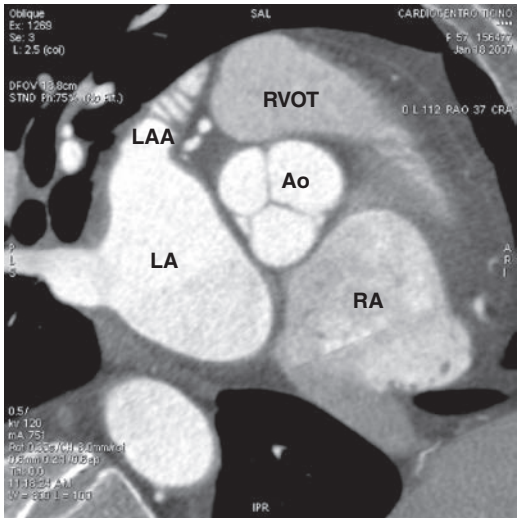

Figure 6.2 Oblique slice showing short-axis view of the heart at its base. Image shows the aorta (Ao), the left atrium (LA), the left atrial appendage (LAA) and the right ventricular outflow tract (RVOT). The aortic valve is located to the right and posterior to RVOT and forms the centerpiece of the heart. RA = right atrium.

Valsalva occupy the greater part of the aortic root. The sinuses are composed primarily of elastic tissue, and they contain the orifices (ostia) of the coronary arteries. In cross-section, the aortic root at this level is trilobed. The trilobed configuration reduces the radius of curvature of the aortic root thus minimizing the diastolic stress against the aortic wall (Fig. 6.8). As first recognized by Leonardo Da Vinci, the sinuses lead to the creation of eddies within the flowing blood during ventricular ejection. This eddy formation assists in two functions: one is valve closure, and the other is aiding or ensuring coronary ostial perfusion. Two of the three aortic sinuses give rise to coronary arteries, hence their designations as right, left and non-coronary sinuses. The latter is usually the largest.

The sinutubular junction is a ridge of aortic wall that is thicker than the adjacent sinuses. It forms a circle joining the peaks of the commissures. It delineates the beginning of the tubular ascending aorta (Fig. 6.9).

The interleaflet triangles

Because of the semilunar attachment of the aortic leaflets, there are three interleaflet triangles that are extensions of the left ventricular outflow tract because they are located beneath the level of the leaflets when the valve is in the closed position. The apex of each triangle reaches near to the sinutubular junction where the attachments of adjacent leaflets meet together forming the "commissures" (Fig. 6.10).

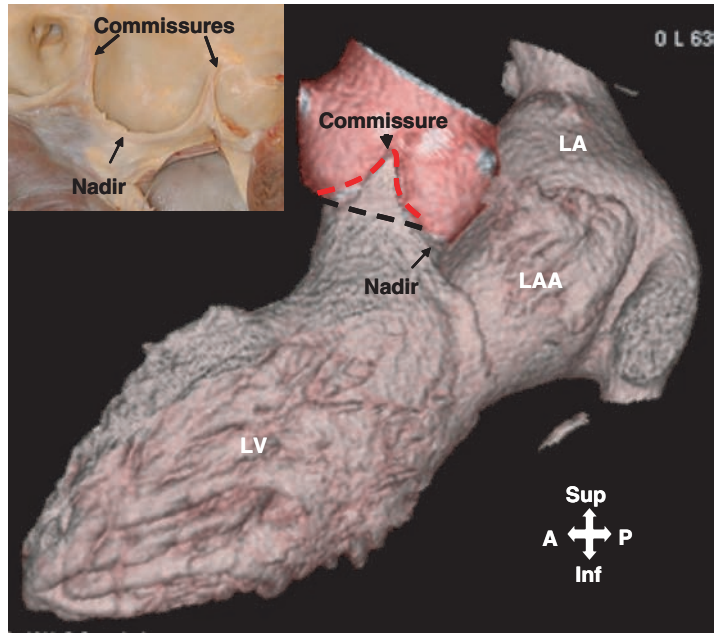

Figure 6.3 3D electronic cast of the left ventricle (LV) and the left atrium (LA) with the aortic root colored in pink and the left ventricle in purple. The semilunar attachments (red dashed line) of the valvar leaflets are arranged in crown-like fashion (see inset of anatomic specimen). The black dashed line marks the ventriculo-arterial junction. Inset: anatomic specimen showing the crown-shaped appearance of the cusps' attachment. LAA = left atrial appendage.

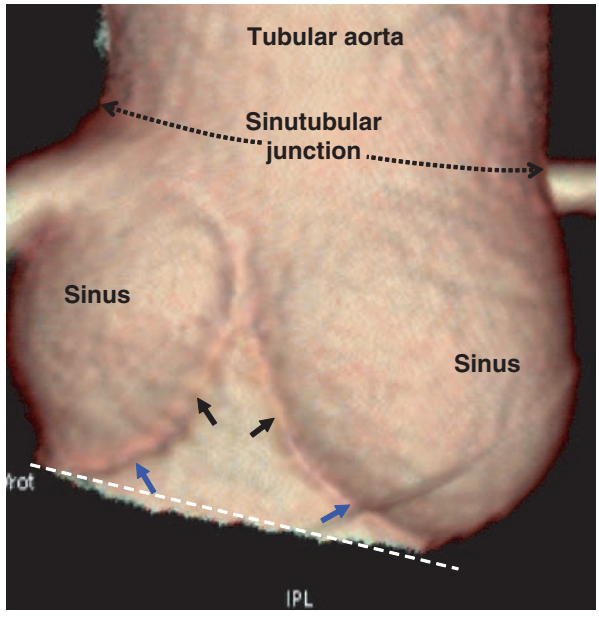

Figure 6.4 3D volume rendering external view of the aortic root. The sinutubular junction distinguishes the tubular portion of the aorta from the sinuses. The arrows point to the condensations of collagenous tissue ("annulus" or hingeline) where the leaflets attach in semilunar (crown-shaped) fashion to the aortic root. The dotted line represents the level of the ventriculo-arterial junction that passes through the hingelines. Anatomically, the lower parts of the sinuses delimited by hingelines (blue arrows) are composed of ventricular tissues. Thus, the right coronary and part of the left coronary sinuses contain ventricular myocardium, a relevant feature for electrophysiologists ablating foci of idiopathic ventricular tachycardia.

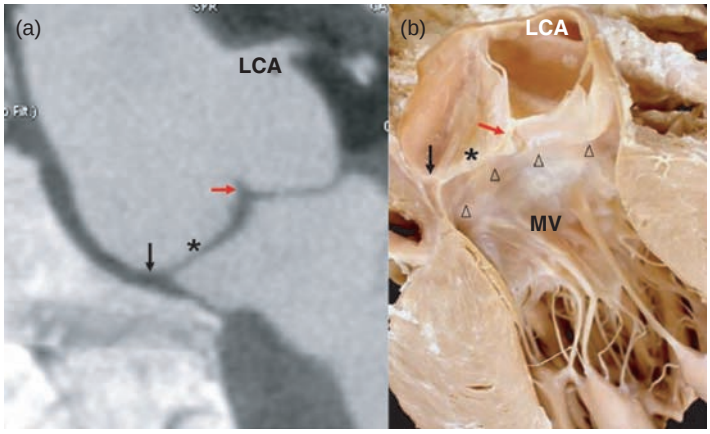

Figure 6.5 (a) Oblique slice and (b) the corresponding anatomic specimen. Each leaflet has a hinge point (black arrow), a body (*), and a coapting surface (red arrow). LCA = left coronary artery; MV = mitral valve.

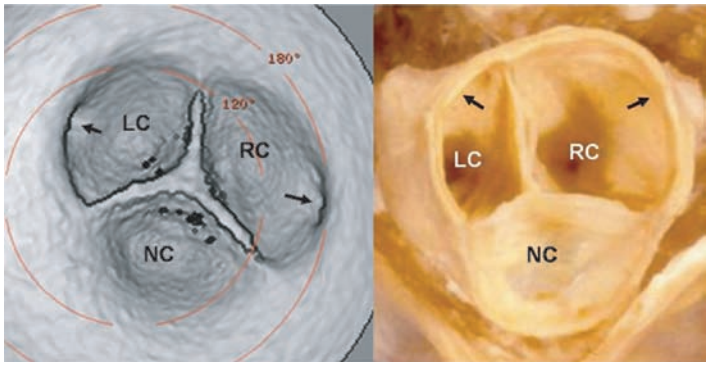

Figure 6.6 3D virtual endoscopic view of aortic leaflets in closed position and a similar display of a heart specimen viewed from the ascending aorta. The arrows indicate the orifices leading to the left and right coronary arteries. LC = left coronary; RC = right coronary; NC = non-coronary leaflet.

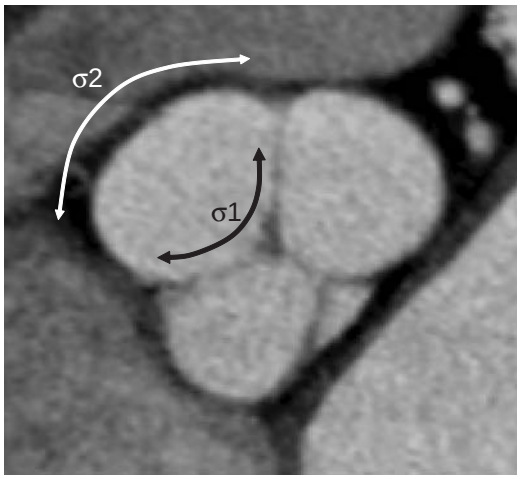

Figure 6.7 Scheme of stress (σ) in leaflets and wall of the aortic root. Because the leaflets are thinner than the wall, the leaflet stresses (σ1) are higher than the root wall stresses (σ2). However, the curvilinear attachment at the sinuses enables the high leaflet stress to be partially transferred to the root wall, thereby decreasing the stress on the leaflets.

The triangle between the right coronary and non-coronary aortic sinuses incorporates within it the membranous part of the septum (Fig. 6.11). The latter is a landmark for the course of the atrioventricular bundle of the cardiac conduction system. The triangle between the left coronary and the non-coronary aortic sinuses forms part of the aortic-mitral valvar curtain (Fig. 6.12). The interleaflet triangles, therefore, are exposed to ventricular hemodynamics.

The ventriculo-arterial junction

Toward the proximal end of the aortic root is the anatomic ventriculo-arterial junction. This is unequivocally circular in shape, and is below the level of origin of the coronary arteries. It is at the ventriculo-arterial junction that surgeons sew prosthetic valves, taking particular care in the region of the membranous septum. The junction crosses the semilunar hingelines, resulting in

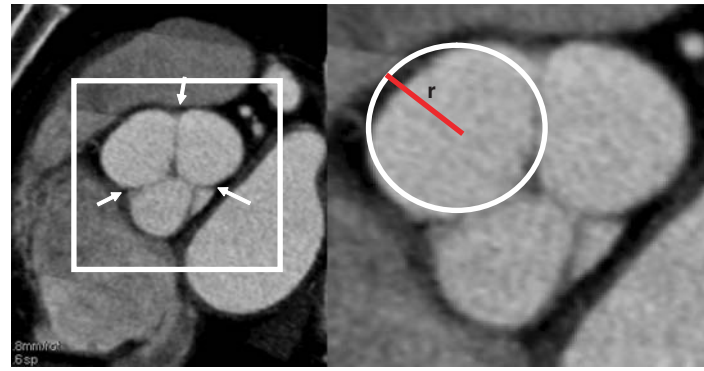

Figure 6.8 The trilobate configuration reduces the radius of curvature, thus minimizing the stress upon the sinuses.

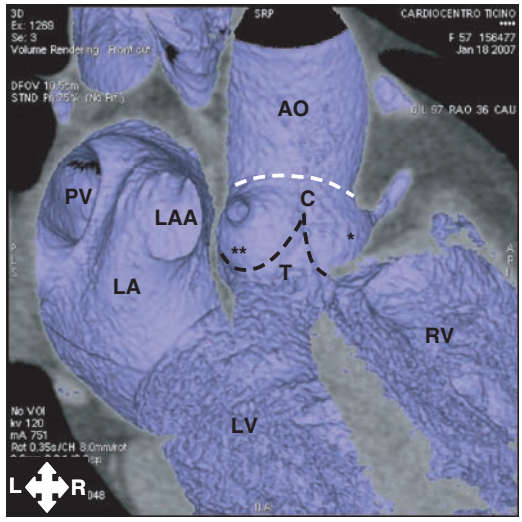

Figure 6.9 3D endocardial surface modality looking from the back of the heart toward the front, depicting the crown-shaped (black dotted line) insertions of the left (**) and right (*) aortic leaflets with the commissure (C) between. The anterior interleaflet triangle (T) adjoins muscular ventricular septum. The dotted white line marks the sinutubular junction. The orifices of the left and right coronary arteries are also visible (arrows). AO = aorta; LA = left atrium; PV = pulmonary vein; LV = left ventricle; RV = right ventricle.

small segments of ventricular myocardium being enclosed within the right sinus and part of the left sinus of the aortic root. The non-coronary sinus has no muscular incorporation because it adjoins the aortic-mitral curtain (Figs. 6.10–6.12).

The basal ring

An imaginary line joining the nadirs of the semilunar hingelines forms a circle, described as the basal ring (Fig. 6.13). This level corresponds to the echocardiographic "annulus" when measurements of the diameter of the aortic valve are made.

Mitral valve

The mitral valve apparatus comprises annulus, valvar leaflets, tendinous cords that attach to the leaflets, and papillary muscles that anchor the cords. Also important for its functioning is the left atrial musculature inserting to the leaflets at the annulus and the ventricular myocardium to which the papillary muscles are attached. The normal mitral valve has two leaflets that, conventionally, are described as anterior and posterior leaflets. With tomographic imaging of the heart *in situ*, it is obvious that these leaflets are not in anterior or posterior positions. But because surgeons continue to use this convention, we will continue to use the term "anterior" for the leaflet that is nearest to the aortic valve and "posterior" for the mural leaflet. Similarly, the "commissures" (ends of the zone of apposition between leaflets), and the papillary muscles are referred to as antero-lateral and postero-medial.

Mitral annulus

The mitral annulus has an elliptical or D-shaped configuration (Fig. 6.14). The straight border accommodates the aortic valve allowing the latter to be wedged between the ventricular septum and the mitral valve (Fig. 6.15a). In this region, the aortic valve is in fibrous continuity with the anterior leaflet of the mitral valve (mitral-aortic continuity or mitral-aortic curtain). Expansions

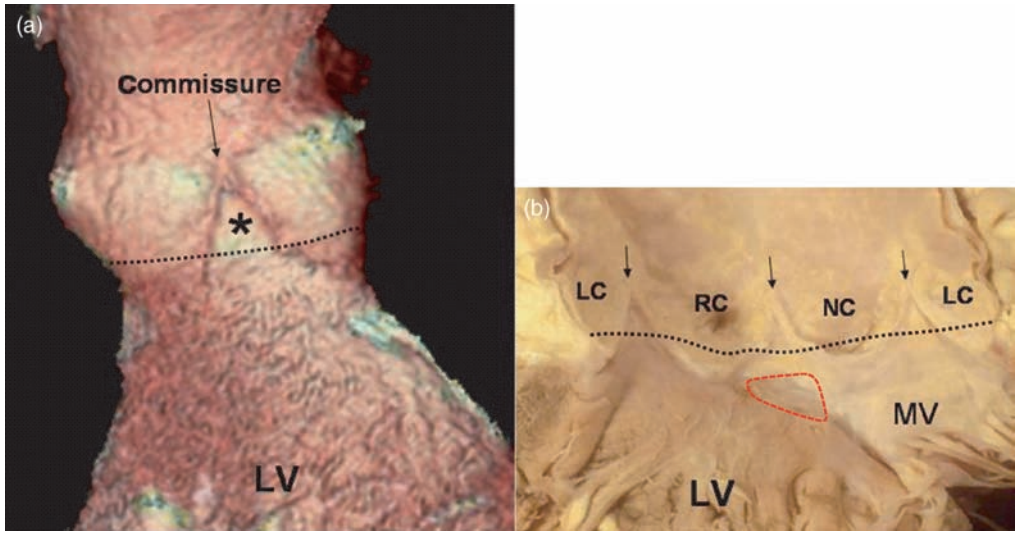

Figure 6.10 (a) 3D volume rendering reconstruction of aortic root, external view, to show the interleaflet triangle (*) between the semilunar attachments of the leaflets. (b) A heart specimen opened longitudinally through the left coronary (LC) sinus of the aortic valve. The leaflets have been removed to show the accretions of fibrous tissue that make up the hingelines that approximate at the commissures (arrows). Note the ventriculo-arterial junction intersects the semilunar hingelines. The nadirs of the right (RC) and left (LC) sinuses contain ventricular myocardium whereas the non-coronary (NC) sinus and part of the left sinus have no ventricular muscle because they are in fibrous continuity with the mitral valve. The interleaflet triangle between the right (RC) and non-coronary (NC) sinuses abuts the membranous septum (encircled by a red broken line), which is in proximity to the atrioventricular conduction bundle. Anatomically, the interleaflet fibrous triangles are arterial and lead outside the heart. Hemodynamically, however, they are ventricular because they occupy the ventricular side of the valve when the leaflets are in the closed position. LV = left ventricle; MV = mitral valve.

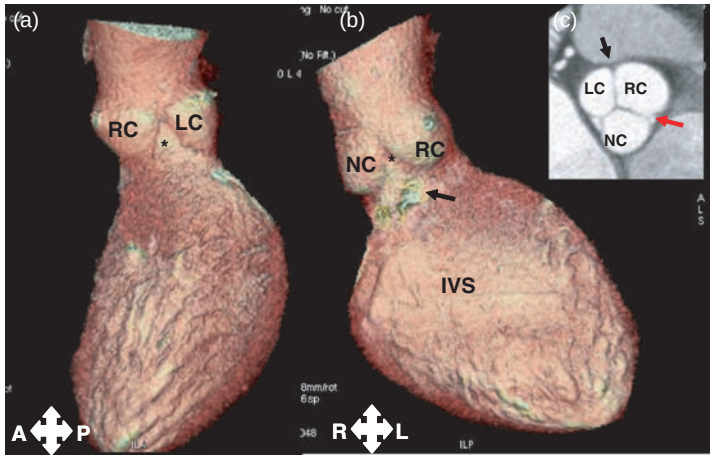

Figure 6.11 (a) 3D volume rendering reconstruction of the interleaflet triangle (*) between the right coronary (RC) and the left coronary (LC) sinuses. (b) The interleaflet triangle (*) between the non-coronary (NC) and the right coronary (RC) sinuses. The arrow marks the membranous septum. (c) Oblique slice showing the interleaflet triangles.

of fibrous tissues at either extreme of the area of continuity form the rigid right and left fibrous trigones (Fig. 6.15b–d). The maximum stress on the mitral valve is at the trigones (Fig. 6.16). The clinical implication is that all annuloplasties must be anchored to the trigones for firm support. The annulus does not lie in a single plane but has a saddle-shaped configuration. There is a "peak" in the midpoint of the anterior segment of the annulus and another "peak" in the midpoint of the posterior segment whereas the "valleys" lie near the commissures (Fig. 6.17). The anterior "peak" rises higher than

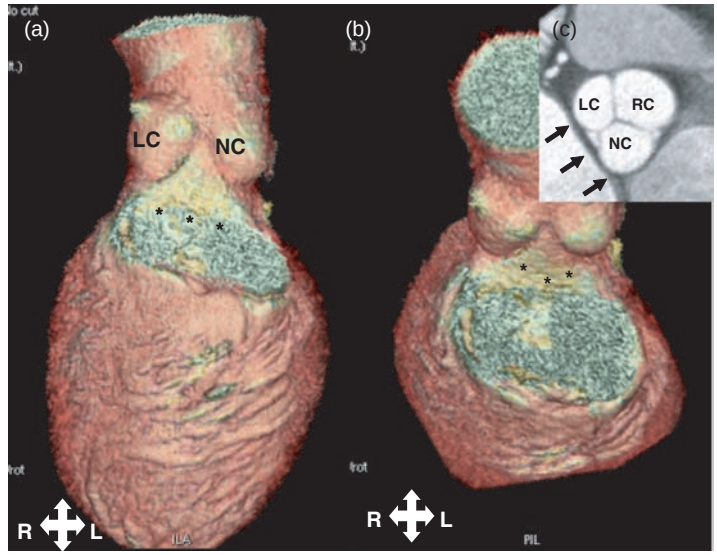

Figure 6.12 (a,b) 3D volume rendering reconstruction of the interleaflet triangle between the left coronary sinus (LC) and the non-coronary sinus (NC) showing the fibrous continuity with the mitral valve (***). (c) Oblique view showing the mitro-aortic continuity. RC = right coronary sinus.

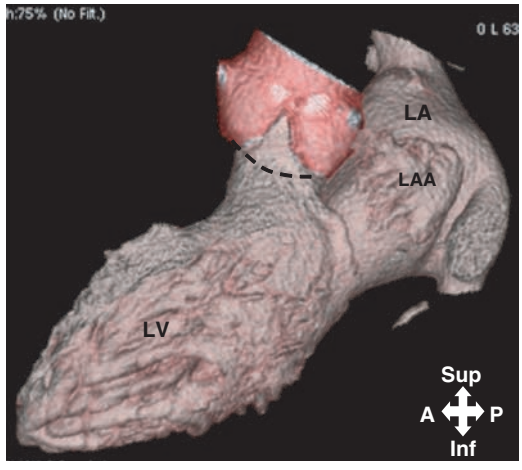

Figure 6.13 3D electronic cast of the left ventricle and the left atrium with the aortic root colored in pink and the left ventricle in purple. The black dashed line marks the basal ring. LV = left ventricle; LA = left atrium; LAA = left atrial appendage.

the posterior "peak." The configuration and size of the annulus vary constantly during the cardiac cycle. This hyperbolic paraboloid shape reduces significantly the mechanical stress. It is this knowledge that motivated the development of flexible rings for mitral annuloplasty.

Leaflets

The leaflets are the most important components of the mitral apparatus for competent valve closure. They meet at the closure line forming a single zone of apposition (Fig. 6.18). The "commissures" are the extreme ends of the zone of apposition. The commissures do not reach the annulus, but end about 5 mm short. Thus from a strictly anatomic point of view, being hinged along the entire annular circumference, the mitral leaflets can be considered as a single veil with the anterior leaflet hanging like a curtain between the left ventricular inflow and outflow tracts (Fig. 6.19). The hingeline of the anterior leaflet occupies one-third of the annular circumference (nearly 3 cm). Being roughly triangular in shape, the anterior leaflet is deeper than the posterior leaflet (Figs. 6.19 and 6.20). The latter is long and narrow and is attached to the two-thirds of the remaining annular circumference. Thus, the overall orifice areas covered by each leaflet are equivalent. Small identations, termed clefts, usually divide the posterior leaflets into three scallops (Figs. 6.18 and 6.21) but quite often there are four or more scallops. Using the surgeon's terminology, these scallops are denoted from lateral to medial as P1, P2 and P3 (P stands for posterior), arbitrarily apportioning the leaflet into thirds. The corresponding areas of the anterior leaflet are denoted A1, A2

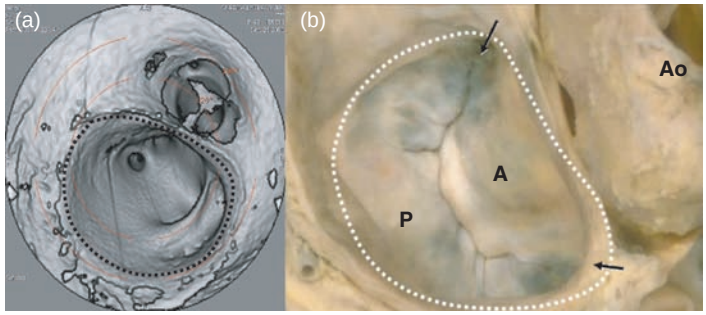

Figure 6.14 (a) Virtual endoscopy and (b) anatomic specimen both showing the "D-shaped" annulus configuration (dotted line). P = posterior; A = anterior.

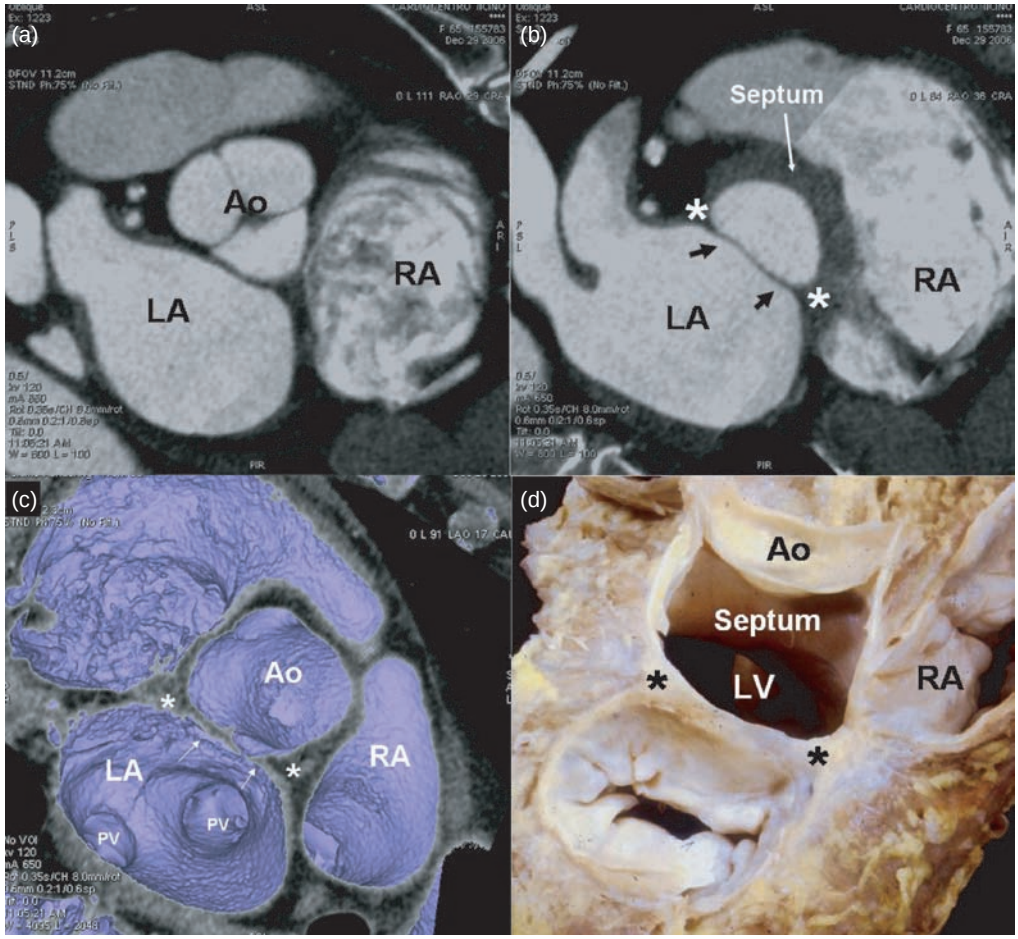

Figure 6.15 (a,b) Axial slices at different levels, (c) 3D endocardial surface modality and (d) anatomic specimen showing the fibrous continuity between aortic and mitral valves. * = trigone; Ao = aorta; RA = right atrium; LA = left atrium; LV = left ventricle; PV = pulmonary vein.

and A3, although any anatomic indentations can be observed (Fig. 6.18). In the normal valve, the total leaflet area is approximately twice that of the mitral orifice. This tissue abundance may account for the success of mitral repair compared with aortic valve repair, where lack of available tissue is a constant limitation. In both leaflets two different zones can be distinguished – a clear and a rough zone. This distinction is more evident in the anterior leaflet. The tendinous cords mainly insert

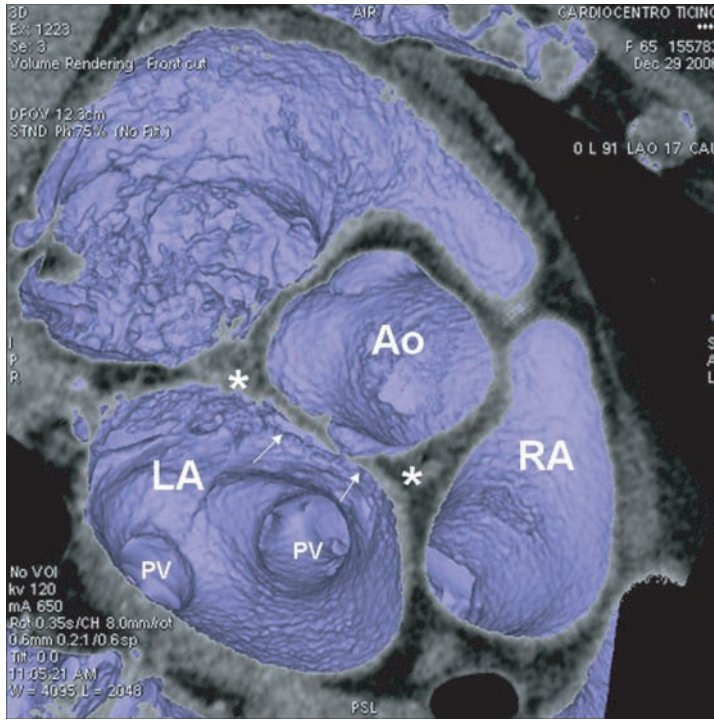

Figure 6.16 Magnified image of panel (c) of Fig. 6.15 showing an endocardial view from the ventricular perspective. Arrows indicate the mitro-aortic curtain. The two asterisks indicate the trigones. Ao = aorta; RA = right atrium; LA = left atrium; PV = pulmonary vein.

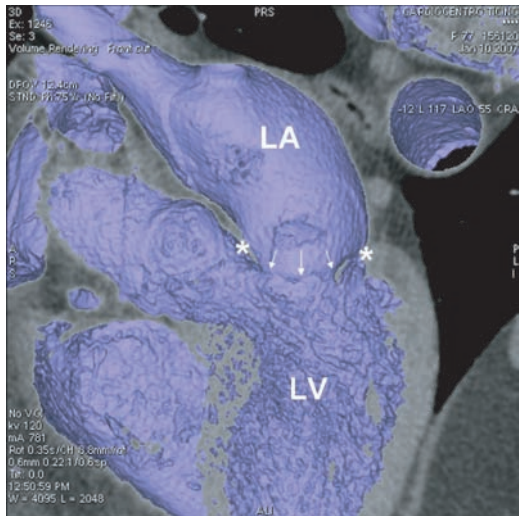

Figure 6.17 3D long-axis endocardial surface modality. Peaks are located in the mid-points of the anterior and posterior segments (*) whereas "valleys" lie near the commissures (arrows). LA = left atrium; LV = left ventricle.

to the ventricular side of the rough zone making the latter appear irregular and thicker than the clear zone. In systole, the atrial sides of both rough zones meet each other to ensure valvar competence along the closure line. The surface of leaflet coaptation is 5–8 mm deep along the zone of apposition allowing the valve to accommodate a moderate degree of annular dilation without becoming incompetent. The clear zone, particularly visible in the anterior leaflet, is thin and translucent. In systole, the clear zone of the anterior leaflet bulges toward the anterior cavity (Fig. 6.23).

Tendinous cords (chordae tendineae)

These cords are fibrous string-like structures on the ventricular surfaces of the leaflets. The majority connect the rough zone and the free edges of leaflets to papillary muscles. Unlike the tricuspid valve, the normal mitral valve does not have cords attaching the leaflets to the ventricular septum. Because cords usually branch several times distal to their origin, there are four or five times more cords attached to the leaflets than to the papillary muscles. There is a wide variability from heart to heart in cordal arrangement and only a general organization can be recognized. One of the more useful classifications distinguishes tendinous cords into first-, second- and third-order cords according to their insertion onto

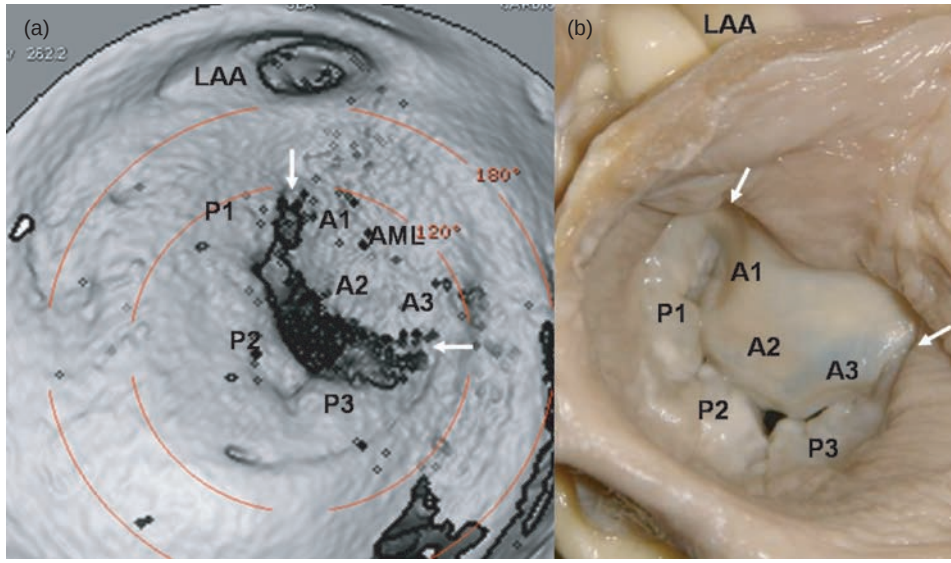

Figure 6.18 Virtual endoscopy (a) and anatomic specimen (b) from an atrial perspective. Two main identations divide the mitral veil in the anterior mitral leaflet (AML) and the posterior leaflets (arrows). Posterior leaflets are subdivided in three scallops (P1, P2 and P3). A1, A2 and A3 are the corresponding regions of the anterior leaflet. LAA = left atrial appendage.

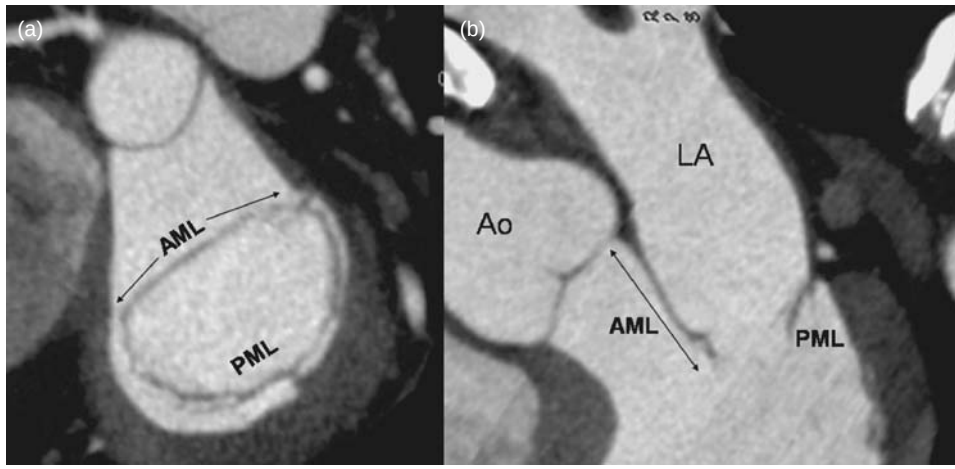

Figure 6.19 Oblique slices. The anterior mitral leaflet (AML) occupies one-third of the annular circumference (a), but is deeper than the posterior mitral leaflets (PML). (b) The overall orifice areas covered by each leaflet are therefore equivalent Ao = aorta; LA = left atrium.

the leaflet's margin, rough zone or basal areas, respectively. The first-order cords are thought to prevent valvar incompetence; the second-order cords, which include some of the thickest cords (known as strut cords), maintain mitral–papillary muscle–ventricle wall continuity, thus supporting longitudinal left ventricle shortening and left ventricular function (Fig. 6.24). The role of the basal cords, which connect the basal area of the posterior leaflet directly to the ventricular wall, is not clear.

At each "commissure" is a distinctive cord (commissural cord) that branches into a fan-shape to insert into the adjacent leaflets. The "fan" is open when the leaflets move apart and it closes when the leaflets come together.

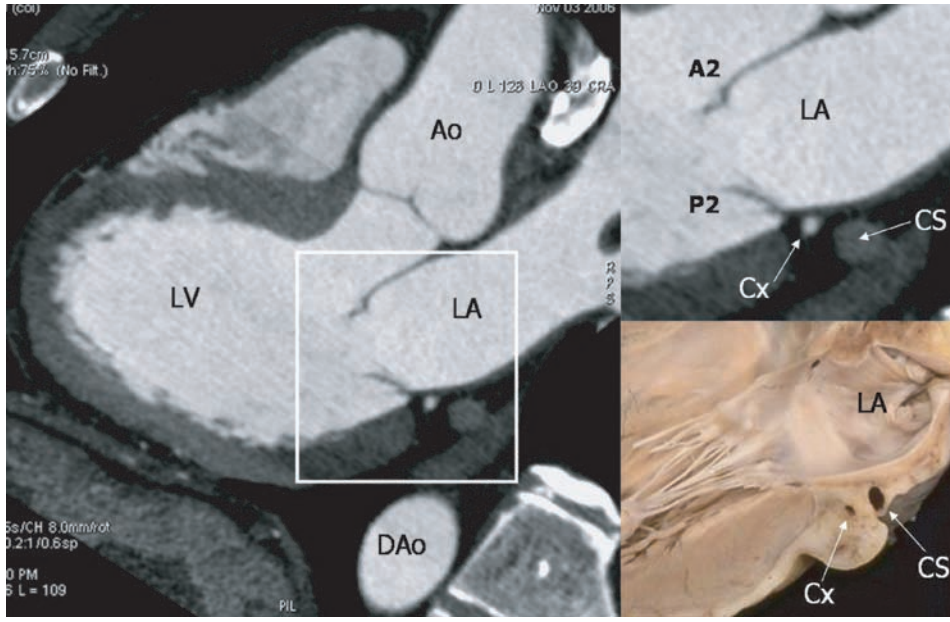

Figure 6.20 Oblique slice showing long-axis view of the left ventricle. Magnified image in the upper right corner and the corresponding anatomic specimen in the lower right corner showing mitral leaflets (A2 and P2), left circumflex artery (Cx) and coronary sinus (CS). Descending aorta (DAo) in the short axis is also displayed in the main panel. LV = left ventricle; LA = left atrium; Ao = aorta.

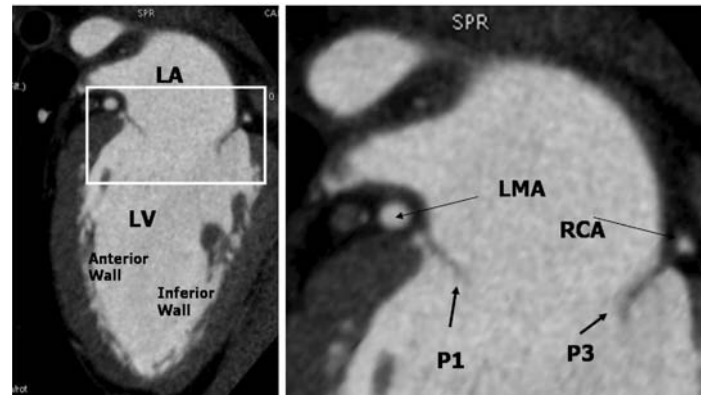

Figure 6.21 Oblique slice showing a two-chamber view in diastole. The lateral (P1) and medial (P3) scallops are shown in the magnified image. Note the left main artery (LMA) and the right coronary artery (RCA) in short-axis view. LA = left atrium; LV = left ventricle.

Papillary muscles

The papillary muscles are considered as a left ventricular muscular protuberance that anchors the cords to the left ventricular wall. Rupture of one of their heads results in severe valvar regurgitation. Viewed from the atrial aspect, the two groups are located beneath the commissures, occupying antero-lateral and postero-medial positions (Figs. 6.25 and 6.26). The arrangement of the papillary muscles in two groups allows the mitral valve to be distinguished from the tricuspid valve. Generally larger than the posteromedial muscle, the anterolateral papillary muscle is supplied by an artery derived from the circumflex or anterior descending branch of the left coronary artery (Fig. 6.27). Because most people have right dominance of the coronary pattern (see Chapter 8), it is the right coronary artery that most often supplies the postero-medial papillary muscle (Fig. 6.28). Papillary muscles are conceptualized as being

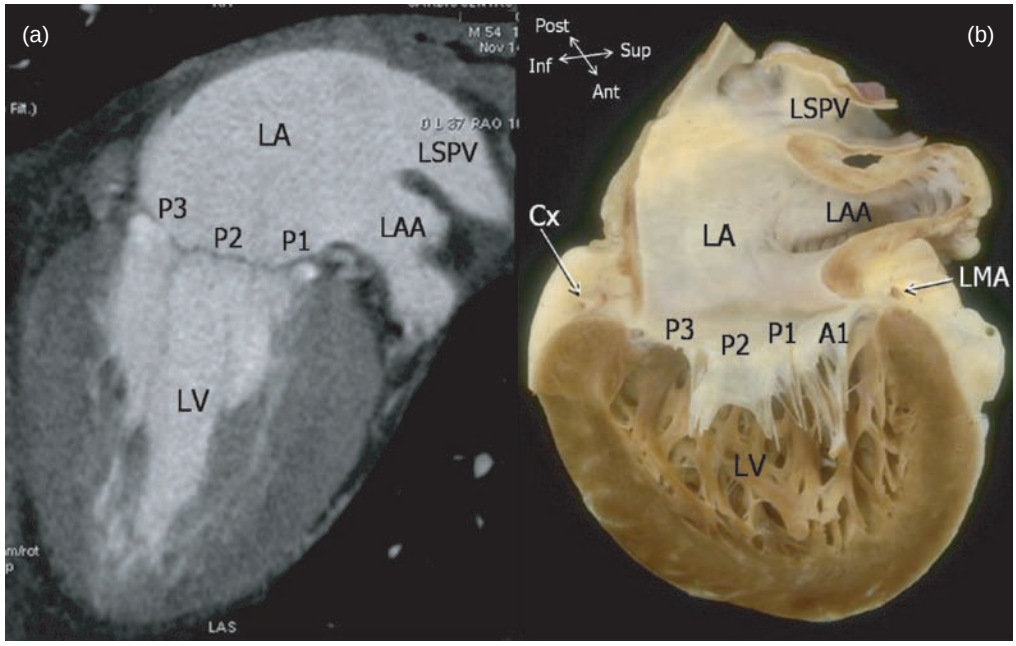

Figure 6.22 (a) Oblique slice showing a two-chamber view in systole. (b) The corresponding anatomic specimen. The three scallops, P1, P2 and P3, of the posterior leaflets are shown. LA = left atrium; LV = left ventricle; LAA = left atrial appendage; Cx = circumflex artery; LMA = left main artery; LSPV = left superior pulmonary vein.

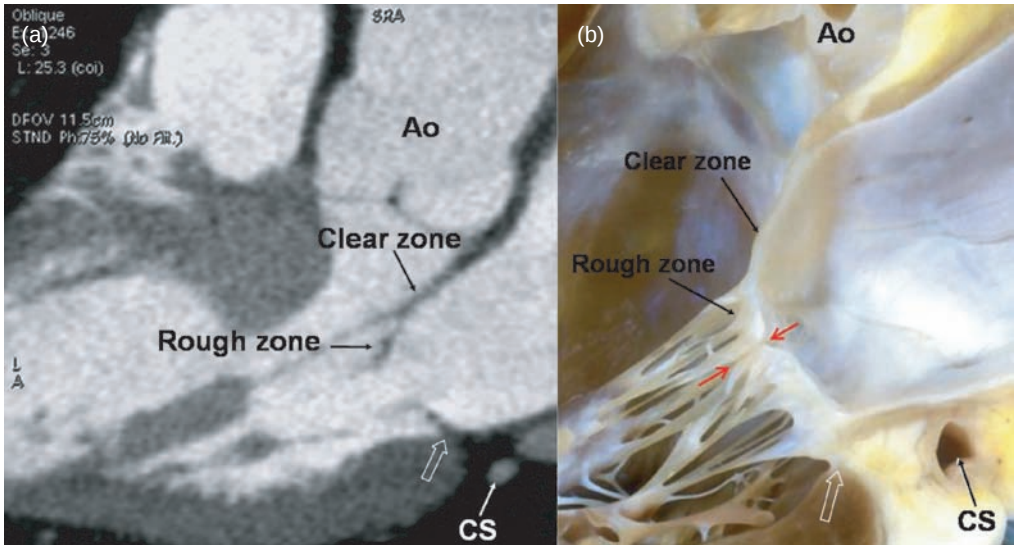

Figure 6.23 Oblique slice (a) and the corresponding anatomic specimen (b) showing the rough and clear zones of the anterior mitral leaflet. Ao = aorta; CS = coronary sinus.

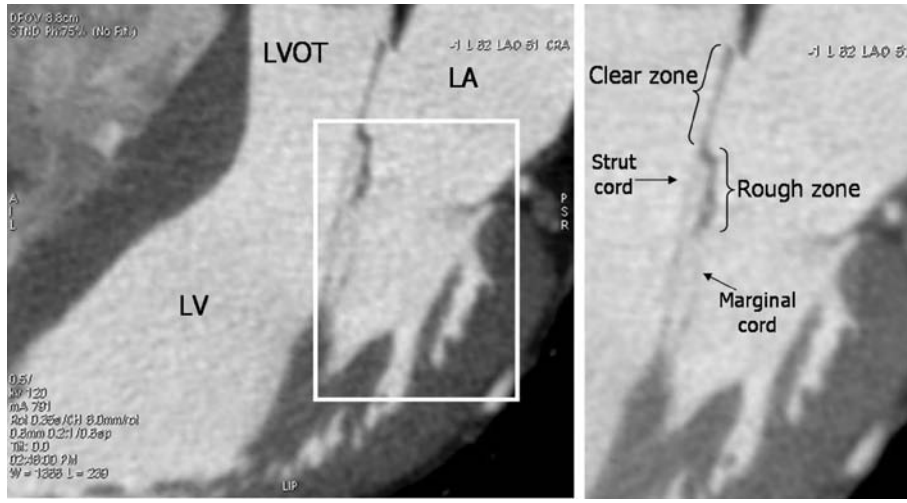

Figure 6.24 Oblique slice. In the magnified image (right) strut and marginal chordae as well as the clear and rough zones can also be distinguished. LA = left atrium; LV = left ventricle; LVOT = left ventricular outflow track.

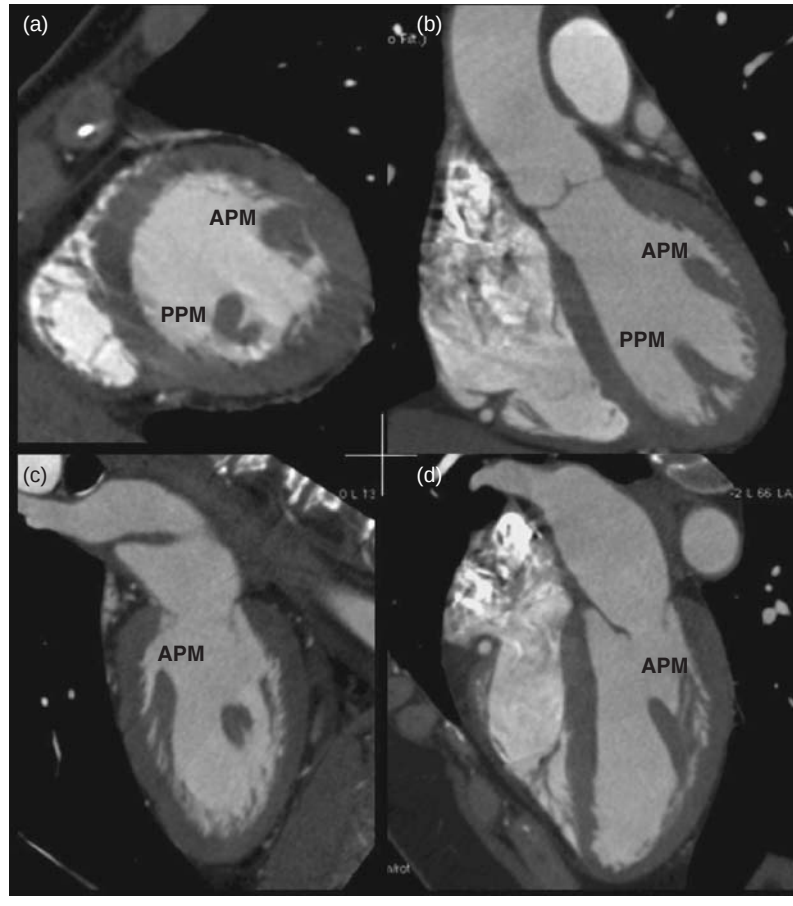

Figure 6.25 (a) Short-axis view, (b) coronal plane, (c) two-chamber and (d) four-chamber view showing anterior (APM) and posterior (PPM) papillary muscles.

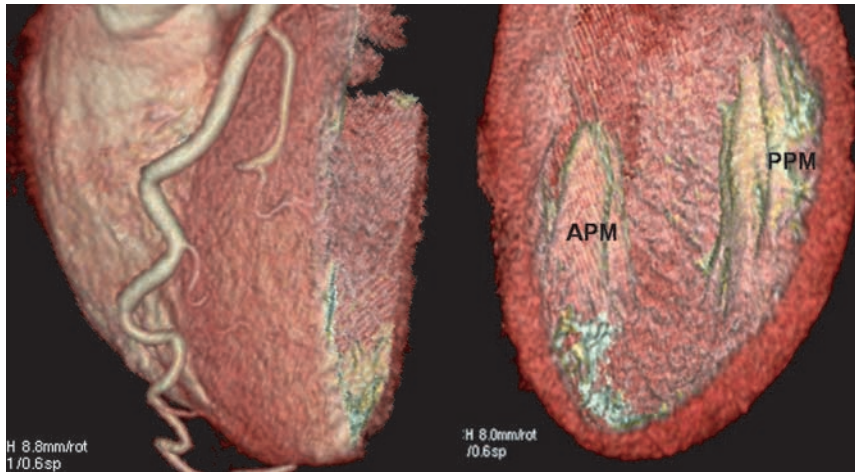

Figure 6.26 3D volume rendering image cropped in long-axis orientation. The lateral wall and the contrast have been "electronically" removed. Both anterior (APM) and posterior (PPM) papillary muscles are shown in 3D volume rendering format.

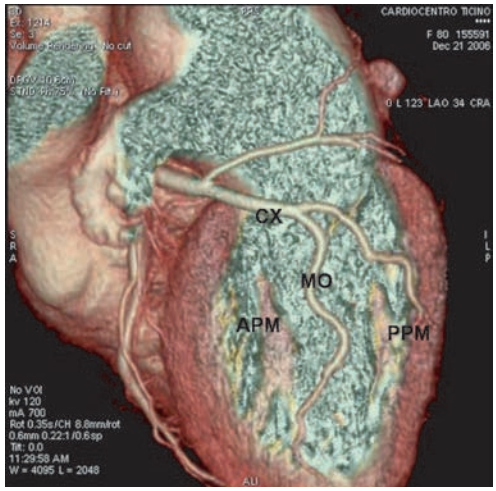

Figure 6.27 3D volume rendering. Image was cropped to visualize both papillary muscles. The coronary vessels were superimposed to show the relationships between circumflex coronary artery (CX), marginal branch (MO) and anterior papillary muscle (APM). PPM = posterior papillary muscle.

directly continuous with the solid portion of the heart wall, the compact myocardium, but tomographic imaging has consistently shown that the bases of the papillary muscles are not solid. Instead, they are composed of muscular continuations from the trabeculations that line the ventricular cavity (Figs. 6.29 and 6.30).

Tricuspid valve

Just like the mitral valve, the tricuspid valve guards the junction between atrium and ventricle and is also described as an atrioventricular valve. Its apparatus comprises "annulus" or hingeline, leaflets, tendinous cords and papillary muscles.

Tricuspid annulus

The tricuspid valve has an "annulus" to which the leaflets are hinged. Although "annulus" implies a well-formed collagenous ring, this is far from the case in the tricuspid valve. Collagenous accretions are seldom found. The hingeline has an elliptical shape that nearly mirrors the mitral "annulus" with straight septal and curved mural components (Fig. 6.31a). Moreover, recent studies have demonstrated a saddle-shaped configuration of the tricuspid "annulus" with the peaks in anterior and posterior positions, and the valley between medial and lateral positions (Fig. 6.31b).

Leaflets

Generally the valve has three leaflets – the medial or septal, the antero-superior and the posterior or inferior leaflets (Figs. 6.32 and 6.33). Attitudinally, antero-superior and inferior describe the locations better than anterior and posterior. Fan-shaped commissural cords support the peripheral ends of the zones of coaptation between adjacent leaflets. The commissures are designated antero-septal,

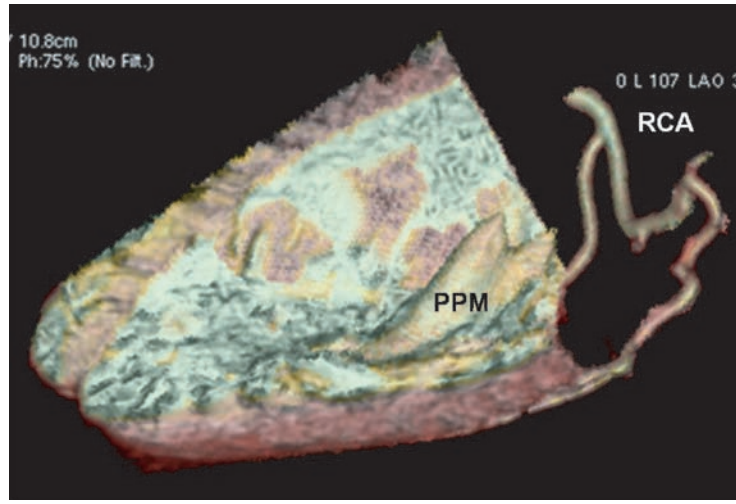

Figure 6.28 3D volume rendering. The heart was "electronically" dissected to show the relationship between the right coronary artery (RCA) and the posterior papillary muscle (PPM).

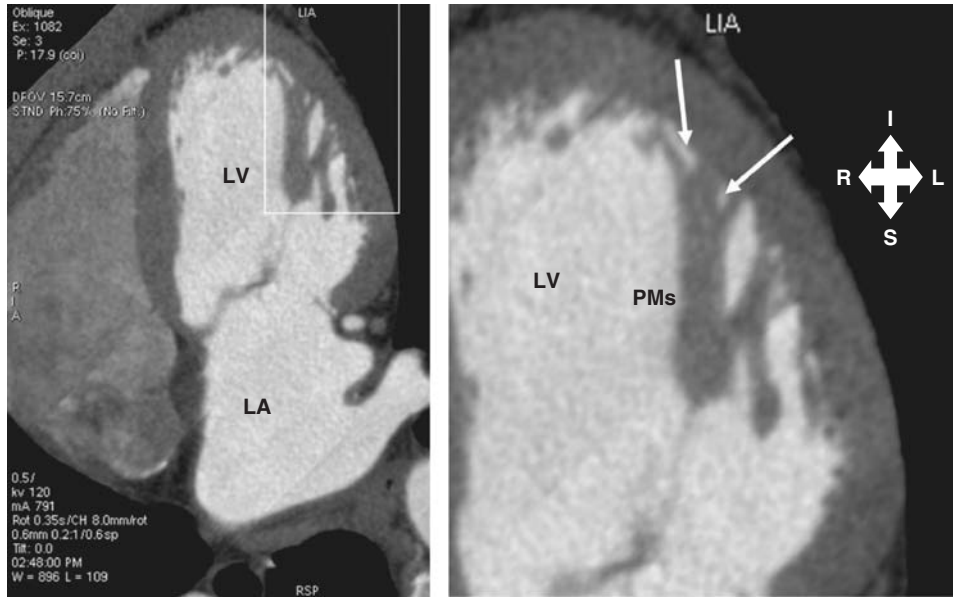

Figure 6.29 Oblique slice in up-down "echocardiographic" format. The base of the papillary muscle (PMs) joins with the network of trabeculae carneae lining the ventricular cavity rather than directly to the solid portion of the heart wall. LA = left atrium; LV = left ventricle.

antero-inferior and inferior. In some hearts, the divisions between leaflets are not so clear and some leaflets may have further subdivisions into scallops. In others, the division between antero-superior and inferior leaflets is not clear so some surgeons consider these as a unique leaflet with several scallops and call it the mural leaflet.

The septal leaflet (Fig. 6.34) has some characteristic features. First, it has multiple tendinous cords attaching it directly to the ventricular septum (Fig. 6.35). Second, its hinge is attached closer to the apex than that of the mitral leaflet. The difference in levels of attachment between the two atrioventricular valves, an offset arrangement, places

Figure 6.30 3D volume rendering images cropped in long-axis orientation. Magnified image of oblique slice in the left upper corner; magnified image of 3D volume rendering in the right upper corner and the corresponding anatomic specimen in the right lower corner showing the same papillary muscle insertion architecture.

(b)

Figure 6.31 (a) 3D volume rendering format. Perspective from above and behind after removing the right atrium. The elliptical shape of tricuspid annulus with straight septal (dashed white line) and curved mural (dashed black line) components. (b) 3D virtual endoscopy. Tricuspid "annulus" has a saddle-shaped configuration with the peak in superior and inferior positions and the valley in medial and lateral positions. Ao = aorta; CS = ostium of coronary sinus.

part of the muscular ventricular septum in an atrioventricular position, and this is evident when cutting the heart just behind the aortic root in a four-chamber slice (Fig. 6.36). Although previously described as the muscular atrioventricular septum, closer examination has shown that it is not strictly septal. Instead, it has a sandwich-like arrangement of right atrial wall and ventricular septum with epicardial fat between. A slice tilted slightly more cephalad will show the hingeline of the septal leaflet bisecting the membranous septum into atrioventricular and interventricular components on the right heart aspect (Fig. 6.37); the aortic root is also revealed on this cut.